Stony Brook University

Repression of Meiotic Gene Expression by Regulated RNA Stability and by Antisense Transcription in *Schizosaccharomyces pombe*

A Dissertation Presented

by

Huei-Mei Chen

to

The Graduate School

in Partial Fulfillment of the

Requirements

for the Degree of

Doctor of Philosophy

in

Molecular and Cellular Biology

Stony Brook University

December 2010

Stony Brook University

The Graduate School

Huei-Mei Chen

We, the dissertation committee for the above candidate for the
Doctor of Philosophy degree,
hereby recommend acceptance of this dissertation.

Dr. Janet K. Leatherwood, Ph.D., Associate Professor
Department of Molecular Genetics and Microbiology, Stony Brook University
Dissertation Advisor

Dr. Bruce Futcher, Ph.D., Professor
Department of Molecular Genetics and Microbiology, Stony Brook University
Chairperson of Defense

Dr. Adrian R. Krainer, Ph.D., Professor
Cold Spring Harbor Laboratory

Dr. Aaron Neiman, Associate Professor
Department of Biochemistry and Cell Biology, Stony Brook University

Dr. Scott Keeney, Ph.D., Professor, Outside Member
Graduate School of Biomedical Sciences, Sloan-Kettering Institute

This dissertation is accepted by the Graduate School

Lawrence Martin
Dean of the Graduate School

Abstract of the Dissertation

Repression of Meiotic Gene Expression by Regulated RNA Stability and by Antisense Transcription in *Schizosaccharomyces pombe*

by

Huei-Mei Chen

Doctor of Philosophy

in

Molecular and Cellular Biology

Stony Brook University

2010

Meiosis produces haploid gametes from diploid germ cells. Many genes are used only for meiosis and cause harm if they are expressed in vegetative (non-meiotic) cells. My dissertation research focused on mechanisms that keep meiotic functions completely off in vegetative cells in a model organism, the fission yeast *Schizosaccharomyces pombe.*

Early meiotic genes drive a specialized S-phase and meiotic recombination events. I found that at least 30 early meiotic genes in S. pombe are transcribed even in vegetative cells where they are kept off by degradation of their transcripts through a novel mechanism directed by Mmi1, an RNA binding protein. I determined that Mmi1 induces hyperadenylation of early meiotic genes, that the exonuclease Rrp6 degrades the hyperadenylated mRNAs, and that the polyA binding protein, Pab2, assists this hyperadenylation and is required for degradation. My work also shows that Mmi1 regulates mRNA splicing. These findings suggest that a polyadenylation quality control mechanism together with splicing regulation regulate early meiotic genes in *S. pombe*.

Middle meiotic genes direct the specialized meiotic division events. Unlike the early meiotic genes, the middle meiotic genes are not transcribed in vegetative cells but are transcriptionally induced just before the first meiotic division. Using Affymetrix tiling arrays, I found that at least 50 middle meiotic genes are transcribed in the anti-sense direction in vegetative cells. Most of these anti-sense RNAs decline coincident with

induction of the corresponding sense transcript during meiosis. To test the idea that anti-sense transcription inhibits expression of middle meiotic genes in vegetative cells, I engineered constructs to block three of the anti-sense RNAs. Using these constructs I found that disruption of the anti-sense RNAs allows sense gene transcription, and I determined that anti-sense mediated repression works together with the forkhead transcription factor, Fkh2 to keep middle meiotic genes fully off in vegetative growth.

This thesis reports my experiments on mechanisms for repression of meiotic genes in vegetative cells including extensive characterization of RNA processing and decay pathways for repression of early meiotic genes, as well as experiments on anti-sense based repression of middle meiotic genes.

For my family, who have been and will always be the best part of my life.

Table of Contents

List of Tables

List of Figures

Acknowledgement

My journey as a PhD student is a great experience, and it is because of the help and support given by faculty, friends and family members.

I am heartily thankful to my supervisor, Dr. Janet Leatherwood, whose encouragement and guidance from the first day and everyday enabled me to develop an understanding and interest of molecular biology. She taught me how to do experiment in the "lazy" way. She inspired me, challenged me and supported me. I also enjoyed the accompany of her family. I have been very fortunate to have her as my thesis advisor.

I would like to show my gratitude to the members of my thesis committee, Dr. Bruce Futcher, Dr. Adrian Krainer, Dr. Aaron Neiman and Dr. Scott Keeney for their precious time, expert advises and unique insights. In particular, Dr. Futcher helped me tremendously with the manuscript writing.

The MCB program provided me a great learning opportunity. I am very grateful for our program director Dr. Rolf Sternglanz for his effort in managing the program and fostering the students. I would like to thank all the co-workers in the Yeast group for providing a stimulating and fun environment.

I am very grateful to all the past and present members of the Leatherwood lab. Dr. Adam Rosebrock helped greatly with microarray experiments and provided brilliant ideas. Hong Qin and Lee Hong See are excellent co-workers and they helped with my experiments in every single aspect. Sohail Khan helped with tiling array analysis. Fellow graduate students Angad Garg and Kaustav Mukherjee make the lab a cheerful place to work and continue all the great lab projects.

My friends here in Stony Brook are very important to me. They are always supportive and awesome. I sincerely cherish their friendship and they will be my friends for life. I also want to thank Nihal for his encouragement and for being my sunshine.

Most importantly, none of this could be possible without the love, understanding and support of my parents, my mom Pin-Yuan Wang and my dad Wen-Chin Chen. It is because of them that I have the strength to go further and reach higher.

Chapter One: Background and Significance

I. Two types of cell division: mitosis and meiosis

Mitosis and meiosis are two types of cell division (Figure 1.1). Somatic cells, or vegetative cells for single celled organisms, divide mitotically. The daughter cells maintain the same genetic makeup as the parent cell. The single celled organism *Schizosaccharomyces pombe*, fission yeast, is one of the model organisms that has been used in cell cycle research. The mitotic cell cycle is well studied, and the functions of many key regulators have been uncovered (Moser and Russell, 2000; Nurse, 1997). Meiosis is a specialized cell division that generates haploid gametes from diploid germ cells. Meiosis is often considered to be an alternate cell cycle because many of the steps in meiosis are similar to those in mitosis except that meiosis is more complex. In a mitotic division there is one round of DNA replication (S phase) followed by chromosome segregation (M phase) cell division, whereas meiosis consists of DNA replication and homologous recombination (pre-meiotic S phase) followed by two rounds of chromosome segregation (MI and MII). In fission yeast, the four resulting nuclei are packed into spores.

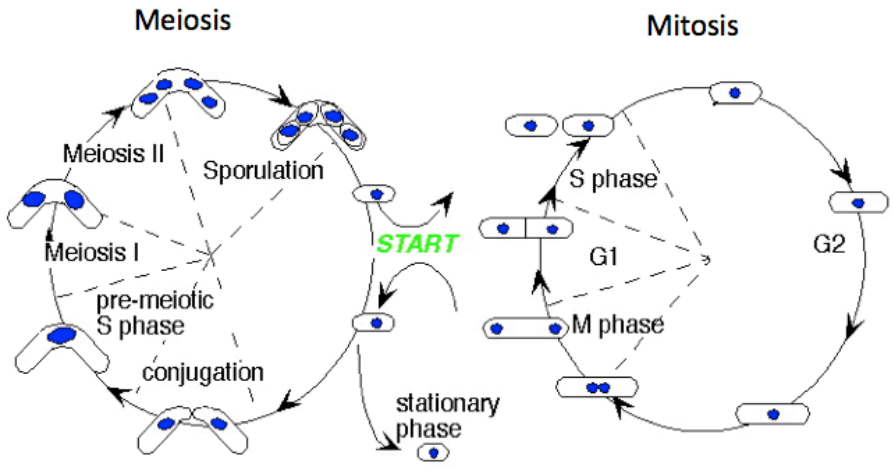

Figure 1.1 Illustration of mitotic and meiotic cell divisions in fission yeast. (Figure adapted from Forsburg Lab *pombe* page)

DNA synthesis is crucial for both cell divisions. Many genes that are required for mitotic DNA synthesis are also expressed during meiotic DNA synthesis (e.g., *cdc18* and *cdt1*) (Hofmann and Beach, 1994; Nakashima et al., 1995; Mata et al, 2002). Similarly, many genes that are required for mitotic chromosome segregation are also important for meiotic chromosome segregation. In addition to shared genes, there are many genes that control meiosis-specific events, and these gene are typically only expressed during meiosis. For example, the early meiotic gene *rec8* (meiosis-specific cohesin subunit) (Parisi et al., 1999) and the middle meiotic genes *spo4*/*spo6* (kinase and regulatory partner for the second meiotic division) (Nakamura et al., 2000; Nakamura et al., 2002) are kept tightly off in vegetative cells. Ectopic expression of meiotic genes in vegetative cells often reduces cell growth or even causes lethality (Averbeck et al., 2005; Mata et al., 2007; Moldon et al., 2008; Shonn et al., 2002). Nevertheless, the mechanisms that prevent mitotic (or vegetative) expression of meiotic genes remain largely unexplored.

II. *S. pombe* meiosis

1. Meiotic stages

S. pombe grows vegetatively as haploids in nutrient rich medium. Starvation stimulates haploids of opposite mating types to mate, which results in diploid cells. If a nutrient source is re-introduced, the diploid cells can be grown vegetatively. Diploids enter meiosis when they are starved. Based on morphological landmarks, the events of meiosis are classified into three stages; namely early (DNA synthesis and recombination), middle (MI and MII), and late (spore maturation).

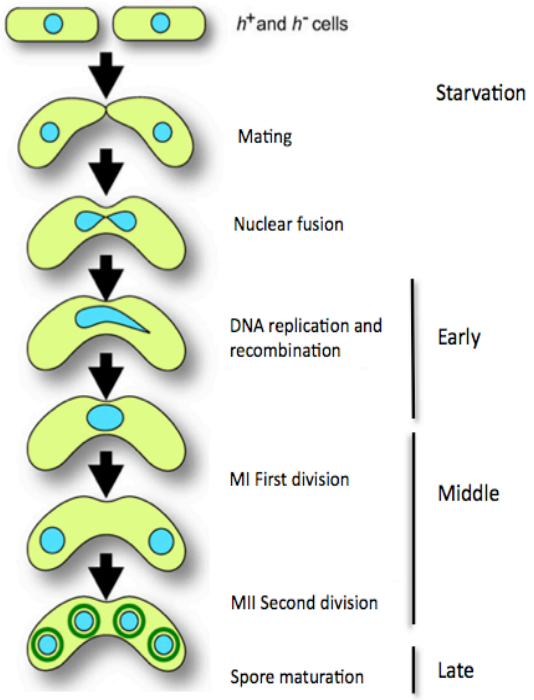

Figure 1.2 Morphological landmarks of meiosis. Figure adapted from (Asakawa et al., 2007).

2. Signal transduction involved in the initiation of meiosis

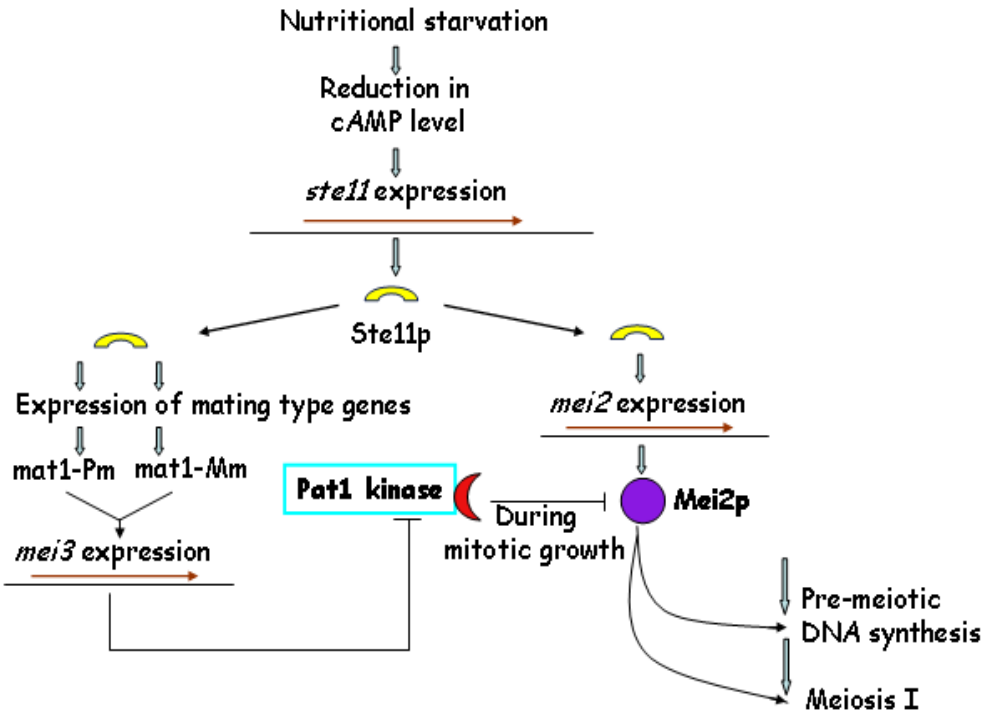

Figure 1.3 Signaling pathway for meiosis in *S. pombe*.
Figure adapted from (Yamamoto, 1996).

Meiosis is coordinated with nutrient status so that cells initiate meiosis when nutrients are low. When cells are starved, cellular cAMP levels decrease due to lower activity of adenylate cyclase, *cyr1* (Young et al., 1989). The reduction of cAMP induces expression of *ste11* which encodes a DNA-binding protein of the HMG (high mobility group) transcription factor family. Ste1 activates a number of genes including genes that encode mating pheromones (*mat1-Pm* of h^+ strain and *mat1-Mm* of h^- strain) and the key meiotic inducer, Mei2 (Sugimoto et al., 1991). The products of *mat1-Pm* and *mat1-Mm* are secreted pheromones, P-factor (Imai and Yamamoto, 1994) and M-factor (Davey, 1992), respectively. These pheromones bind and then activate their corresponding G protein coupled transmembrane receptors, present on the surface of opposite mating type cells. Activation of the G protein coupled receptor stimulates a MAP kinase cascade and further enhances the expression of *ste11* and additional genes, including *mei3* (McLeod et al., 1987; Neiman et al., 1993).

The interactions between Mei2, Pat1 and Mei3 control entry into meiosis. Mei2 is the key meiotic inducer. Mei2 activation causes ectopic meiosis irrespective of the signaling pathways (Watanabe et al., 1997). In vegetative cells, Mei2 is inhibited by the protein kinase Pat1. Pat1, also known as Ran1 in older literature, is a Ser/Thr kinase that phosphorylates Mei2 (McLeod and Beach, 1988; Watanabe et al., 1997). Phosphorylation inhibits Mei2 activity by two mechanisms. First, phosphorylation targets Mei2 for ubiqutination-dependent protein destruction (Kitamura et al., 2001). Second, phosphorylated Mei2 is not able to bind its RNA partner, meiRNA (Sato et al., 2002). *mei3* is induced by Ste11 when haploid cells mate or when diploid cells are starved. *mei3* encodes a pseudo-substrate that binds and inactives Pat1 kinase (Li and McLeod, 1996). Similar to ectopic expression of Mei2, over expression of Mei3 or inactivation of Pat1 also induces meiosis irrespective of the cell ploidy or signaling cascades. All together, these results demonstrated the importance of Mei2.

3. Function of Mei2, the key meiotic inducer

Mei2 is an RNA binding protein that contains three RRM-type RNA binding motifs (Birney et al., 1993; Watanabe and Yamamoto, 1994). Mei2 homologs are also key regulators of differentiation and meiosis in Arabidopsis (Kaur et al., 2006). Mei2 is essential for karyogamy (nuclear fusion, our unpublished result), meiotic DNA synthesis, and the first meiotic division (Watanabe and Yamamoto, 1994). However, the mechanisms of Mei2 action are poorly understood. The only known RNA partner of Mei2 is meiRNA, a polyadenylated non-coding RNA transcribed from the *sme2* gene (Watanabe and Yamamoto, 1994). Mei2, together with meiRNA, forms a single dot in the nucleus during meiotic prophase and the formation of this dot correlates with the ability to perform the first meiotic division (Yamashita et al., 1998).

mes1 was the first gene reported to be regulated by splicing in *S. pombe*. That is, the introns are not spliced during vegetative cell growth, and they become spliced during meiosis. In addition, *mes1* unspliced pre-mRNA accumulates in *mei2*$^{-}$*/mei2*$^{-}$ diploid cells under nitrogen starvation conditions (Kishida et al., 1994). However, *mes1* is constitutively spliced in vegetative growth in my experiments. The discrepancy between results might be due to different strain backgrounds or strain handling methods.

Nevertheless, the published observation suggests that Mei2 might be involved in mRNA processing. It is likely that the Mei2 dot forms a meiosis-specific mRNA processing machinery during meiosis.

Two papers have reported Mei2-based mechanisms promoting meiosis (Shinozaki-Yabana et al., 2000). First, in a search of high copy number suppressors that rescue Mei2 induced ectopic meiosis, a novel gene, *mip1*, was identified (Mei2 interacting protein-1) (Shinozaki-Yabana et al., 2000). Similar to the mTOR pathways (Target of Rapamycin, TORC1 and TORC2) in mammalian cells, *S. pombe* has two Tor pathways, Tor1 and Tor2 (Alvarez and Moreno, 2006; Weisman and Choder, 2001). Mip1 was later identified as a Raptor homolog that inhibits the Tor2 (mammalian TORC1) signaling pathway. The Tor2 pathway promotes mitotic cell growth and represses meiotic cell differentiation (Alvarez and Moreno, 2006). Mip1 is cytoplasmic and immunoprecipitation analysis has shown that Mip1 and Mei2 interact in vivo (Shinozaki-Yabana et al., 2000). The Mei2-Mip1 interaction suggests that Mei2 has a cytoplasmic function to regulate Tor2. The other function of Mei2 is to inactivate Mmi1, a protein that degrades meiotic mRNAs in vegetative cells (Harigaya et al., 2006). This Mmi1-mediated mRNA removal is discussed in a later section (p.10).

4. Meiotic transcription program

The *S. pombe* meiotic transcription program involves up-regulation of ~1/7th of the transcriptome (Mata et al., 2002) The upregulated genes were classified based on temporal expression pattern as (1) starvation- or pheromone-induced genes (250 genes), (2) pre-meiotic S phase and recombination (early meiosis, 108 genes), (3) nuclear divisions (middle meiosis, 561 genes), or (4) spore formation (late meiosis, 133 genes) (Mata et al., 2002).

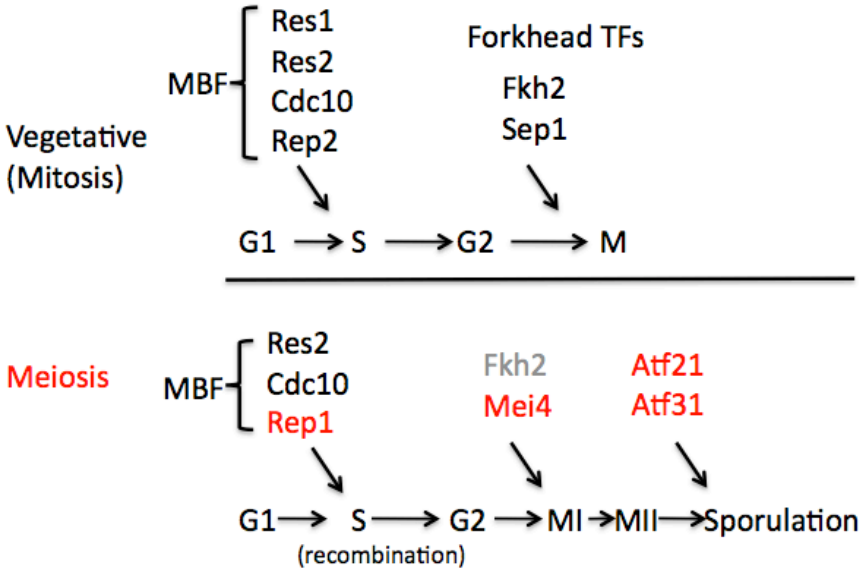

Figure 1.4 Comparison of mitotic and meiotic transcription factors. Meiosis-specific transcription factors are colored in red.

There are apparent similarities and differences between mitotic and meiotic transcription factors (Figure 1.4). The MBF transcription factor complex induces genes required for both mitotic and meiotic S phase (Ayte et al., 1995; Ding and Smith, 1998), and the forkhead transcription factors regulate both mitotic and meiotic G2/M phase (Buck et al., 2004; Horie et al., 1998). However, the specific factors involved are distinct. The MBF complex in meiosis contains Rep1, instead of Rep2 (Nakashima et al., 1995). The major forkhead transcription factor in meiosis is Mei4, but not Sep1 (Mata et al., 2007). Fkh2 is required for proper meiotic progression, but the molecular mechanism of Fkh2 in regulating meiosis is unknown (Szilagyi et al., 2005).

Half of the early meiotic genes do not require Rep1 for the observed meiotic increase in transcript levels (Mata et al., 2007), strongly suggesting the existence of some other regulatory mechanisms. Because several early meiotic genes seem to be regulated by meiosis-specific splicing (Averbeck et al., 2005), we expected that other regulatory mechanisms might act by changing RNA processing, which would in turn change the RNA stability, allowing accumulation of meiotic transcripts in mitosis, independent of meiotic specific transcription factors. In Chapter Two, I focus on the molecular mechanism that regulates early meiotic genes.

Mei4 is the major meiotic transcription factor responsible for induction of almost all middle genes (Mata et al., 2007). Four genes code for forkhead transcription factors in *S. pombe* (Table 1.1): *mei4* is expressed only in meiosis, while *fkh2*, *sep1* and *fhl1* are expressed in vegetative cells. Forkhead transcription factors contain the signature FKH domain that binds to DNA in a sequence-specific manner. The core DNA binding motif (GTAAAYA) for forkhead transcription factors is well conserved in fission yeast (Horie et al., 1998; Oliva et al., 2005) and likely across species (Kaufmann et al., 1994; Pierrou et al., 1994). Little is known about how forkhead transcription factors choose among similar binding motifs to achieve specificity of each factor.

Forkhead	Function	FHA
Fkh2	G2➔M, (meiosis?)	Yes
Sep1	G2➔M	No
Mei4	Meiotic G2➔M	No
Fhl1	Growth (ribosomal synthesis)	Yes

Table 1.1 Forkhead transcription factors in *S. pombe*.

The FHA (Forkhead-Associated) domain was originally identified as a conserved region in forkhead transcription factors. Fkh2 and Fhl1 contain the FHA domain, while Mei4 and Sep1 lack an FHA domain. The FHA domain interacts with phosphorylated proteins (Mahajan et al., 2008). Forkhead transcription factors can exert opposite functions (i.e., transcription activation or repression) depending on their interacting proteins. One of the best examples is Fkh2 in budding yeast. Fkh2 forms a complex with Mcm1 at target promoters of G2/M genes, but this complex does not activate transcription. Transcription is activated when the co-activator, Ndd1, is phosphorylated and recruited to the Mcm1-Fkh2 complex in a cell cycle-dependent manner (Darieva et al., 2006; Reynolds et al., 2003). It is likely that the FHA domain and interacting proteins determine both the specificity and transcription activity of the forkhead transcription

factors. In Chapter Three, I discuss the repression activity of Fkh2 for middle meiotic genes in vegetative cells.

Two transcription factors, Atf21 and Atf31, have overlapping functions accounting for half of late meiotic gene expression (Mata et al., 2007). Mei4 induces Atf21 and Atf31, and this provides a mechanism by which the late gene expression wave follows the middle meiotic events.

III. Meiosis-specific RNA processing

1. Meiosis-specific splicing

More than half of *S. pombe* genes have introns, and genes with multiple introns are frequent (Wood et al., 2002). To splice the large number of introns of different sizes and sequences, *S. pombe* has a sophisticated splicing apparatus (Kaufer and Potashkin, 2000). Our previous post-doctoral researcher Dr. Averbeck has shown that meiosis-specific splicing regulates a dozen meiotic genes, including 3 early, 8 middle and 1 late meiotic genes (Averbeck et al., 2005). That is, these genes are transcribed in vegetative cells; however, to keep these genes from making functional proteins, their introns remain unspliced. During the course of meiosis, these introns are spliced, corresponding to the functional timing of their genes. This observation suggests that splicing regulation applies to all stages of meiosis. Several other groups have reported meiosis-specific splicing (Kishida et al., 1994; Moldon et al., 2008; Wilhelm et al., 2008). However, all of these investigations, including the one from our lab, used splicing assays that lack strand specificity and therefore can be complicated by antisense transcription (see Chapter Three for details). To differentiate splicing regulation from antisense regulation, I used strand specific splicing assay on a dozen meiotic genes and found that only the early meiotic genes have the meiosis-specific splicing pattern, while all the middle and late genes are not expressed as sense transcripts in vegetative cells. My data suggest that splicing regulation only applies to the early meiotic genes.

Dr. Averbeck also found that the 3' UTR (untranslated region) of *crs1* (early meiotic cyclin) confers the splicing inhibition in vegetative cells. Replacing the 3'UTR of *crs1* with *nmt1*-terminator sequences de-represses splicing of *crs1* (Averbeck et al.,

2005). For a second gene, *rem1*, it has been reported that the promoter confers splicing regulation (Averbeck et al., 2005). For these two meiotic genes, *crs1* and *rem1*, DNA sequences far away from the introns, not the intron sequences themselves, are important for inhibiting splicing in vegetative cells. That the regulatory sequences are located at the opposite ends for these two genes suggests that at least two mechanisms exist to regulate meiosis-specific splicing. Moreover, the locations also suggest that the process of splicing may be coordinated with mRNA 3' end processing and transcription.

Aýte's group investigated the splicing regulation of *rem1* extensively (Malapeira et al., 2005; Moldon et al., 2008). Because the promoter region is important for *rem1* splicing inhibition and the meiosis-specific forkhead transcription factor, Mei4, induces both transcription and splicing of *rem1,* they tested the splicing status of *rem1* in strains carrying mutations affecting forkhead transcription factors. In summary, they concluded that *rem1* regulation involves coupling between a transcription factor and the splicing machinery, a phenomenon that was previously observed in mammalian cells (Cramer et al., 1997). However, our tiling array data indicated that the "unspliced" RT-PCR signal of *rem1* in vegetative cells may have come from antisense RNA. I hypothesized that Fkh2 might regulate a switch between antisense and sense transcription, rather than splicing (See Chapter Three for more details).

To identify the *trans*-acting factors involved in splicing inhibition of early meiotic genes, I screened a panel of factors that participate in mRNA processing, including splicing, 3' end processing and RNA degradation, and specifically looked for mutants that allow splicing of meiotic genes in vegetative cells. Mutation of several factors allowed splicing of meiotic genes. However, these factors influence different genes at variable degrees, suggesting meiosis-specific splicing is regulated by a complex regulatory system (See Chapter Two for more detail). One of these factors is Mmi1, an RNA binding protein. The discovery of Mmi1 and function of Mmi1 is described in the following section.

2. Regulation of RNA stability

As described above, many early meiotic genes do not depend on any known transcription factors. In addition, several early meiotic genes, including *crs1* and *rec8*, are

transcribed in vegetative cells possibly as much as in meiotic cells based on transcription run-on assays and analysis of published RNA pol II ChIP-on-chip data (McPheeters et al., 2009; Wilhelm et al., 2008). Regulation of RNA stability seems to the major mechanism to keep these genes off in vegetative cells and turn them on in meiotic cells.

The key factor to this regulation is Mmi1. Mmi1 was discovered because it promotes *mei4* mRNA decay in vegetative cells. Mmi1 contains a putative RNA binding domain, the YTH domain. In vegetative cells, Mmi1 directly binds the Mei4 mRNA, and somehow "targets" the mRNA for exosome-mediated degradation. In an *mmi1-ts* mutant, several other meiosis-specific mRNAs become stabilized in vegetative cells at restrictive temperature. These other meiosis-specific mRNAs are also bound by Mmi1 and targeted for exosomal degradation in vegetative cells. The Mmi1-binding sequences on these various RNAs have been mapped and have been named "DSRs" (Determinant of Selective Removal). But no consensus sequence or structure has been identified in the DSR (Harigaya et al., 2006; McPheeters et al., 2009). Many of the genes regulated by Mmi1 at the level of RNA stability contain introns, and I found that Mmi1 also regulates splicing of most of these genes; however, my experiments in Chapter Two suggest that intron retention is not likely to be the cause of RNA instability for most of these genes. When meiosis is induced, the key meiotic regulator Mei2, together with meiRNA, sequester and inactivate Mmi1. When Mmi1 is inactivated, Mmi1-regulated mRNAs are spliced and accumulate (Harigaya et al., 2006; and Chapter Two). Thus, regulation of this set of meiotic genes appears to be largely post-transcriptional (Harigaya et al., 2006) (Figure 1.5). In Chapter Two, I described studies of the "targeting" mechanism of Mmi1.

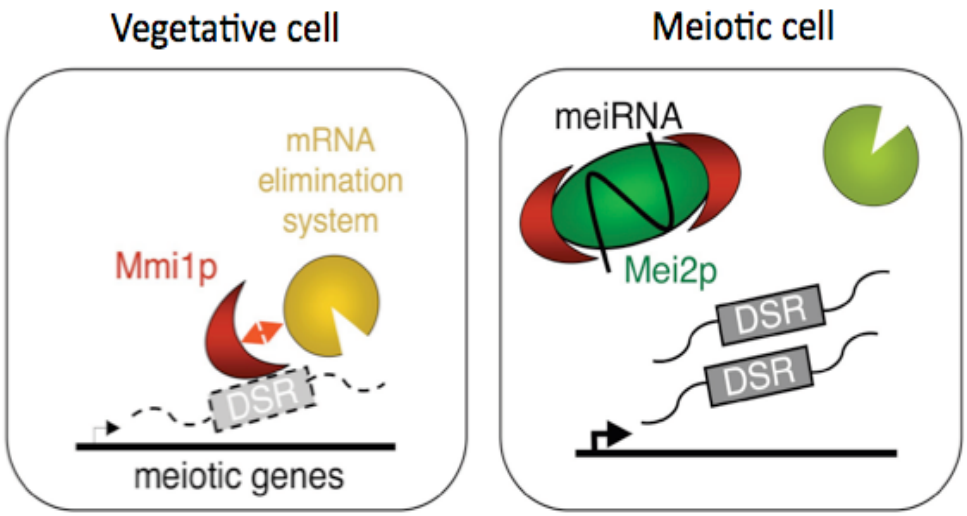

Figure 1.5 Regulation of RNA stability by Mmi1. A number of meiosis-specific mRNAs carry a region designated the "DSR", which interacts with Mmi1 in vegetative cells. Mmi1 causes the elimination of these mRNAs in the nucleus, probably cooperating with the nuclear exosome. During early meiosis (meiotic prophase), Mei2 and meiRNA form a dot structure which sequesters Mmi1 and inactivates Mmi1. The meiosis-specific mRNAs thereby become stably expressed. (Image adapted from Harigaya et al., 2006)

Mmi1 interacts with Rrp6, a 3' to 5' exonuclease associated with the exosome, and thereby brings RNAs to the exosome for degradation (Harigaya et al., 2006). The exosome is involved in a wide range of RNA processing and RNA decay reactions in both the nucleus and the cytoplasm. For excellent recent reviews on the structures and functions of the exosome, please see (Ibrahim et al., 2008; Lebreton and Seraphin, 2008; Schmid and Jensen, 2008). The exosome is a large complex with a 9-subunit barrel-like core structure. In eukaryotic cells, the core complex itself does not possess nuclease activity (Figure 1.6 A).

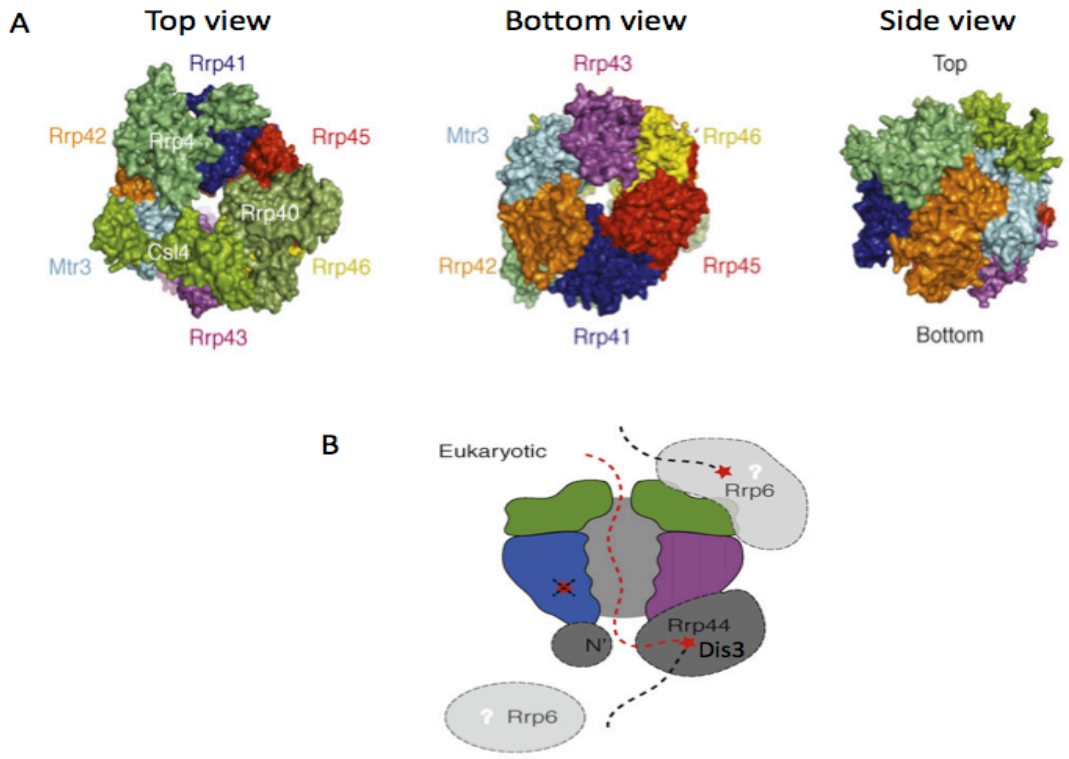

Figure 1.6 Structure of RNA exosome complexes. (A) Surface representation of exosome central core structures. Individual subunits are color-coded: Rrp41/Ski6 (blue), Rrp42 (orange), Mtr3 (cyan), Rrp43 (magenta), Rrp46 (yellow), Rrp45 (red), S1–KH domain proteins Rrp4, Csl4, Rrp40 (greens). The gene names were derived from *S. cerevisiae* and were followed in naming *S. pombe* and mammalian exosomal genes. (B) Cartoon sliced side view of the exosome showing the central channel (gray). Rrp44 (*S. cerevisiae*)/Dis3 (*S. pombe*) (dark gray) and Rrp6 (light gray) have the exonuclease activity and associate with the core. Dotted lines depict potential paths of the RNA substrate, and red stars denoted the active sites. Figure adapted from (Schmid and Jensen, 2008).

The catalytic activity comes from two exosomal associating factors: Rrp44 (*S. cerevisiae*) /Dis3 (*S. pombe*) which has 3' to 5' exonuclease as well as endonuclease activities (Dziembowski et al., 2007; Mitchell et al., 1997) and Rrp6, which has 3' to 5' exonuclease activity (Allmang et al., 1999b). In fission yeast, Dis3 localizes to in both the cytoplasm and the nucleus, while Rrp6 is only in the nucleus. Path(s) for RNA substrates through the exosome are postulated in Figure 1.6 B. The difference of the predicted substrate paths for Rrp6 and Dis3 suggests that these two exonucleases may recognize substrates with different properties. Because the exonuclease activity is 3' to 5', the 3' end of the RNA substrate is important for initial recognition. It was recently identified

that short A tails at the 3' end help to target rRNAs and snoRNAs for exosomal processing (LaCava et al., 2005; Vanacova et al., 2005). In contrast, long polyA tails are bound by polyA binding proteins that protect RNAs from exosome degradation. Interestingly, Rrp6 interacts with polyA polymerase (Burkard and Butler, 2000) and polyA binding protein (Lemay et al., 2010). These interactions suggest that Rrp6 might monitor the quality and/or quantity of the polyadenylation reaction.

IV. Quantitation of RNA: Expression microarray and Tiling array

The accurate measure of RNA levels and RNA structures on a genome wide scale is fundamental to my research. In this work I have used two microarray formats: Spotted arrays that are manufactured in the Stony Brook Microarray Facility and Affymetrix tiling arrays *S. pombe* 1.0. It is important to note that microarrays measure the steady state of the RNA, which is a balance between RNA synthesis and RNA degradation.

Spotted array

Our lab has used two color spotted PCR arrays for more than a decade. These arrays were designed, printed, processed and hybridized in Stony Brook Microarray Facility by Dr. Futcher, Dr. Leatherwood, Dr. Rosebrock, Lei-Hoon See and Hong Wang. Probes printed on these arrays are PCR amplicons with a 3' bias for each gene/feature, and the average size of the PCR amplicon is 150nt. Each probe was printed on the array multiple times (ranging from 2 to 8). This spotted array is mainly designed to measure gene expression level by comparing "control" and "experimental" samples, and the relative ratio of the two is the output data. I have used the spotted array on meiotic expression time course and on various mRNA processing mutants in Chapter Two.

Tiling array

In contrast to the spotted array in which each gene is represented by one probe, the tiling array covers much more than the coding sequence. The Affymetrix *S. pombe* 1.0 array consists of ~2.5 million probes. The probes are *in situ* synthesized 25nt oligos, with 5nt overlap with the adjacent probe and tile the entire *S. pombe* genome on both DNA strands. Tiling arrays are versatile; they can be used for identifying protein-binding sequences (ChIP-on-chip), splicing efficiency, absolute transcript level, transcript

boundaries and so on.

At the beginning of my research I discovered differential 3' end processing on several meiotic genes using a traditional 3' RACE method. That is, the 3' end cleavage of these transcripts is directed by different *cis*-elements, sequences that are recognized and cleaved by the 3' end processing machinery. In vegetative cells the functional cleavage site(s) is generally down stream to the site(s) used during meiosis. Although the traditional 3' RACE yielded informative results, it can only analyze one gene at a time, is labor intensive and expensive. To study 3' end processing more efficiently I decided to utilize tiling arrays. The work presented in Chapter Three related to tiling array was a collaborative work with Dr. Rosebrock and Sohail Khan. Dr. Rosebrock spent a tremendous amount of time and effort in initially analyzing these array data. Details about array analysis methods including probe mapping, normalization within and between samples and visual presentation can be found in Dr. Rosebrock's thesis (Regulation of Transcription in the Fission Yeast *Schizosaccharomyces pombe*. Stony Brook University, August 2009). The subsequent tiling array analysis was accomplished with great help from Sohail Khan.

V. Research overview: Keeping meiotic genes off in mitotic cells

I have undertaken a study of different gene repression mechanisms that prevent meiotic genes from expression in vegetative cells. I started this research on meiosis-specific splicing by screening for genes that show regulated splicing patterns and by screening for factors that de-regulate splicing. At the time of my proposal exam, I had finished the screening for 650 genes across many conditions using RT-PCR method and I suspected that the splicing data might be complicated by the presence of antisense RNA. Soon after the proposal, I acquired solid results to demonstrate that splicing regulation applies to some early meiotic genes but not to middle or late meiotic genes.

In Chapter Two, I focus on the repression mechanism of early meiotic genes. Unexpectedly, I found that many of these early meiotic genes are highly transcribed in vegetative cells and are rapidly degraded by a novel mechanism. The core factor of this mechanism is Mmi1, an RNA binding protein that binds to target meiotic mRNAs through interaction between the RNA binding domain of Mmi1 and a special RNA motif, termed DSR (Determinant of Selective Removal), of the target mRNAs. Mmi1 confers

RNA instability and inhibits splicing. I determined that splicing inhibition by Mmi1 is separable from 3' end processing and RNA stability. The most significant discovery is that Mmi1 induces hyperadenylation of early meiotic genes and that Rrp6, a 3' to 5' exonuclease, degrades such hyperadenylated mRNA. A polyA binding protein, Pab2, seems to assist hyperadenylation and degradation. This suggests that cells use polyadenylation quality control as a regulatory mechanism to control gene expression.

In Chapter Three, I study the repression mechanism of middle meiotic genes. Unlike early meiotic genes, the middle meiotic genes are not transcribed in vegetative cells. Using Affymetrix tiling arrays, I determined that at least 50 middle meiotic genes associate with abundant antisense RNAs in vegetative cells. Moreover, the levels of many meiotic antisense RNAs decrease during meiosis. These observations suggest that antisense RNA inhibits meiotic gene transcription. Supporting this idea, disrupting the synthesis of antisense RNA allows sense RNA expression. Another repression mechanism acting on middle meiotic genes involves a forkhead transcription factor, Fkh2. I discovered that many meiotic-induced genes accumulate in *fkh2Δ* strain, suggesting that Fkh2 functions as a transcriptional repressor of these genes. This FKh2-mediated repression possibly operates through promoter competition with Mei4, a meiosis-specific forkhead transcription factor. These two mechanisms can function on the same gene to achieve maximum repression in vegetative cells.

All these repression mechanisms have been identified sporadically in organisms from bacteria to mammals. In Chapter Four, I discuss the important finding of each repression mechanism in other organisms and future directions that will move this research forward.

Chapter Two: Regulation of Early Meiotic Genes by RNA Stability

Paper title: The RNA-binding protein Mmi1 targets transcripts to Rrp6 for degradation using hyperadenylation, and thereby controls expression of early meiotic genes in fission yeast

Abstract

Polyadenylation is required for mRNA stability and is monitored by the exosome as a quality control mechanism. Here we report that the fission yeast, *Schizosaccharomyces pombe*, adopts this RNA quality control mechanism to regulate meiotic genes. In vegetative cells the RNA binding protein Mmi1 alters 3' processing of target transcripts to promote an extremely long polyA tail, sometimes as much as a kilobase. These hyperadenylated transcripts are rapidly degraded by the nuclear exonuclease Rrp6. The nuclear polyA binding protein Pab2 assists this hyperadenylation-mediated RNA decay. Experiments with a ribozyme-generated polyA tail suggest that alteration of 3' processing is a key step in the Mmi1-mediated decay pathway. Microarray analyses of meiosis and *mmi1, rrp6, dis3, pfs2, cid14* and *pab2* mutants defined an RNA regulon controlled primarily by the Mmi1 pathway. In some cases, Mmi1 also inhibits splicing and we show that splicing regulation is separable from 3' processing and stability control. This work advances our mechanistic understanding of regulated mRNA processing in the developmental switch to meiosis.

I. Introduction:

Gene expression involves intertwined steps of transcription, RNA processing, export and decay (Maniatis and Reed, 2002). The steady-state RNA level in the cell represents an equilibrium between transcription and degradation. In many cases, genes are regulated at the transcriptional level; however, regulation can also occur in other ways, including changes in RNA processing. One striking example of coordinated gene regulation via RNA processing is found in the fission yeast *S. pombe*. When this yeast first enters meiosis, there are at least a dozen meiotic genes that become functionally expressed

mainly because of changes in RNA processing (Averbeck et al., 2005; Harigaya et al., 2006). That is, these genes are actively transcribed in vegetative cells, but the primary transcripts are not processed into mature mRNAs, but instead are highly unstable and therefore unproductive. Upon meiotic entry, the processing of these transcripts changes dramatically, mature mRNAs are formed, and proteins are produced. Central to this regulation is the protein Mmi1, which is active in vegetative cells, but inactivated in meiotic cells. In vegetative cells, Mmi1 binds to a target region—the DSR (Determinant of Selective Removal)—often found near the 3' end of the transcripts, and somehow directs the destruction of the transcripts (Harigaya et al., 2006). The DSR is a transferable element; if it is deleted from a native gene, then the transcript becomes stable in vegetative cells; and if the DSR is added to a heterologous, reporter gene, then the transcript becomes destabilized in vegetative cells. It has been suggested that Mmi1 works with Rrp6, a nuclear 3' to 5' exonuclease component of the exosome, to target transcripts containing a DSR for degradation in vegetative cells (Harigaya et al., 2006).

Previously, we studied in some detail the RNA processing of *crs1*, an Mmi1 regulated gene (McPheeters et al., 2009). Transcription of *crs1* is equally high in both vegetative cells and meiotic cells, but mRNA only accumulates in meiotic cells. In vegetative cells (where Mmi1 is active), the *crs1* transcript that is detectable in WT (vegetative) cells is not polyadenylated, not spliced, and does not accumulate, and this lack of processing and stabilization depends on Mmi1. When meiosis is induced, or when Mmi1 is inactivated by mutation, the *crs1* transcript accumulates in its polyadenylated form, all four introns are spliced out, and the mature mRNA is relatively stable, resulting in protein expression. The involvement of the exonuclease Rrp6 was confirmed, since in an *rrp6* mutant, the *crs1* transcript was polyadenylated, spliced, and stabilized, even in vegetative cells. Finally, we found that mutation of *pfs2*, a component of the complex directing cleavage and polyadenylation of nascent transcripts, allowed splicing and accumulation of the targets of Mmi1. This suggested that Mmi1 probably affects 3' cleavage of the primary transcript, polyadenylation of the transcript, and splicing, in addition to affecting RNA stability.

Although splicing can be studied as an independent process, it is coupled with transcription and 3' processing (Bentley, 2005; Maniatis and Reed, 2002). Evidence

emerging over the last decade has indicated that splicing and 3' processing affect each other. For instance, mutation of splice sites decreases 3' processing along with splicing (Millevoi et al., 2002) and mutation of polyadenylation signals decreases splicing along with polyadenylation (Cooke et al., 1999). Interactions of the spliceosome with the 3' processing complex seem to be important to this coupling. We suggest that the mechanism of Mmi1 action may take advantage of the normal coupling between RNA processing steps. A study of Mmi1-mediated RNA turnover may provide a window on the mechanisms linking 3' cleavage, polyadenylation, splicing, and the degradation of aberrant transcripts.

To that end, we have done further analysis of a selection of genes with regulated splicing, finding that although they have behaviors in common with *crs1*, there are also significant gene-to-gene differences. Finally, we have used a polyA-encoding ribozyme to cleave and "polyadenylate" a transcript from the Mmi1-regulon in order to answer cause-and-effect questions about the relationship between cleavage, polyadenylation, splicing, and RNA stability.

II. Results

2.1 Identification of transcripts affected by Mmi1, RNA processing mutants, and meiosis.

To gain a more comprehensive idea of the range of genes regulated by Mmi1 and RNA processing, we did a series of microarray experiments. These included experiments on meiosis, *mmi1* and *rrp6* mutants (three conditions known to affect Mmi1 target genes), as well as other mutants that might or might not affect Mmi1 targets. The other mutants included *dis3-54*, *cid14*Δ, *pfs2-11* and *pab2*Δ. Figure 1 shows the 50 genes that accumulate most in the *mmi1-ts*3 mutant. As previously shown by Yamamoto and co-workers (for a smaller number of genes), the most strongly Mmi1-responsive genes are early meiotic genes (labeled in light yellow in Figure 2.1) (Harigaya et al., 2006). Hierarchical clustering reveals a 31-gene sub-group of these 50 genes with highly correlated expression in the meiotic, *mmi1*, *rrp6*, and *pab2*Δ experiments; these genes are almost entirely early meiotic or mid-meiotic genes and include *mei4*, the mid-meiotic

transcription factor. Thus Mmi1 is involving in priming gene expression of the mid meiotic genes by regulating their major transcription factor. The 19 genes that are responsive to Mmi1, but not in the "Mmi1 regulon" include several nitrogen starvation, late meiotic and non-meiotic genes, but most of these genes do not respond to Mmi1 as strongly as the early meiotic genes. An interesting member of this group is *pho1*, an acid phosphatase, which does accumulate strongly in *mmi1* mutants, but has no obvious relationship to meiosis.

Previously we showed that *crs1*, one of the Mmi1 regulated genes, is transcribed in vegetative cells as highly as in meiotic cells, but the transcript accumulates only during meiosis due to Mmi1-dependent decay in vegetative cells (McPheeters et al., 2009). To see if the other Mmi1 target genes were regulated in a similar fashion, we used three approaches. First, we looked for positive evidence that these genes are transcriptionally activated in early meiosis. This would suggest that their transcription is relatively low in vegetative cells in contrast to the case of *crs1*. The only transcription factor clearly documented to be specifically important for early meiotic genes is Rep1, and we found that induction of the Mmi1 regulated early meiotic genes during meiosis was independent of Rep1 (Figure 2.2). This finding is consistent with the model that Mmi1 target genes are constitutively transcribed. Second, we analyzed the amount of RNA polymerase II associated with Mmi1 target genes using ChIP-on-chip data from vegetative cells (Wilhelm et al., 2008). Many of the Rep1 independent genes, show strong RNA pol II ChIP signals along the open reading frame during vegetative growth, indicating robust transcription, despite a virtual absence of steady-state mRNA (an example of one Mmi1 regulated gene, *rec8*, is shown in Figure 2.3). Finally, we considered the data from our expression microarrays in which the Mmi1 regulated early meiotic genes accumulate during vegetative growth in *mmi1*, *rrp6* (exonuclease) and *pab2Δ* (polyA binding protein) mutant strains (Figure 2.1). Because both Rrp6 and Pab2 presumably regulate RNA stability (see below) rather than transcription, we conclude that the genes of the Mmi1 regulon are constitutively transcribed during vegetative growth, a condition that expression of meiotic genes often causes slow growth or even cell death.

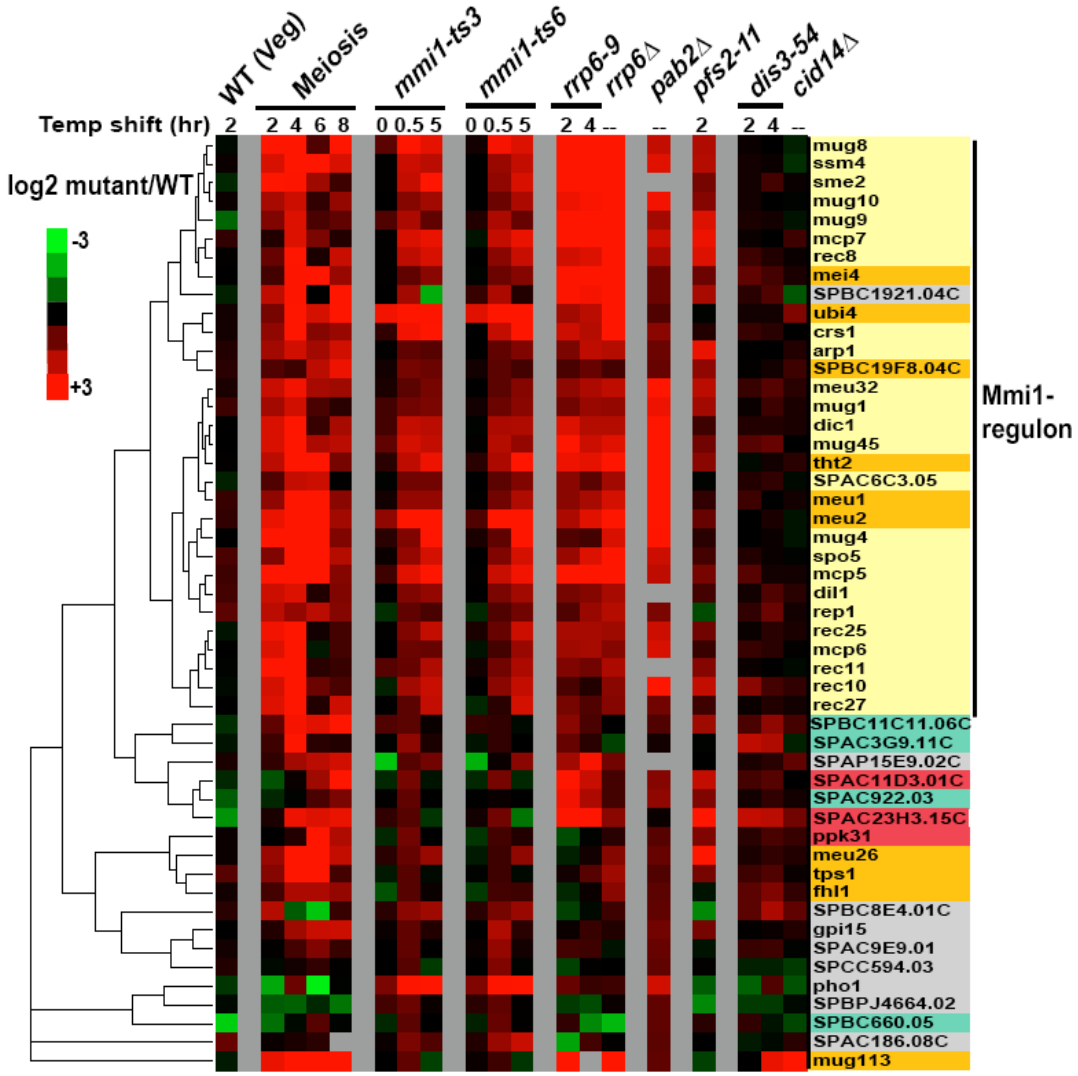

Figure 2.1 Behavior of Mmi1 responsive genes during meiosis and in RNA processing mutants. Hierarchical clustering of the top 50 genes that accumulate in the *mmi1-ts3* mutant is shown for microarray analyses of meiosis as well as *mmi1, rrp6, dis3, pfs2, pab2* and *cid14* mutants. Synchronized meiosis was induced in diploid strain F277, other strains were grown vegetatively and conditional mutants were shifted to respective temperature (see materials and methods for details). Colors represent transcript levels as log2 ratio (mutant/wild-type), such that red is higher in mutant and green is lower in mutant. The cluster of genes enriched for strongest accumulation in *mmi1-ts3*, *mmi1-ts6*, *rrp6-9* and *pab2Δ* is designated the "Mmi1 regulon". Genes names are color coded; yellow=early meiotic, orange=mid meiotic, red=late meiotic, green=nitrogen starvation and grey=non-meiotic.

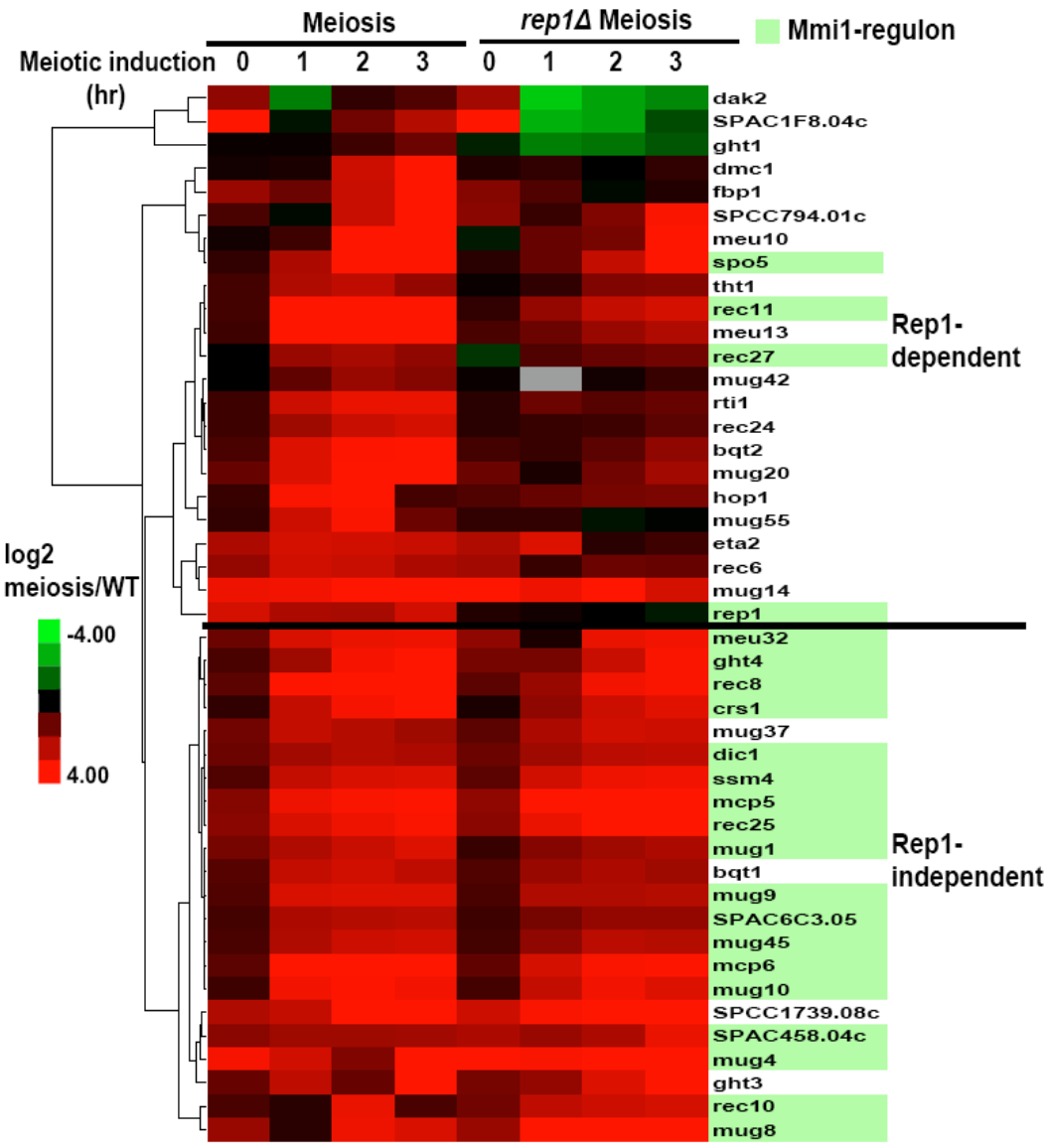

Figure 2.2 Most of the Mmi1 regulated genes are independent of the early meiotic transcription factor Rep1. 45 early meiotic genes that appear to be meiosis-specific based on low vegetative expression levels were analyzed by hierarchical clustering of published microarray data for meiosis and meiosis lacking *rep1*. Genes that belong to Mmi1 regulon were labeled in light green. Colors represent transcript levels as log2 ratio (meiosis/vegetative), such that red is higher in meiosis and green is lower in meiosis. Microarray data required from (Mata et al., 2007).

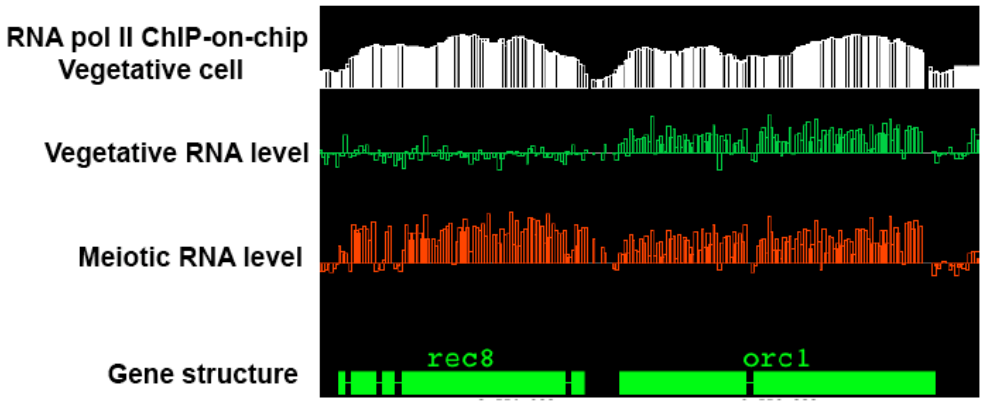

Figure 2.3 Evidence that *rec8* is transcribed in vegetative cells. RNA pol II chromatin IP efficiency across *rec8* and the adjacent gene *orc1* is shown (white bar) together with data on transcript levels in vegetative cell (green bar) and meiotic cell (red bar). Affymetrix tiling array data is shown using the Integrated Genome Brower software (Affymetrix). The signal intensity of probes are represented by bars, and the taller the bar the higher the intensity. RNA pol II CHIP-on-chip data required from (Wilhelm et al., 2008).

Mmi1 keeps its target genes off in vegetative cells by somehow targeting them for degradation through Rrp6, a nuclear 3' to 5' exosomal exonuclease (Yamanaka et al., 2010). Not all mutants affecting the exosome affected the Mmi1 targets. In budding yeast, the processivity of Rrp6 is assisted by the TRAMP complex (Trf4/Air2/Mtr4) (Callahan and Butler, 2010; LaCava et al., 2005; Vanacova et al., 2005). In this complex, Trf4 is a non-canonical polyA polymerase that adds oligoA tail to the 3' ends of RNAs. This oligoA tail is thought to provide a non-structured single strand 3' end for easy access to the Rrp6 exonuclease. The subunits of the TRAMP complex also exist in *S. pombe*, in which Cid14 is functionally homologous to Trf4 (Win et al., 2006). However, a *cid14Δ* mutant did not affect the Mmi1 targets, so this particular role of Rrp6 is independent of the TRAMP complex.

Like *rrp6*, *dis3* encodes a 3' to 5' exonuclease associated with the exosome, and, like *rrp6*, a *dis3* mutant was previously reported to stabilize *crs1*, a member of the Mmi1 regulon. However, in the more global microarray experiments here, it is apparent that Dis3 does not affect the same set of genes as Mmi1 or Rrp6, and the level of *crs1* accumulation in the *dis3* mutant is much less than in the *rrp6* mutant (Figure 2.1). It

seems that even though the exosome has two exonucleases associated with it, the Mmi1 pathway uses mainly or only Rrp6. The fact that Rrp6 plays a role in the nuclear surveillance pathway to degrade aberrantly polyadenylated RNA species in budding yeast (Davis and Ares, 2006; Kadaba et al., 2006; Milligan et al., 2005; Wyers et al., 2005) prompted us to include the nuclear polyA binding protein, Pab2 (St-Andre et al., 2010), in our study. Many Mmi1 targets also accumulate in *pab2*Δ mutants, suggesting that Pab2 may work together with Rrp6 in the decay pathway for these genes.

Another factor influencing Mmi1 targets is Pfs2, a scaffolding component of the 3' cleavage and polyadenylation complex. Because 3' cleavage is defective in the *pfs2-11* mutant, the resulting transcripts are long read-through transcripts lacking polyA tails. Such transcripts are generally unstable. However, many Mmi1 targets accumulate in the *pfs2-11* mutant, indicating that what normally happens at the 3' end in the presence of Mmi1 makes these transcripts even more unstable than without 3' processing.

In summary, we find that Mmi1 primarily regulates early meiotic genes, keeping them off in vegetative cells due to rapid RNA turnover. Additional factors involved in this regulation appear to be Rrp6, Pab2 and Pfs2, but not Dis3 or Cid14 (representing the TRAMP complex).

2.2 Mmi1 affects splicing and polyadenylation

RNA processing steps, such as splicing and polyadenylation, determine RNA stability. Previously, we identified a number of early meiotic genes that were spliced in early meiosis, but not in vegetative cells (Averbeck et al., 2005). To know if splicing is a major factor in regulating RNA stability and if Mmi1 is involved in splicing regulation, we chose four genes with meiosis-specific splicing for further study. Figure 2.4 (lane 1 and 3) shows that splicing of these four genes was repressed in vegetative cells (unspliced) and this repression was removed during meiosis (spliced). For *rec8* and *crs1*, genes identified as Mmi1 targets above, splicing inhibition was fully removed when *mmi1* was inactivated (Figure 2.4, lane 4). For *mek1* and *meu1*3, genes for which RNA does not accumulate in the *mmi1* mutant, *mek1* was slightly spliced and *meu13* was mostly spliced in the *mmi1* mutant. This suggests that Mmi1 inhibits splicing, yet splicing inhibition does not strongly correlate with RNA instability or RNA level.

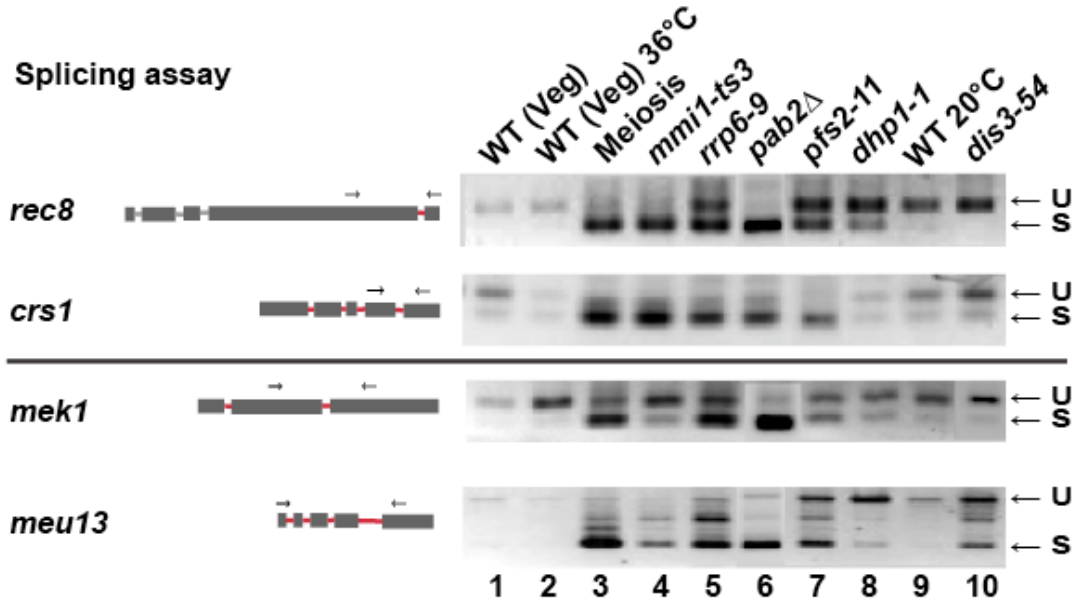

Figure 2.4 Mmi1 inhibits splicing of early meiotic genes. Left: Exon/intron structure of the early meiotic genes *rec8, crs1, mek1*, and *meu13* (drawn to scale). Regulated introns are red and constitutively spliced introns are grey; small arrows show locations of primers used for splicing assays. Right: RT-PCR based splicing assays for transcripts of wild type vegetative (F31), meiotic (F277) and mutant cells. For strain growing conditions, please see Materials and Methods. Arrows show unspliced (U) and spliced (S) products.

rec8 is different from the other three genes in that only the 3' most intron (4th intron) of *rec8* shows meiosis-specific splicing, while the three 5' proximal introns are spliced at all time (Figure 2.5). Given that *rec8* is one of the genes that accumulate the most in the *mmi1* mutant, we tested if splicing of the 3' most intron determines RNA stability. Three versions of *rec8* were constructed; namely normal *rec8*, 4th intron deleted *rec8* (int4Δ, spliced) and branch point mutated *rec8* (BPmut, unable to be spliced), and measured the RNA level of each construct by Q-PCR. In WT vegetative cells the RNA level from the three forms of *rec8* was nearly the same (Figure 2.6), indicating that splicing inhibition of *rec8* is not the major cause of RNA instability in vegetative cell.

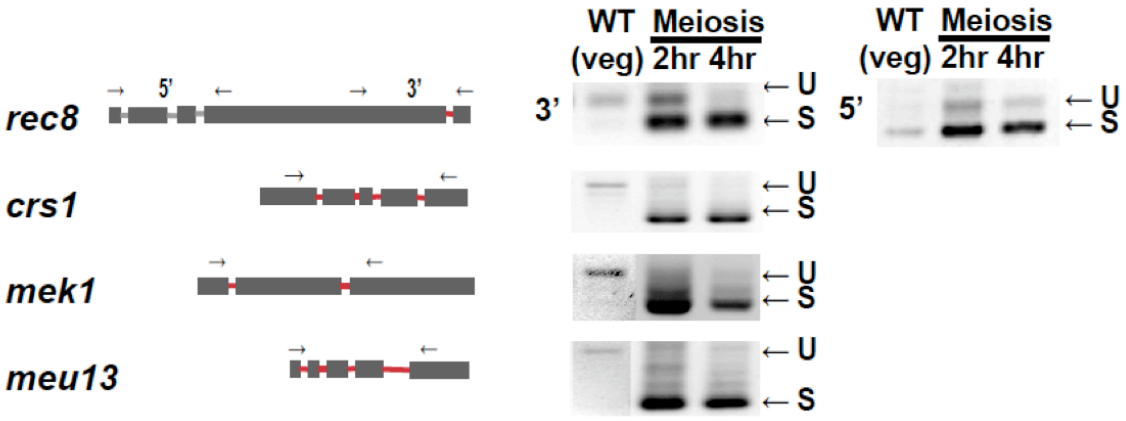

Figure 2.5 *rec8* is different from other genes in that only the 3' most intron is regulated. Left: Exon/intron structure of the four genes. Note that the primer locations are different from the those in Figure 2.4. Right: RT-PCR based splicing assays for transcripts of wild-type vegetative cells and meiotic cells (2hr and 4hr after meiotic induction). Arrows indicate unspliced (U) and spliced (S) products. This figure shows the meiosis-specific splicing pattern of these four genes. All the introns in *mek1, meu13, and crs1* appear to be coordinately regulated. That is, in vegetative cells both introns in *mek1*, all five introns in *meu13*, and all four introns *in crs1* are retained, and then when cells enter meiosis all the introns are efficiently spliced. *rec8* is distinct in that only the 3' most intron is regulated while three introns near the 5' end are spliced both in meiotic and in vegetative cells.

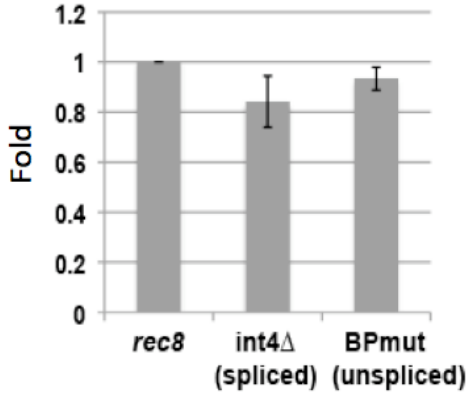

Figure 2.6 Splicing status does not influence *rec8* mRNA stability. Three forms of plasmid bound *rec8* were tested: WT *rec8*, 4th intron deleted *rec8* (int4Δ, spliced) and branch point mutated *rec8* (BPmut, unable to be spliced). Two independent transformants for each plasmid were analyzed with duplicate Q-PCR reactions. Results depicted as mean ± STD.

Polyadenylation status of *rec8, crs1, mek1* and *meu13* was determined by RACE-PAT (rapid amplification of cDNA end-polyadenylation assay) (Salles and Strickland, 1999). For all four genes, polyadenylation assays showed little if any polyadenylated transcript in vegetative cells and then the appearance of polyadenylation during meiosis (Figure 2.7), the time when the transcripts become spliced and accumulate. These data suggest two possibilities. First, polyadenylation is inhibited for these transcripts in vegetative cells, and without polyadenylation these transcripts are highly unstable. Or, alternatively, these transcripts are polyadenylated in vegetative cells, but then degraded so rapidly that they are not detected. It is interesting to note that for all four genes we observed two major forms, which ended at one of the two PolyAdenylation Sites (Figure 2.7, PAS1 and PAS2). We currently do not know if the existence of multiple polyA sites for a gene is a special feature for meiotic genes or is a common feature.

For *rec8* and *crs1* (Mmi1 regulon), the polyadenylated transcripts appear in the *mmi1* and *rrp6* mutants; while for *mek1* and *meu13* (not Mmi1 regulon), the polyadenylated transcripts appear only in the *rrp6* mutant, but not in the *mmi1* mutant (Figure 2.7, lane 4 and 5). The presence of polyadenylated transcripts in vegetatively grown *rrp6* mutant strongly supports the second possibility that polyadenylated transcripts are made in vegetative cells, but are removed rapidly by Rrp6. Mmi1 affects polyadenylation only for the genes that belong to the Mmi1 regulon. We expect that other factor(s) may affect polyadenylation of *mek1* and *meu13*. How Mmi1 influences polyadenylation and how Mmi1 targets polyadenylated transcripts for Rrp6 degradation are the questions we next tried to answer.

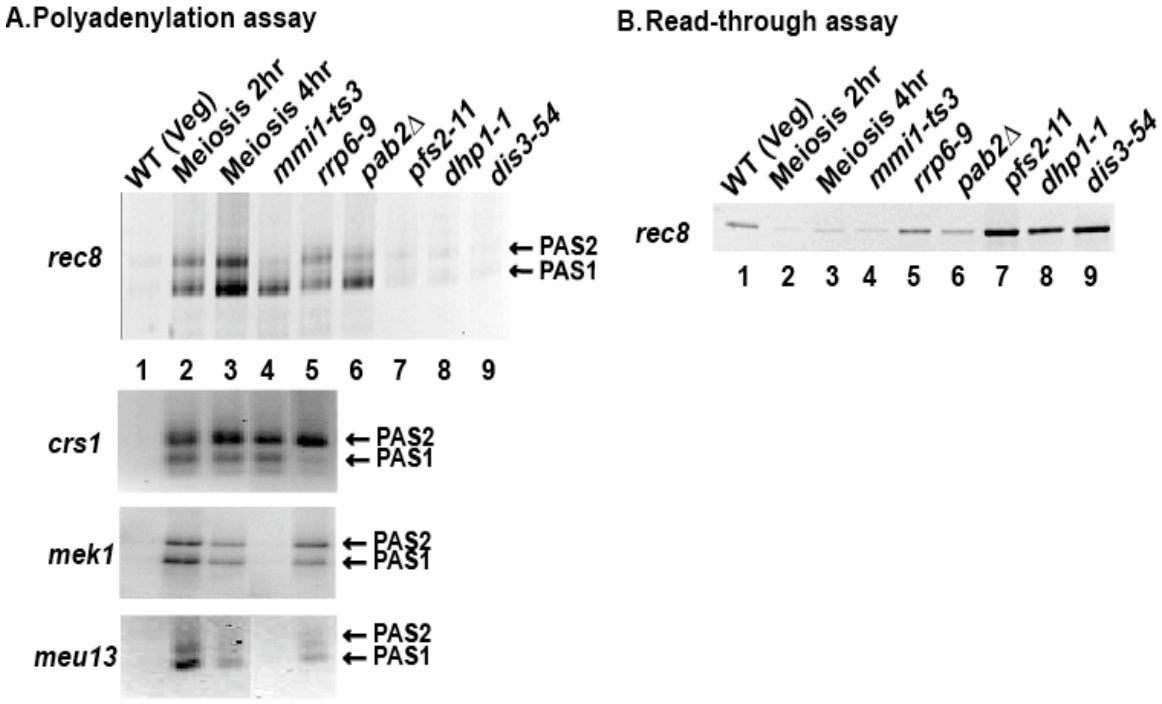

Figure 2.7 Mmi1 regulates polyadenylation. (A) Polyadenylation assay of early meiotic genes. Polyadenylation assay to determine "cleavage/polyadenylation sites" of "polyadenylated transcripts" of early meiotic genes from vegetative, meiotic and mutant cells. Two major polyadenylation sites for each gene are indicated (PAS1, PAS2). Every band was cloned and confirmed by sequencing to be polyadenylated at the indicated cleavage site. (B) Read-through assay of *rec8*. RT-PCR with primers across the two polyadenylation sites. Only read-through transcript would provide template for this PCR reaction.

2.3 Mutants that generate an *mmi1*-like phenotype

To further understand the mechanism of Mmi1 action, we examined a panel of other mutants that affect mRNA splicing, 3' end processing, transcription termination and mRNA turnover (Figure 2.8). Mutant cells were grown vegetatively, shifted to restrictive conditions for the given mutant, and then analyzed for splicing pattern, looking especially for mutants that mimic the *mmi1*$^-$ phenotype of splicing of meiotic genes in vegetative cells. Figure 2.4 shows that both *rec8* and *crs1* became fully spliced in the *mmi1-ts3* mutant; similarly, both genes became spliced to some degree in *rrp6-9*, *pfs2-11* and

dhp1-1 (subunits of 3' cleavage and polyadenylation complex), or *pab2Δ* mutants. The other two genes examined, *meu13* and *mek1*, which are not in the Mmi1 regulon, showed a different spectrum of responses to the various mutations, suggesting the splicing regulation of *mek1* and *meu13* may be distinct from that of *rec8, crs1* and other Mmi1-responsive genes.

Having found that mutations of *mmi1, rrp6, pab2, pfs2* and *dhp1* could generate "meiosis-specific" splicing of Mmi1 regulon genes in vegetative cells, we analyzed molecular details of their effects on *rec8.* To compare the effects of the two exonucleases, *rrp6* and *dis3*, we also analyzed *dis3*. In addition to assaying splicing in vegetative cells, we examined the generation of polyadenylated transcripts at the PAS1 and PAS2 polyadenylation sites, and also looked for read-through transcripts (i.e., transcripts not cleaved at the polyadenylation sites). The results (Figure 2.7) show that these six mutants fall into two classes. First, the *mmi1-ts3, rrp6-9*, and *pab2Δ* mutants generate vegetative transcripts that are cleaved and polyadenylated at PAS1 and PAS2, like the transcripts seen in meiosis. These mutants appear to stabilize *rec8* transcripts in vegetative cells, and also allow splicing (though the splicing is not due to the stabilization, see below). Second, and in contrast, *pfs2-11, dhp1-1* and *dis3-54* do not generate such polyadenylated PAS1 or PAS2 transcripts, but instead accumulate read-through transcripts (Figure 2.7 A and B, lane 7 to 9); these are not like the transcripts seen in meiosis. Consistent with other report

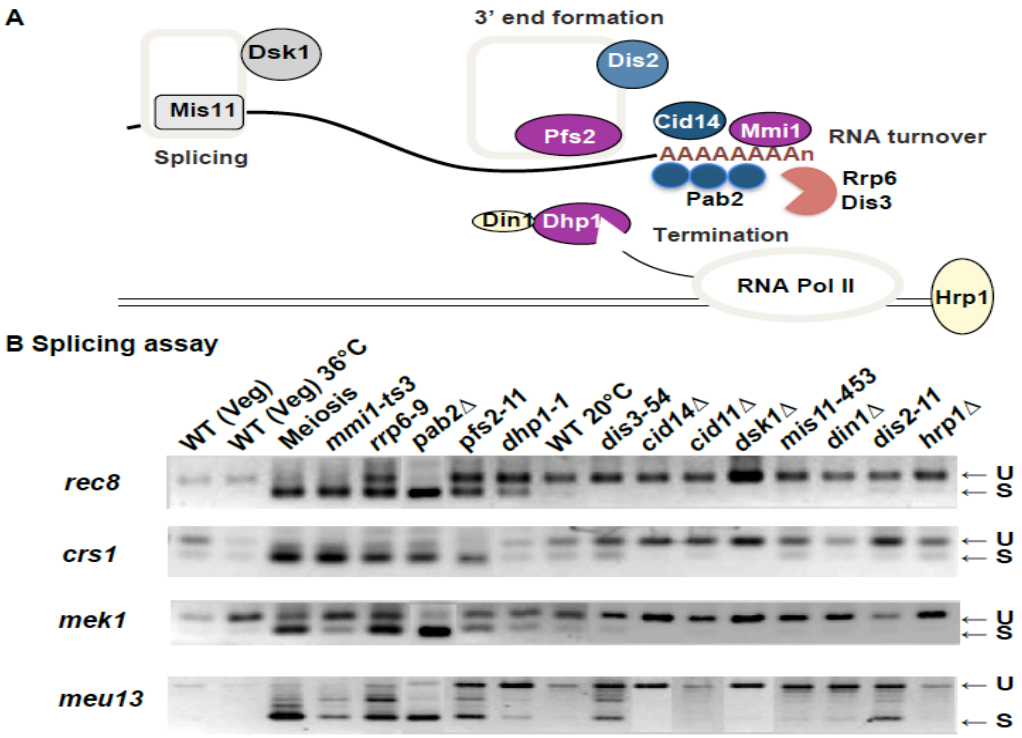

Figure 2.8 Identification of mRNA processing factors involved in early meiotic gene regulation. (A) Cartoon of factors for which mutant alleles were tested. Related functions are color coded, grey=splicing, purple/blue = 3' cleavage/adenylation, orange=exosome, yellow = transcriptional termination. For factor function and homologs, please see Table 2.3 (p.63). (B) Splicing assays by RT-PCR for transcripts from wild-type vegetative, meiotic and mutant strains. RNA was analyzed by RT-PCR for splicing of the 4th intron of *rec8*, *crs1*, and *mek1* or all introns of *meu13*; arrows show unspliced (U) and spliced (S) products. Results for *rec8* and *crs1* were discussed in the main text. *meu13* and *mek1*, which did not appear strongly Mmi1-responsive in our microarray analysis, showed a different spectrum of responses to the various mutations comparing to *rec8* and *crs1*. *mek1* in particular is only weakly responsive to Mmi1 inactivation and *meu13* accumulates spliced products in two additional mutants, *dis3* (the other 3'-5' riboexonuclease of the exosome) and *dis2* (a phosphatase involved in 3' end processing), suggesting the splicing regulation of *mek1* and *meu13* may be distinct from that of *rec8, crs1* and other Mmi1-responsive genes.

(Kim et al., 2004; Wang et al., 2005), *pfs2-11* and *dhp1-1* are defective in cleavage and polyadenylation, and instead yield longer, read-through transcripts.

The mechanism by which read-through transcription allows a degree of splicing is unclear. One possibility is that the read-through transcripts, though unstable in absolute terms, may nevertheless be more stable than the very highly unstable, Rrp6-degraded transcripts. In this model, the (relative) stability of the read-through transcripts might simply allow extra time for splicing. However, other data (see below) suggest that this is not the whole story. Given that Mmi1 is an RNA binding protein, we propose a second model, according to which the (relatively) stable read-through transcripts (presumably including all Mmi1 regulon genes) in the *pfs2-11* mutant provide a sink for Mmi1, titrating it out, leading to a partial *mmi1*$^{-}$ phenotype. In this model, the splicing of *rec8* (and other intron containing genes of the Mmi1 regulon) in *pfs2-11* mutant is a reflection of an inadequate supply of Mmi1. Supporting the second model, shifting the *pfs2-11* mutant to non-permissive temperature for longer periods (to accumulate more Mmi1 target transcripts that may titrate out Mmi1) allows increasing amounts of spliced *rec8* to appear (Figure 2.9 A, top panel). More importantly, over expression of Mmi1 suppresses the partial splicing of *rec8* transcripts in the *pfs2-11* mutant strain (Figure 2.9 A, bottom panel). Similarly, splicing repression was restored to *rec8* in the *pab2Δ* mutant when Mmi1 was over-expressed (Figure 2.9 B). Based on the polyadenylation and read-through assay results, we think that Rrp6 and Pab2 are likely to be in the Mmi1 pathway, but that Pfs2, Dhp1 and Dis3 are not, and instead work indirectly by allowing accumulation of read-through transcripts, resulting in partial titration of Mmi1 molecules. Since Mmi1 may physically interact with the 3' cleavage and polyadenylation complex, and since the *pfs2* mutant disrupts this complex, some *pfs2* phenotypes could also be due to an altered interaction between Mmi1 and the cleavage and polyadenylation complex (see Discussion).

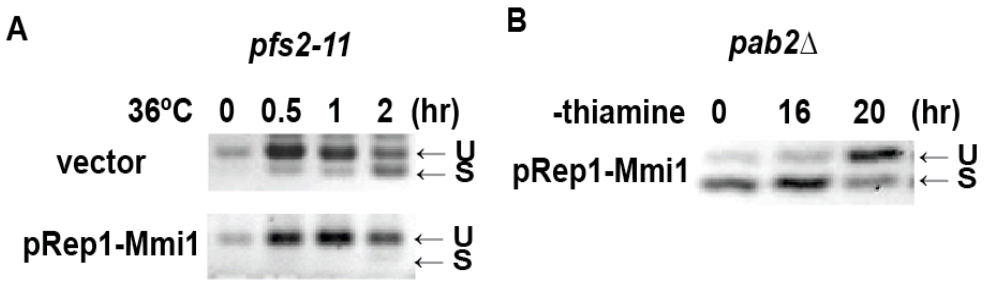

Figure 2.9 Titration of Mmi1 in *pfs2-11* and *pab2Δ* strains allows partial splicing of *rec8*. The 4th intron of *rec8* was analyzed by RT-PCR splicing assay. (A) Over expression of Mmi1 restored splicing repression to *rec8* transcripts in the *pfs2-11* strain. *pfs2-11* mutant strain was transformed with pRep1- empty vector or pRep1-Mmi1 vector. Mmi1 was induced in minus thiamine medium for 24hr and then cells were shifted to 36°C to inactivate Pfs2 function for indicated time. Top: *rec8* became partial spliced in the *pfs2-11* mutant strain, and more spliced mRNA appear in the later time points. Bottom: over expression of Mmi1 restored the splicing repression in *pfs2-11* strain. (B) Over expression of Mmi1 restored splicing repression to *rec8* transcripts in the *pab2Δ* strain. *Pab2Δ* strain was transformed with pRep1-Mmi1 and grown at 30°C in EMM-UAH plus thiamine (5ug/ml). Cells were washed and resuspended in EMM-UAH lacking thiamine to induce Mmi1 and cells were harvested at 0, 16, or 20 hours after the medium change.

As noted above, Rrp6 and Dis3 are both 3' to 5' exonucleases associated with the exosome, but the splicing assays (Figure 2.4, lane 5 and 10) and the polyadenylation and read-through assays (Figure 2.7 A and B, lane 5 and 9) suggest that their roles are rather different: the *rrp6* mutant preferentially stabilizes polyadenylated transcripts ending at the normal polyadenylation sites (Figure 2.7 A, lane 5), and allows splicing of both *rec8* and *crs1*, whereas the *dis3* mutant preferentially stabilizes read-through transcripts (Figure 2.7 B , lane 9), and has only a small effect on splicing of genes in the Mmi1 regulon. This finding of different substrates specificities for Rrp6 and Dis3 agrees with other recent results (Kiss and Andrulis, 2010; Lebreton and Seraphin, 2008). Detection of both processed (polyadenylated and spliced) and unprocessed (read-through and unspliced) forms in vegetatively grown exonuclease mutants suggests that both forms naturally occur in vegetative cells.

Another gene with splicing and polyadenylation phenotypes resembling *mmi1* is *pab2*, the homolog of mammalian nuclear polyA binding protein PABPN1. In

mammalian cells PABPN1 is involved in stimulating polyadenylation (Kerwitz et al., 2003) and controlling polyA tail length (Wahle, 1995). In *S. pombe*, deletion of *pab2* results in slow growth; yet the expression level of the majority of mRNAs does not change (Lemay et al., 2010). Significantly, many genes that do accumulate in *pab2Δ* strains are also genes of the Mmi1 regulon (St-Andre et al., 2010). These results indicate that Pab2 plays a vital role in the Mmi1-mediated mRNA decay pathway.

2.4 Mmi1 promotes hyperadenylation on Mmi1 target genes

Our polyadenylation assay does not reflect the length of polyadenylation; rather during the PCR reaction most PCR products collapse to the minimum length that reflects the "cleavage/polyadenylation site" of "polyadenylated transcripts". Therefore, to examine the polyA tail of *rec8* by an alternative approach, we used Northern analysis to measure the lengths in the WT*, mmi1-ts3, rrp6-9* and *pab2Δ* mutants. Strikingly, the *rec8* transcripts in the *rrp6-9* mutants, but not the other mutants assayed, were found in a high molecular weight smear, one or perhaps even two kilobases longer than the *rec8* transcript in meiotic cells (Figure 2.10).

To test if this extra length is due to polyadenylation, we incubated transcripts with RNase H and oligo d(T), which would destroy any polyA tail. As shown in Figure 4A this RNase H/oligo d(T) treatment had little effect on *rec8* transcripts from meiotic and *mmi1-ts3* mutant cells, but shortened the long transcripts from *rrp6-9* mutants back to the same length as the transcripts in the *mmi1-ts3* and meiosis. This shows that the high-molecular weight *rec8* transcripts in the *rrp6-9* mutant have extremely long polyA tails. (Similar results were recently obtained by Yamanaka et al. 2010).

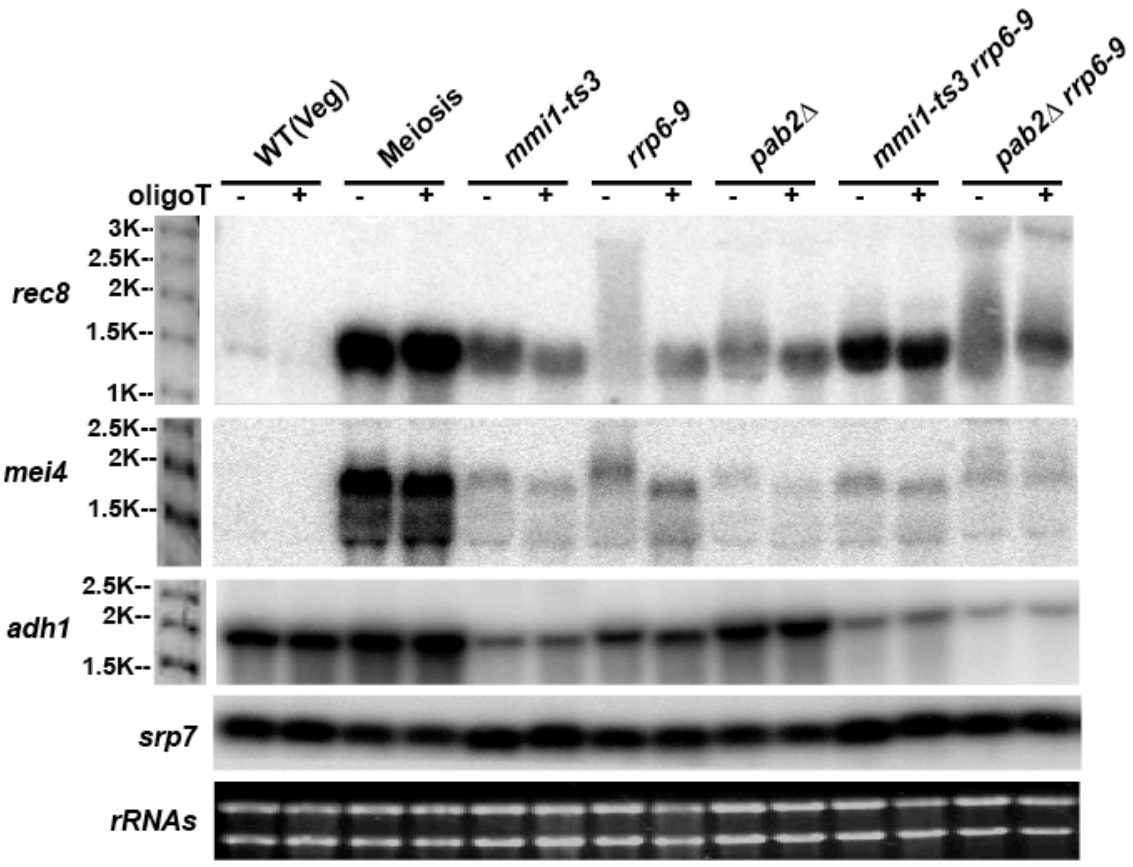

Figure 2.10 Mmi1 induces hyperadenylation on target mRNAs, *rec8* and *mei4*. Total RNA was isolated from wild-type vegetative, meiotic and mutant cells. RNA was treated with RNase H in the presence (+) or absence (-) of oligo d(T) and then analyzed by strand specific Northern blot. *rec8* and *mei4*, genes that accumulated in both *mmi1-ts3 and rrp6-9* mutants, shown hyperadenylation phenotype in *rrp6-9* mutant. Control gene *adh1* was not hyperadenylated in *rrp6-9* mutant. *Srp7* Northern blot and rRNAs ethidium bromide staining) are shown below each blot, indicating equal amount of loading and the RNA integrity.

To see if the long polyA tails are a general feature of the *rrp6-9* mutant, or, on the other hand, if they are connected to Mmi1, we looked at several other genes that either are or are not members of the Mmi1 regulon. *rec8, mei4* (Figure 2.10) and *ssm4* (data not shown), genes that do respond to Mmi1, did have a long polyA tail in the *rrp6-9* mutant. *adh1* (Figure 2.10) and *LEU2* (Figure 2.14 B, *LEU2* is from budding yeast), genes that do not respond to Mmi1, did not have long polyA tails in the *rrp6-9* mutant. We asked if the

long polyA tail depends on Mmi1. Strikingly, in *mmi1-ts3 rrp6-9* double mutants, the long polyA tail was absent, showing that indeed, Mmi1 activity is needed to create the hyper-long polyA tails, while Rrp6 activity is needed to degrade these hyperadenylated molecules.

Since the *pab2Δ* mutant phenocopies the *mmi1* mutant, we wished to know how Pab2 is involved in Mmi1-mediated decay. Deletion of *pab2* in *S. pombe* causes hyperadenylation of total RNA, but this hyperadenylation is only ~200nt longer than normal (Perreault et al., 2007). Many of these short hyperadenylated RNA species are snoRNAs and snRNAs, while polyadenylation of the two tested mRNAs (*adh1* and *pyk1*) remained normal (Lemay et al., 2010). However, gene-specific regulation by Pab2 may exist, in which polyadenylation of selected mRNAs is affected. Figure 2.10 shows that *rec8* transcripts had some hyper-polyadenylation in the *pab2Δ* strain, though not nearly as much as in the *rrp6-9* mutant. Because the slight hyperadenylation is seen on genes with the Mmi1 regulon, but not with control genes, Mmi1 may provide the gene-specificity to Pab2. Next, we asked if the Mmi1-dependent hyperadenylation depends on Pab2. The results show that in the *pab2Δ rrp6-9* double mutant, the *rec8* transcript was hyper-polyadenylated, but not to the same degree as in the *rrp6-9* single mutant. This observation is consistent with the idea that Pab2 is important, but not essential, for creating the hyperadenylated tails, and that it is transcripts with the longest tails that are targeted for degradation. It is also consistent with the idea that Pab2 is important for degrading the hyperadenylated messages. However, the *pab2Δ rrp6-9* double mutant has a severe growth defect even at the permissive temperature for *rrp6-9* (data not shown), so the reduced hyperadenylation compared to the *rrp6* mutant could be an indirect effect.

Not all genes in the Mmi1 regulon behave the same. An obvious difference is the hyperadenylation length of different Mmi1-targeted genes. *rec8*, a strongly Mmi1 responsive gene with the mapped DSR very close to the polyadenylation sites, has a >1 kilobase polyA tail in the *rrp6-9* mutant. *Mei4*, a weaker Mmi1 responsive gene with a ~500nt polyA tail in the *rrp6-9* mutant, has the mapped DSR far from the polyadenylation site. Another gene we tested, *ssm4*, has a 0.5-1 kilobase hyperadenylated tail and has its DSR mapped close to the stop codon (data not shown). At least for these three genes, the closer the Mmi1 binding site is to the polyadenylation site, the longer the

polyA tail gets, and the more responsive the gene is to Mmi1. Overall, these results are most consistent with the idea that Mmi1 promotes hyperadenylation in a pathway involving Pab2, and that the hyperadenylated transcripts are degraded by Rrp6.

2.5 Hyperadenylation is not limited to the Mmi1 regulon

From microarray experiments, there were around 280 genes that accumulated more than 2 fold in the *rrp6-9* mutant, but were not members of the Mmi1-regulon (Figure 2.12). We wondered if hyperadenylation is a common feature of Rrp6 substrates, or is a feature that only occurs on Mmi1 target genes. To this end, we used Northern blot analysis on four genes that accumulated in the *rrp6-9* mutant in the microarray experiment, but were unchanged in the *mmi1-ts3* mutant. These four genes were: TFIIB, the general transcription factor; SPCC1442.04c, a gene with unknown function; *Ish1* and SPCC757.03c, two stress responsive genes. Figure 2.11 shows that two out of the four, THIIB and SPCC1442.04c, had a hyperadenylation phenotype in the *rrp6-9* mutant. Moreover, this hyperadenylation persisted in the *mmi1-ts3 rrp6-9* double mutant, indicating that Mmi1 is irrelevant to this hyperadenylation. The other two genes, *Ish1* and SPCC757.03c, also accumulated in the *rrp6-9* mutants (confirming the microarray results), but were not hyperadenylated (data not shown). These data suggest that the link between hyperadenylation and RNA instability is not restricted to meiotic regulation, or even to Mmi1. Moreover, in addition to a hyperadenylation related mechanism, Rrp6 must use other mechanism(s) for regulating RNA stability in a gene-specific manner.

In summary, we found that many genes that are degraded by Rrp6 share the hyperadenylation phenotype in the *rrp6-9* mutant. This is consistent with the idea that hyperadenylation is targeting these genes for degradation by Rrp6. For the Mmi1 regulated genes, hyperadenylation depends on the activity of Mmi1, and Pab2 seems to assist hyperadenylation and degradation. What regulates and promotes hyperadenylation of the non-Mmi1 regulated genes remains an open question.

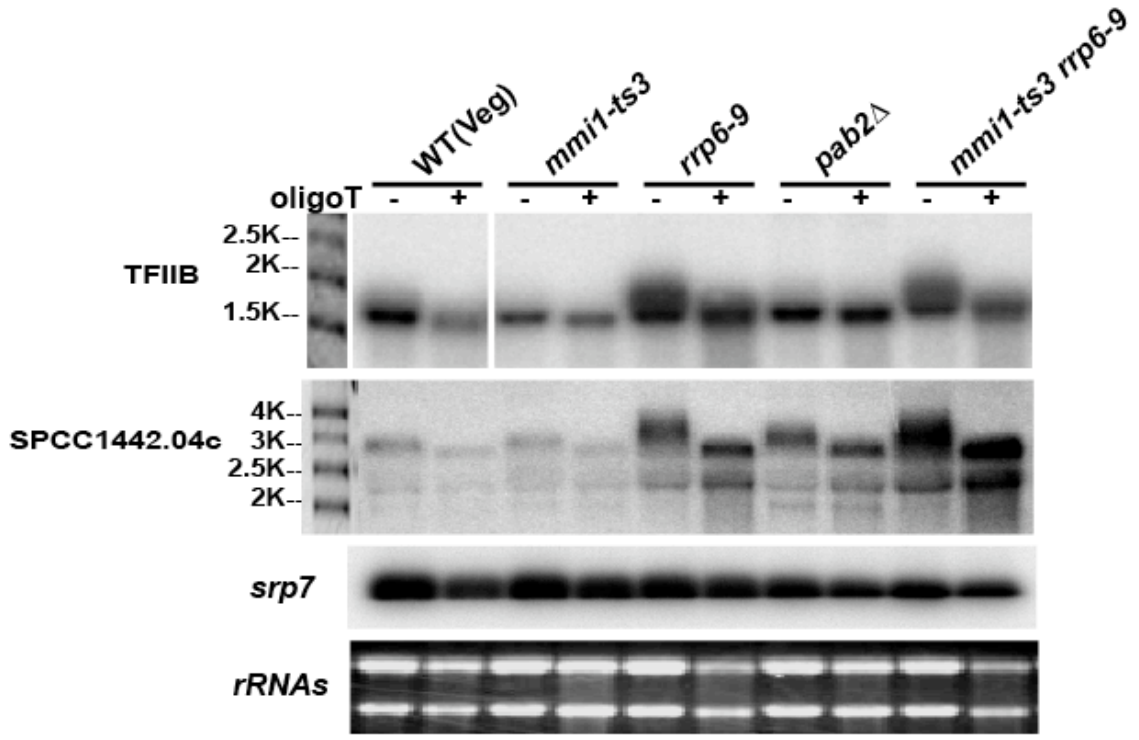

Figure 2.11 Hyperadenylation is not limited to Mmi1-regulated genes. Northern blot analysis of two genes that were not regulated by Mmi1, but were degraded by Rrp6. Hyperadenylation phenotype was observed in rrp6-9 strain, and Mmi1 was not required for this hyperadenylation.

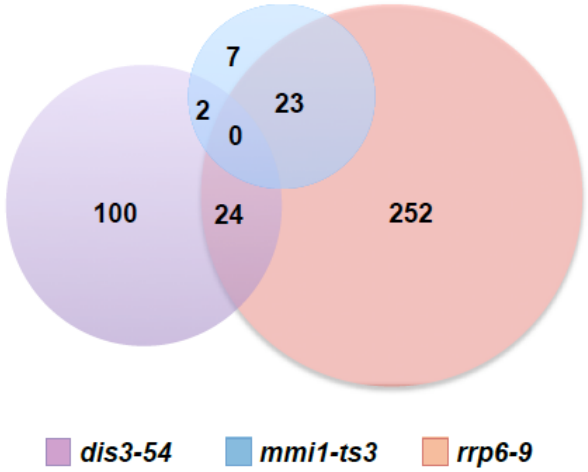

Figure 2.12 Distinct and shared substrates between *mmi1-ts3*, *dis3-54* and *rrp6-9* mutant strains. Genes that accumulated above 2 fold in *mmi1-ts3* (36°C, 0.5hr), *dis3-54* (20°C, 2hr) and *rrp6-9* (36°C, 1hr) were represented in the Venn diagram, which shows that (1) most (23 of 32 total) Mmi1 responsive genes also respond to Rrrp6. For the 7 genes that accumulated mainly in the *mmi1-ts3* mutant, 3 of them (including *pho1*) also slightly accumulated in the *rrp6-9* mutant and 4 of them did not accumulate in the *rrp6-9* mutant at all. None of the 7 genes are meiotic genes. (2) Rrp6 has many targets in addition to the Mmi1 regulated genes. (3) Dis3 and Rrp6 have many distinct substrates and (4) only 2 out of 32 Mmi1 targeted genes accumulated in the *dis3-54* mutant (*rec10* and SPAC3G9.11c).

2.6 Use of ribozyme constructs to dissect cause-and-effect relationships

As described above, 3' cleavage, polyadenylation, splicing and RNA stability are coordinately regulated in the WT cells for several Mmi1 regulated genes. It is unclear what the cause-and-effect relationships are. To separate events of 3' cleavage and polyadenylation from other events, we used a hammerhead ribozyme and a DNA encoded polyA sequence to generate 3' ends with polyA tails without using any of the machinery for 3' end processing. The hammerhead ribozyme catalyses the site-specific hydrolysis of a phosphodiester bond (Birikh et al., 1997), in this case leaving the encoded polyA tail at the end of the transcript. We constructed a series of vectors containing *rec8* followed by an encoded polyA tail (65 As) and a hammerhead ribozyme. The vectors differed in whether the ribozyme was active (*rec8*-A_{65}RZ vector), or, alternatively,

contained a point mutation that inactivated the self-cleavage activity (*rec8*-A_{65}RZmut vector) (Samarsky et al., 1999). The vectors also differed in whether the two usual polyadenylation sites (PAS1 and PAS2) were included 5' of the ribozyme or not (*rec8*-A_{65}RZ PAS or *rec8*-A_{65}RZ ΔPAS vector, respectively) (see Figure 2.13 A for vector diagrams).

To characterize the self-cleavage of the ribozyme in this system, *rec8*-A_{65}RZ and *rec8*-A_{65}RZmut constructs were transformed into the *pfs2-11* mutant strain, which gives mainly read-through transcription (i.e., PAS1 and PAS2 are inefficiently used in this mutant). We assayed for transcripts going beyond the ribozyme cleavage site, and found that such read-through transcripts were readily detected for the RZmut construct, but were completely undetectable for the cleavable RZ construct (Fig 2.13 B, top panel, comparing lane 1 and 2). This demonstrates that ribozyme cleavage is efficient in our system.

Notably, when we looked for this same read-through product with the inactive ribozyme in the WT, *mmi1-ts3*, and *rrp6-9* cells, the read-through product was seen in the WT and *rrp6-9* mutant, but not at all in the *mmi1-ts3* mutant (Figure 2.13 B, lanes 3 through 8), where instead all transcripts were cleaved at the normal PAS1 and PAS2 sites. This suggests that the Mmi1 protein may be inhibiting 3' cleavage to some extent, allowing a degree of read-through in *mmi1*$^{+}$ cells. In the *pfs2-11* mutant the read-through transcripts from *rec8*-A_{65}RZ seemed to be stabilized by the encoded polyA tail (Figure 2.14 A, lane 6, RZ end). This result shows that the encoded polyA tail with 65 A residues can provide stability for the transcript. Consistent with previous observations that Mmi1 causes inefficient 3' end cleavage (Figure 2.7 B, Figure 2.13 B), the "RZ end" band was detectable in the WT and *rrp6-9* mutant, but not in the *mmi1-ts3* mutant (Figure 2.14 A, lane 3 to 5).

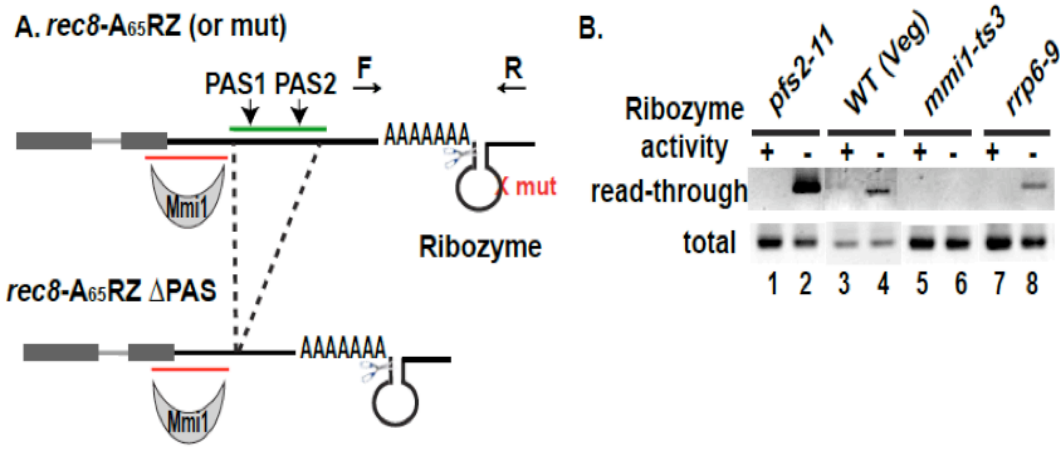

Figure 2.13 Use of *rec8*-polyA-ribozyme chimeras to test roles of 3' cleavage/adenylation in *rec8* regulation. (A) Illustration of *rec8*-A_{65}RZ and *rec8*-A_{65}RZ ΔPAS constructs showing 3' region starting at the 4th and 5th exons of *rec8* (boxes). Features shown include the mapped Mmi1 binding sequence (DSR) (red line), two polyadenylation sites (PAS1 and PAS2), the region directing cleavage and polyadenylation (green line), which is deleted in *rec8*-A_{65}RZ ΔPAS. For *rec8*-A_{65}RZ, sequence encoding 65 As (called A_{65}) is inserted after the normal PASs (-91nt away from PAS2). A_{65} is immediately followed by hammerhead ribozyme sequence (called RZ and shown as a stem loop). Scissors show the ribozyme self-cleave site. The construct for *rec8*-A_{65}RZmut, is identical to *rec8*-A_{65}RZ except for the point mutation that disrupts ribozyme self-cleavage activity (red cross). F and R arrows show primers used to detect read-through transcripts. (B) Read-through assay on *rec8*-A_{65}RZ (+) and *rec8*-A65RZmut (-) to assay RZ self-cleavage activity and *rec8* 3' end cleavage (at PAS1 and PAS2) efficiency in the respective strains. Top panel: read-through assay with primers across the ribozyme sequence. Bottom panel: total *rec8* measured by primers within the *rec8* ORF.

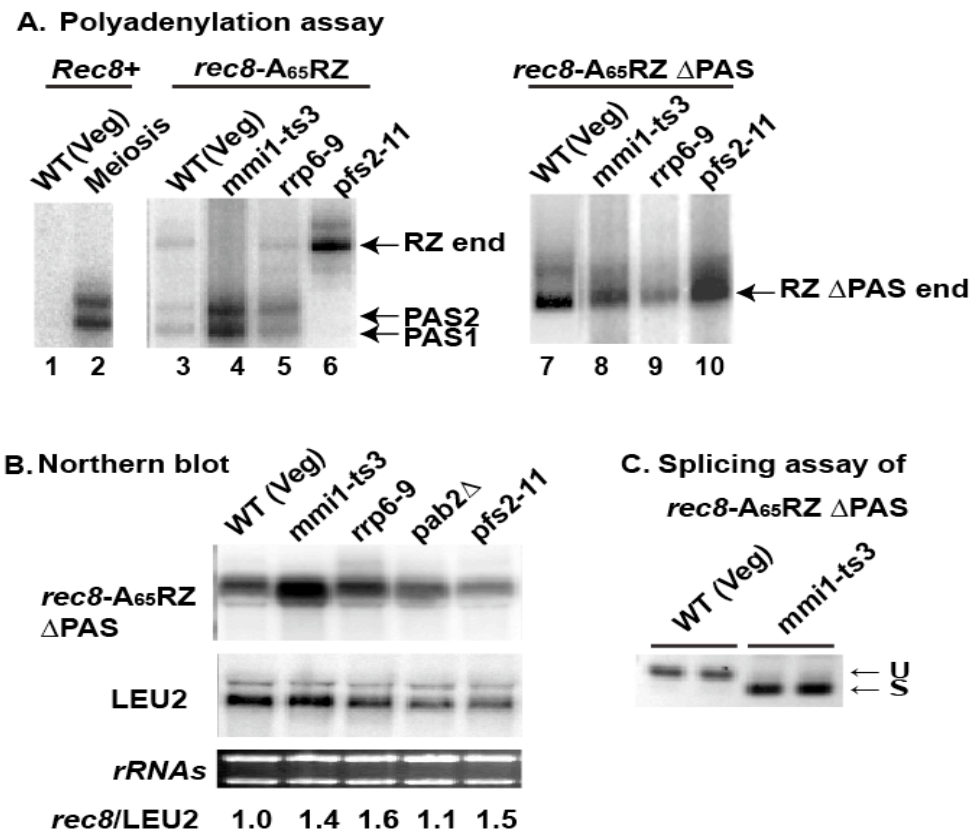

Figure 2.14 Mmi1 does not target *rec8* for degradation, when the 3' end of *rec8* is generated by the ribozyme. (A) Polyadenylation assay to determine the cleavage sites of polyadenylated transcripts. Left panel: assay on endogenous *rec8*$^{+}$ in vegetative and meiotic cells. Transcripts ending at the two major polyadenylation sites were marked as PAS1 and PAS2. Middle panel: assay on transcripts of *rec8*-A_{65}RZ in *rec8Δ* strains. Transcripts ending by ribozyme with 65 As is marked as RZ end. Right panel: assay on transcripts of *rec8*-A_{65}RZ ΔPAS in *rec8Δ* strains. Transcripts ending by ribozyme with 65 As is marked as RZ ΔPAS end. RZ end and RZ ΔPAS end bands were confirmed by sequencing. (B) Northern blot analysis of *rec8*-A_{65}RZ ΔPAS in *rec8Δ* strains. Upper panel: Level of *rec8* transcripts from *rec8*-A_{65}RZ ΔPAS. Middle panel: LEU2 was hybridized for a normalization control. Lower panel: rRNAs. The numbers shown were calculated for the ratio of *rec8*-A_{65}RZ ΔPAS/ LEU2 from the average of two experiments using two independent transformants. (C) Splicing assay on *rec8*-A_{65}RZ ΔPAS of *rec8Δ* WT and *rec8Δ mmi1-ts3* mutant strains. Results of two independent transformants are shown.

Most of the transcripts from *rec8*-A_{65}RZ construct still ended at endogenous PAS1 and PAS2, even in the presence of Mmi1, very similar to transcripts from endogenous *rec8*. This construct did not allow us to separate 3' processing from splicing and RNA stability. To increase the number of transcripts that have a polyA tail generated by the ribozyme, we used *rec8*-A_{65}RZ ΔPAS, in which the two PAS sequences have been deleted while leaving the mapped DSR intact (Figure 2.13 A). In the absence of the native PAS sequences, it is expected that transcription will continue through the ribozyme, and therefore most transcripts will end by ribozyme cleavage with the DNA-encoded polyA tail. Indeed, polyadenylation assays show that most or possibly all the transcripts from the *rec8*-A_{65}RZ ΔPAS construct were terminated by ribozyme self-cleavage, and ended with the encoded 65 A residues (Figure 2.14 A, right panel). These results indicate that the RZ ΔPAS end can be generated at high efficiency.

Most importantly, the transcript from the *rec8*-A_{65}RZ ΔPAS construct is about equally abundant in all strains (Figure 2.14 B), suggesting that the ribozyme-generated transcripts, which have intact Mmi1 binding sites, are stable even in the WT strain containing active Mmi1. Moreover, transcripts from *rec8*-A_{65}RZ ΔPAS in the *rrp6-9* strain were not hyperadenylated (Figure 5D). This strongly suggests that hyperadenylation occurs as part of, or as a consequence of, the normal process of 3' end formation. Ends generated in other ways, even though they contain seed polyA tails, do not become hyperadenylated.

Transcripts from *rec8*-A_{65}RZ ΔPAS in the WT vegetative cells were abundant and therefore presumably stable, but strikingly, remained almost entirely unspliced (Figure 5E, left). That is, the encoded polyA tail is apparently sufficient to stabilize the *rec8* transcript, but neither the polyA tail nor the stability allows splicing. The lack of splicing strongly suggests that Mmi1 is bound to these transcripts, especially since the same transcripts are efficiently spliced in the *mmi1-ts3* mutant (Figure 5E, right). This key result suggests that the lack of splicing of the 4th intron of *rec8* in the WT vegetative cells is not due to the lack of polyadenylation or RNA stability; more likely, it is due directly to Mmi1 binding. Furthermore, it suggests that simple binding of Mmi1 to a transcript is not sufficient for transcript degradation.

2.7 Mmi1 genetically interacts with Pfs2

Pfs2 is required for cleavage and polyadenylation. As we suspect Mmi1 interferes with cleavage and polyadenylation, the opposite function of Pfs2, these two genes could be mutually suppressive (i.e., synthetic rescue). We generated *mmi1-ts3 pfs2-11* double mutants and compared the growth rate to *pfs2-11* and *mmi1-ts3* single mutants over a range of temperatures from 28°C to 34°C. Notably, the double mutants were viable at 34°C, while the *pfs2-11* single mutant was dead (Figure 2.15 A). The DAPI-staining phenotype of the *mmi1-ts3* mutant at 34°C is similar to haploid meiosis, which shows abnormal nuclear segregation and many cells have 2 to 4 nuclei (Figure 2.15 B). At 34°C, *pfs2-11* rescues this multi-nuclei phenotype of the *mmi1-ts3* mutant (Figure 2.15 B). Moreover, over-expression of Mmi1 in the *pfs2-11* mutant strain causes a severe growth defect even at the permissive temperature (Figure 2.15 C). Notably, the morphology of Mmi1 over-expression in the *pfs2-11* mutant strain at 24°C is similar to the morphology of the *pfs2-11* mutant at 36°C, in that cells were elongated and chromosomes mis-segregated (Figure 2.15 D). Collectively, mutation of Mmi1 rescues the growth defect of the *pfs2-11* mutant and over-expression of Mmi1 kills the *pfs2-11* mutant. These results strengthen our model that Mmi1 interferes with the 3' end processing machinery.

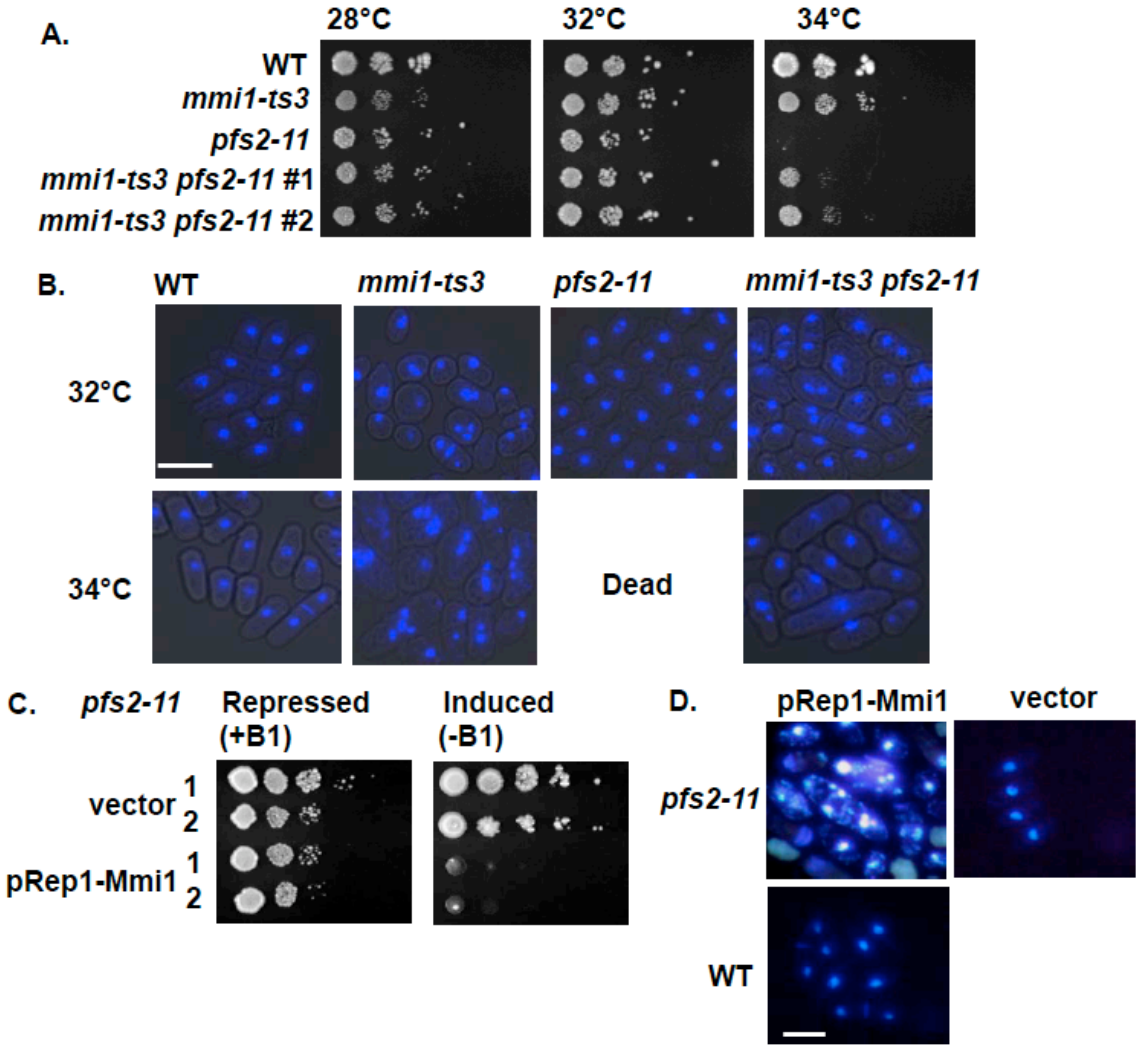

Figure 2.15 Genetic interactions between *mmi1* and *pfs2*. (A and B) Synthetic rescue relationship between *mmi1-ts3* and *pfs2-11* mutants. (A) *mmi1-ts3* rescues the temperature sensitive growth defect of *pfs2-11*. 10-fold serial dilutions of cells were plated on YES and incubated at 28°C, 32°C, or 34°C for 3 days. (B) *pfs2-11* rescues the defective nuclear division morphology of *mmi1-ts3*. Cells were grown to mid-log phase in YES, stained with DAPI, and photographed; scale bar = 10 microns. (C and D) Synthetic lethality of Mmi1 over expression in the *pfs2-11* mutant. Mmi1 was cloned into pREP1 vector under inducible *nmt1* promoter (no message in thiamine). Empty vector and pREP-Mmi1 vector were transformed into *pfs2-11* mutant strain. Cells were then spotted on plates with (repressed, no Mmi1 over-expression) or without (induced, Mmi1 over-expression) 5µg/ml thiamine and incubated at 32°C for 4 days. Two independent transformants are shown for each plasmid. (D) Over-expression of Mmi1 in the *pfs2-11* mutant causes cell elongation and nuclei mis-segregation. Cells were grown in EMM without thiamine for 36 hours at 24°C, stained with DAPI, and photographed.

III. Model and Discussion

Using expression microarrays, we defined a group of 31 genes, mostly important for early meiosis, that are regulated by the RNA-binding protein Mmi1. Most of these genes are transcribed in vegetative cells, but due to the action of Mmi1, these vegetative transcripts are unprocessed and, as a consequence, highly unstable. As cells enter meiosis, the Mmi1 protein is inactivated and the Mmi1-regulated transcripts become processed, stabilized, and expressed.

We and others (McPheeters et al., 2009; St-Andre et al., 2010; Yamanaka et al., 2010) have investigated the molecular mechanisms of RNA processing and degradation in the Mmi1 pathway. One issue in comparing these studies is that the detailed effects of Mmi1 vary from gene to gene, a point we will address further below. Here, we primarily discuss the effects of Mmi1 on the *rec8* transcript; when information is available, we attempt to highlight similarities with, and differences between, *rec8* and other transcripts.

A model of Mmi1 action at *rec8*

Our current model for Mmi1-regulated RNA processing and turnover is illustrated in Figure 2.15 using *rec8* as an example. Transcription of *rec8* is active in vegetative cells (Figure 2.15 A). When RNA pol II transcribes the DSR (i.e., the Mmi1 binding site), Mmi1 binds to this DSR (shown as a red box on the nascent transcript), prior to 3' end formation. Mmi1 then interferes with 3' end processing in two ways. First, Mmi1 interferes to some extent with cleavage at the endogenous polyadenylation sites, thus generating read-through transcripts (Figure 2.15B). These read-through transcripts are rapidly degraded by Dis3. Despite reduced 3' end cleavage, the majority of *rec8* transcripts are cleaved at PAS1 and PAS2. We suggest that the second and most important effect of Mmi1 is to promote hyperadenylation of these cleaved transcripts (Figure 2.15 C). The hyperadenylated 3' tail is synthesized by the canonical polyA polymerase Pla1 (Yamanaka et al., 2010) and is partially dependent on Pab2. The hyperadenylated transcripts are now attacked by the exonuclease Rrp6, rendering them extremely unstable. With or without 3' end cleavage, Mmi1 inhibits splicing of the 3' most intron of *rec8*. The binding of Mmi1 close to the 3' intron-exon junction may directly inhibit the splicing of this particular intron, perhaps simply by steric hindrance of spliceosome assembly.

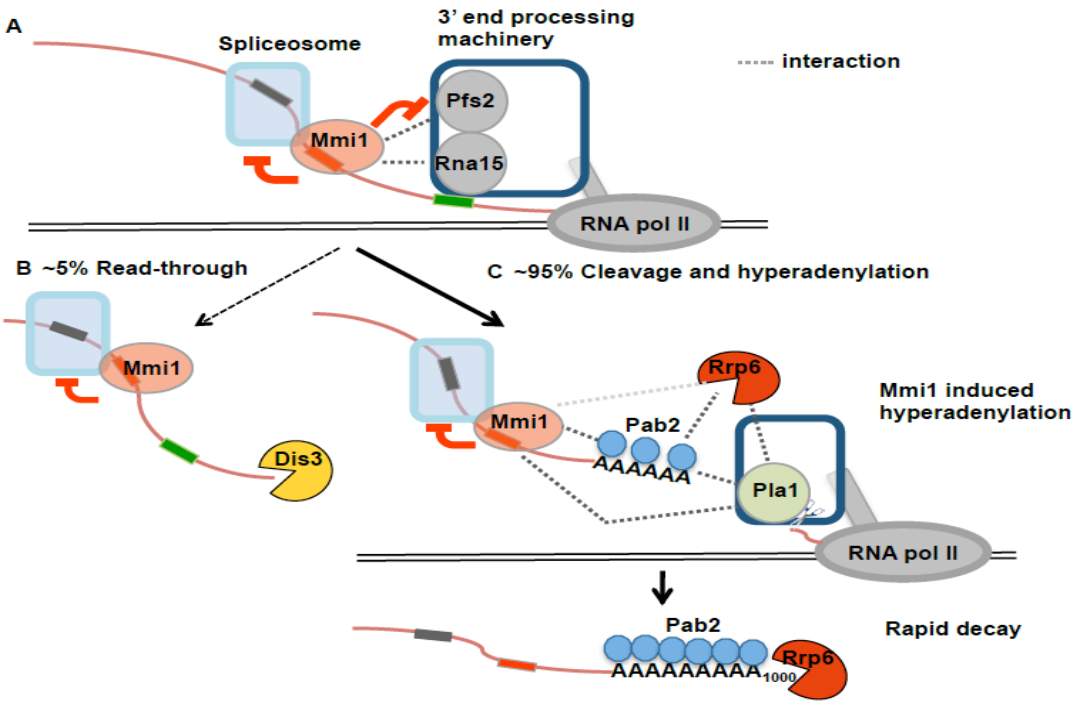

Figure 2.15 Model of Mmi1's function. (A) Mmi1 (orange ball) binds DSR sequences (orange box) in the nascent transcript and inhibits splicing (gray box, intron; light-blue square, spliceosome). (B) Mmi1 also affects 3' end processing (dark blue, 3' end processing complex), such that cleavage is inhibited on ~5% transcripts. These read-through transcripts are removed by Dis3 (yellow pacman). (C) Mmi1 alters 3' end processing of the majority of transcripts to promote hyperadenylation. This hyperadenylation depends on the canonical polyA polymerase Pla1 (green ball)(Yamanaka et al., 2010), also a subunit of 3' end processing complex. The polyA binding protein Pab2 (blue ball) may assist such hyperadenylation and recruit exonuclease Rrp6 (red pacman) to clear these hyperadenylated transcripts. Protein-protein interactions are shown by dotted line according to following evidence. (A) Mmi1-Pfs2: mutual suppression (this study); Mmi1-Rna15: yeast two-hybrid and co-IP (Yamanaka et al., 2010). Both Pfs2 and Rna15 are essential for 3' cleavage event. (C) Mmi1-Pab2 and Mmi1-Pla1: yeast two-hybrid and co-IP (Yamanaka et al, 2010); Mmi1-Rrp6: unpublished observation (Harigaya et al., 2006); Rrp6-Pab2: co-IP (Lemay et al., 2010); Rrp6-Pla1: synthetic rescue in budding yeast (Burkard and Butler, 2000) and Pab2-Pla1: biochemical interaction in mammalian cell (Kerwitz et al., 2003).

Evidence for the model and comparisons with other work

The first effect we have noted is that Mmi1 interferes with cleavage at the normal polyadenylation sites, and so promotes read-through transcription. The main evidence for this comes from the *rec8*-A_{65}RZ construct. Read-through transcripts are prominent in WT vegetative cells and the *rrp6* mutant, but are not seen in the *mmi1* mutant (Figure 2.13). Moreover, the polyadenylation assay (Figure 5C, middle panel) detecting read-through transcripts stabilized by the encoded polyA tail (RZ end) shows a considerable amount of such read-through transcript in the WT and the *rrp6* mutant, but not in the *mmi1* mutant. These results indicate that Mmi1 inhibits cleavage. Mmi1 physically interacts with Rna15 (Yamanaka et al., 2010) and genetically interacts with Pfs2 (Figure 2.15). Both Rna15 and Pfs2 are essential for cleavage. It is likely that the physical interaction between Mmi1 and the 3' cleavage machinery reduces the cleavage efficiency of genes in the Mmi1 regulon. Nevertheless, read-through *rec8* transcripts are only a minority of total transcripts, given that the RZ end band intensity is low in WT cells (~5%) compared to *pfs2* mutant (Figure 2.14 A, lane 3 and 6), which generates ~100% read-through transcription. The majority of rec8 transcripts are cleaved, but are extremely unstable and not detectable in WT cells.

Previously, we and our collaborators studied the regulation of *crs1*, another gene of the Mmi1-regulon (McPheeters et al., 2009). The inability to detect cleaved *crs1* transcript led to the conclusion that Mmi1 primarily works by blocking the use of the cleavage and polyadenylation sites. We note that the critical experiments of McPheeters et al. involved mutating the region in and around the 3' cleavage and polyadenylation site; the effects of these mutations were interpreted as effects on the cleavage and polyadenylation signals. However, since the DSR often lies at least partly in the 3' untranslated region, the mutations may instead have acted by affecting the DSR, and diminishing Mmi1 binding.

The most striking part of our current model is that Mmi1, in co-operation with Pab2, leads to the hyperadenylation of the cleaved transcripts. This hyperadenylation seems to target the transcripts for rapid degradation via Rrp6. In the case of *rec8*, the polyA tail was extraordinarily long (Figure 2.10). Hyperadenylation was also seen on the two other Mmi1-targets investigated, *mei4* (Figure 2.10) and *ssm4* (data not shown), but

not on two control genes. We investigated the cause-and-effect relationships between Mmi1, hyperadenylation, and transcript instability using a ribozyme construct that allowed formation of a polyA tail independent of the cleavage and polyadenylation machinery. Experiments with the ribozyme constructs showed that an encoded polyA tail stabilized the *rec8* transcript, and that the stability of this transcript was not greatly affected by the presence or absence of Mmi1, Rrp6 or Pab2 (Figure 2.14 B). That is, the Mmi1 pathway was unable to target a DSR-containing transcript for degradation, if the polyA tail was formed independently from the 3' processing machinery. Based on this result, we suggest that Mmi1, working in co-operation with Pab2, and probably also with the 3' processing machinery, promotes hyperadenylation of transcripts, and this hyperadenylation targets these transcripts to Rrp6 for degradation. In the absence of hyperadenylation, for instance when a polyA tail of 65 As is encoded, the transcript is stable despite the presence of Mmi1 and Pab2. Consistent with the model that hyperadenylation targets a transcript for degradation via Rrp6, we found two examples of other genes, *TFIIB* and SPCC1442.04c, that are not Mmi1 targets, but appear to be targeted to Rrp6 via hyperadenylation. This suggests that hyperadenylation may be a general method of targeting transcripts to Rrp6, and Mmi1 may be one of several methods of achieving hyperadenylation.

It might seem paradoxical that the hyperadenylated RNA is so unstable, since the polyA tail generally helps stabilize mRNA. However, polyadenylation-triggered mRNA decay is well established in prokaryotes (Dreyfus and Regnier, 2002; Steege, 2000) and in the DNA containing compartments of plant cells (Lange et al., 2009). Interestingly, a recent paper proposed a novel mRNA decay mechanism induced by Kaposi's sarcoma-associate herpesvirus (KSHV) that also involves hyperadenylation (Lee and Glaunsinger, 2009). This viral SOX protein shuts off host cell mRNA expression by hyperadenylation-associated RNA decay. In the KSHV system hyperadenylation depends on the canonical polyA polymerase PAPII, which is equivalent to the dependency of the canonical polyA polymerase Pla1 in the Mmi1 system. The similarities between the two systems, one in fission yeast and one in virus-mammalian cells, suggests that the polyadenylation quality control has been converted (or hijacked by virus) into an efficient regulatory mechanism.

For normal transcripts, the length of the polyA tail is well controlled within a defined range, ~70-90nt in budding yeast (Brown and Sachs, 1998) and ~250nt in mammalian cells (Brawerman, 1981). In mammalian systems, polyA addition is distributive until the tail reaches 10-12nt, the minimal length to stabilize polyA binding protein PABPN1 (Wahle, 1991), homologous to *S. pombe* Pab2. (Note: distributive means that the polyA polymerase can only add a few nucleotides before dissociating from the RNA.) The interaction between polyA polymerase, the 3' end processing complex and PABPN1 then induces processive polyadenylation (Kuhn et al., 2009). Once the polyA tail reaches ~250nt, the interaction between the three factors is disrupted and processive polyadenylation ceases (Kuhn et al., 2009). PABPN1, with 200~300nt of polyA, forms a 21nm compact particle, which may be responsible for disrupting the simultaneous interaction and protecting the RNA 3' end (Kuhn et al., 2009). Thus, PABPN1/Pab2 may function as a molecular ruler for polyA tail length. The interaction of Mmi1 with Pab2 (Yamanaka et al., 2010) could somehow disturb this measuring device, allowing much longer lengths of polyA.

During preparation of this manuscript, Yamanaka et al. published a report making a number of observations similar to ours. In particular, they also showed that several targets of Mmi1 become hyperadenylated in an Mmi1-dependent fashion, and that Pab2 is involved. Like us, they designed an experiment to test causal relationships by making a construct with an encoded polyA tail. Strikingly, however, their experiment gave essentially the opposite result as ours: in their case, a transcript with an encoded polyA tail of 50 nucleotides was not stabilized, and the turnover continued to be dependent on Mmi1 and Pab2. In addition, the turnover depended on the 50 nucleotides of polyA, but not polyT. These findings led to conclusions that are different from ours. For instance, Yamanaka's results suggest that although a polyA tail is required, it does not have to be particularly long; i.e., hyperadenylation is not required. In addition, Yamanaka's results would suggest that the Mmi1 pathway can function without necessarily interacting with or influencing the cellular 3' end processing machinery.

There are a number of possible reasons for the apparent difference in experimental results. First, the experiment of Yamanaka et al. was done in the context of the reporter gene GFP fused with the DSR from *spo5* at the 3' end. Second, there are

differences between the experiments in the distance from the DSR to the 3' end of the transcript. Third, for both experiments, there is an issue as to whether the encoded polyA tail is exposed at the very 3' end. But fourth, and perhaps most importantly, very different methods of terminating the transcript were used. Whereas we terminated the *rec8* transcript using a completely heterologous ribozyme, Yamanaka et al. used the *S. pombe snu2* terminator (i.e., the terminator of the U2 snRNA), which does not use the usual cleavage and polyadenylation complex, and which does not normally lead to polyadenylation. Instead, the formation of the 3' end of *snu2* is a two-step process: internal cleavage at a stem-loop at the 3' end by endonuclease Pac1, and then 3' to 5' exonuclease trimming to form the mature 3' end (Zhou et al., 1999). Perhaps importantly, this trimming is most likely carried out by Rrp6 (Allmang et al., 1999a). One possibility is that, whereas in most Mmi1-target genes, Rrp6 is recruited by the hyper-long polyA tail, in the case of the GFP reporter with a *snu2* terminator, Rrp6 may be recruited by the *snu2* terminator, one of its natural substrates. The combination of Mmi1, some Pab2 bound on a 50-nucleotide polyA tail, and recruitment of Rrp6 via the natural *snu2* substrate could achieve the same end effect as Mmi1 and a hyperadenylated tail.

Splicing

We originally began working on Mmi1-regulated genes because some of them have meiosis-specific splicing (Averbeck et al., 2005). But different Mmi1-regulated, intron-containing genes, manifest different effects. For some, such as *crs1*, splicing of all the introns is co-regulated. In other cases, such as *rec8*, splicing of the first three introns is not inhibited by Mmi1, while splicing of the 4th and 3' most intron is inhibited by Mmi1 in vegetative cells. The *rec8*-A_{65}RZ ΔPAS construct (Figure 2.14 C) showed that Mmi1 inhibits splicing of this 3' most intron even when the transcript is stabilized by an encoded polyA tail, and even when transcript termination does not depend on the 3' end processing machinery. This suggests that splicing inhibition by Mmi1 is separable from interfering with 3' end processing and RNA stability. Consistent with this view, the transcript levels of *mek1* and *meu13* did not increase in the *mmi1* mutant, even though transcripts from both genes became partially spliced.

We now see at least three ways that Mmi1 affects splicing. First, Mmi1 leads to the very rapid turnover of vegetative transcripts, so that these transcripts may never survive long enough to be spliced. In this model, splicing is kinetically slow. Second, Mmi1 leads to an increased proportion of read-through transcripts. Although these are unstable, they may be more stable than the hyperadenylated, Rrp6-targeted transcripts, and these read-through transcripts seem to be the transcripts we detect in vegetative cells. These read-through transcripts are largely unspliced. This may be partly due to the lack of 3' end processing, and partly also a kinetic issue, given their instability. Finally, some introns, such as the 3' most intron of *rec8*, are truly regulated in a specific way by Mmi1, since even when the transcript is stabilized, this intron is not spliced in vegetative cells (Figure 2.14 C). A straightforward model is that the binding of Mmi1 very close to the intron-exon junction directly interferes with splicing.

Protein domains of Mmi1 and homologues of Mmi1

The only identified motif of Mmi1 is YTH, named for human YT521-B homology, proposed to have RNA binding activity. YT521-B acts as a pre-mRNA splicing factor and modulates alternative splice site selection (Hartmann et al., 1999). YT521B co-localizes with active transcription sites in mammalian cells, suggesting that this protein family may function co-transcriptionally (Hartmann et al., 1999). In Arabidopsis, the YTH domain is found in the longer form of CPSF30 (cleavage and polyadenylation specificity factor) which is important for both 3' cleavage and polyadenylation (Delaney et al., 2006). Incidentally, the CPSF30 homologue in budding and fission yeasts is called Yth1, yeast thirty kD homology, but does not have the YTH domain. The presence of the splicing-related YTH domain in the major 3' end processing factor CPSF30 in plants perhaps provides the most direct link between the two functionalities. In our experiments, Mmi1 regulates both splicing and 3' end processing of *rec8*. The fact that homologs of Mmi1 are sometimes found as integral components of the 3' cleavage and polyadenylation machinery strengthens the view that Mmi1 works in part by interacting with this machinery.

RNA binding factors such as Mmi1 potentially regulate individual genes by substantially different mechanisms. For *rec8* our results show that Mmi1 keeps *rec8* off

in vegetative cells by combined mechanisms of inhibiting splicing, inhibiting 3' cleavage, and targeting of the 3' cleaved hyperadenylated transcripts for a rapid decay pathway. Further investigation of the Mmi1 regulon may yet hold additional surprises.

IV. Materials and Methods

Yeast cell culture

General *S. pombe* culture methods have been described previously (Cervantes et al., 2000; Moreno et al., 1991). Strains used in this work are listed in Table 2.1. Except where specifically stated in figure legends, growth conditions were as follows: cells were grown in minimal media (MP biomedicals) with required supplements at 24°C to OD600=0.3 to 0.5 upon harvest. For temperature sensitive strains, cells were grown at 24°C to OD600=0.3 to 36°C for 1 hour for *mmi1-ts3, rrp6-9, mmi1-ts3 rrp6-9* and *pab2Δ rrp6-9*, or to 36°C for 2 hours for *pfs2-11, dhp1-1*, *mis11-453*, and a wild-type control. *pab2Δ* cells were routinely grown at 30°C. The cold sensitive mutants *dis3-54* and *dis2-11* were grown at 34°C to OD600=0.3 and shifted to 20°C for 4hr. Ice was added to each culture at the time of harvest. Cells were collected by centrifugation, washed 1X with ice-cold water, frozen in liquid nitrogen, and stored at -80C.

Meiotic time-course

A synchronous meiosis was achieved as described (Cervantes et al., 2000). Briefly, a diploid strain homozygous for the *pat1-114* mutation (F277) was grown in EMM2* (without adenine) at 24°C to OD600 0.3. Cells were washed with water and resuspended in EMM2* without NH_4Cl at 24°C for 16hr to obtain a culture of G1 arrested cells. Cells were shifted to 34°C to inactivate Pat1 and were re-fed with 5mg/ml NH_4Cl (time = 0 hours). 2ml samples were harvested each hour for 8 hours for flow cytometry and DAPI staining (Figure 7) and large samples of 2×10^8 cells were collected at the same times for RNA isolation.

Expression microarrays

Microarrays were manufactured and hybridized at the Stony Brook microarray

facility as described (Oliva et al., 2005). RNA from each mutant strain or meiotic time-point was converted to Cy3 labeled cDNA and hybridized together with a reference cDNA. Wild-type (F31) grown to early log phase in minimal medium was the source of RNA for making Cy5 labeled cDNA used as the common reference in all cases. Data were analyzed by hierarchical clustering by the agglomerative algorithm (Eisen et al., 1998) and are presented using Java TreeView (available at http://jtreeview.sourceforge.net/). Microarray data are available at Array Express.

RT-PCR based splicing, readthrough and polyadenylation assays

Total RNA was isolated using the RiboPure™-Yeast kit (Ambion). 20ug of total RNA was treated with 4 U TURBO DNase in 40µl at 37°C for 1hr (Ambion). RNA was then tested for genomic DNA contamination using the 7SL primer pair in a 32 cycle PCR reaction. If no 7SL product was generated, then the RNA was used for cDNA syntheses described below. cDNA was synthesized from 2-4µg total RNA using SuperScript III reverse transcriptase (Invitrogen) according to manufacturer's instructions and with addition of 50ng actinomycin D to prevent second strand cDNA synthesis (Ruprecht et al., 1973). 250ng random hexamer was used for random primed cDNA (for splicing and readthrough assays). For each random primed cDNA synthesis a mock reaction (-RT control) lacking reverse transcriptase was performed in parallel. For the polyadenylation assay, 100ng P1-T_{16} primer was used and the cDNA was then purified to remove free primer (QIAquick PCR purification column (Qiagen)). For all reactions, final cDNA volumes were adjusted to 40µl.

1µl of cDNA was amplified by PCR (28 cycles) for splicing and readthrough assays followed by agarose gel electrophoresis and ethidium bromide staining. For polyadenylation assays, 1µl of P1-T_{16} primed cDNA was amplified in two steps. The first step was 10 cycles of PCR was with forward primer (F1) and P1 reverse primer. 1µl of the first PCR product was used in a second PCR of 15 cycles with p^{32}-αdCTP, a different forward primer (F2) down stream of F1 and the same P1 reverse primer. PCR products were resolved on 5% polyacrylaminde gels. Signals were detected and analyzed using the Phosphoimager Storm system (GE) and ImageQuant software (GE).

3'RACE and cloning

To enrich mRNA, 10μg total RNA was selected by Poly(A)purist (Ambion) to remove rRNAs. The remaining RNA was 2-5% of the input and was largely enriched with mRNA. 100ng mRNA was used for 3' ligation with adenylated 3' cloning linker. Ligated mRNA was used as template for cDNA synthesis with primer complement to 3' cloning linker. The 3' cloning linker, RNA ligation and cDNA synthesis materials were from mirCat kit and followed manufacture instruction (Integrated DNA technologies). cDNA was used for PCR reaction with rec8 3'F primer (see primer list) and primer complement to 3' cloning linker. PCR product was cloned into pSC-A vector (Stratagene) and transformed to E. coli. Single colonies were sent for sequencing with rec8 3'F primer.

Northern blot analysis

10ug total RNA was analyzed for each sample. Electrophoresis (1% agarose, 2.2M formaldehyde ,1X MOPS) was followed by capillary transfer onto a nylon membrane (Hybond-XL, Amershan) as described (ref. protocol). Membranes were hybridized with 10μl of radiolabled probe (~0.5-1 X 10^6 CPM) at 68°C over night in ULTRAhyb buffer (Ambion) and then washed at 68°C (3 washes 10 minutes each in 1XSSC 0.1% SDS and 3 washes 20 minutes each in 0.1XSSC 0.1% SDS). Signals were detected and analyzed using the Phosphoimager Storm system (GE) and ImageQuant software (GE).

Strand specific p^{32}-labeled RNA probes were synthesized by in vitro transcription with T3 or T7 RNA polymerase using the MAXIscript kit (Ambion), purified using Microcon YM-30 (Millipore) and eluted in 50ul water. Templates for transcription were generated by PCR amplification of genomic DNA using primers listed in Supplemental table 2.

RNase protection assay

RNA probe synthesis was the same as described in Northern blot section. RNA probe was further gel purified to ensure full-length probe recovery. Probe was quantified with scintillation counter and estimated the specific activity. In multiple experiments, the

probes were consistently measured ~0.5-1 X 10^6 CPM/µl, or ~0.5-1 X 10^9 in terms of specificity activity. 2µl probe was hybridized with 10ug total RNA at 42°C overnight. In this ratio, probe was in molar excess to target mRNA. The hybridization and RNase digestion procedure were followed RPAIII kit (Ambion). The RNA samples were resolved on 10% acrylamide-8M Urea TBE gel.

Fluorescence microscopy

Cells were collected, washed with water and fixed in 70% ethanol. Cells were then rehydrated prior to fluorescent staining with DAPI (Vectashield) and 5ug/ml calcoflour. Cells were examined using anAxioplane2 microscope (Zeiss). Images were obtained and analyzed using Axiovision Rel. 4.7 (Zeiss).

Plasmid construction

Primer sequences are provided in Table 2.2. All clones derived from PCR products were sequenced. QuikChange kit (Stratagene) was used for site-directed mutagenesis.

p*Rec8* is a replicating plasmid containing the sequences extending from 1kb upstream of the *rec8* ATG to 1kb downstream of the *rec8* stop codon. This region was amplified from genomic DNA by PCR and cloned between the *Sph*I and *Sac*I sites of pJR2-41XL (Moreno et al., 2000) thereby replacing *nmt* promotor and terminator sequences with those of rec8.

p*Rec8*-int4Δ and p*Rec8*-BPmut were made by site directed mutagenesis of p*rec8* with primers *rec8*_int4D_F and *rec8*_int4D_R or *rec8*_BPmut_F and *rec8*_BPmut_R, respectively.

p*Rec8*-A_{65}RZ was constructed using overlapping PCR to join the *rec8* 3' region with A's and the ribozyme (A_{65}RZ module is originated from GFP A150RZ) (Dower et al., 2004). *rec8* 3' region was amplified using template p*rec8* and primers *rec8*_exo4F_*Nco*I and *rec8*_-248R_*Sac*IIRZ. A_{65}RZ was amplified using template GFP A150RZ and primers RZ5'_*Sac*II-2 and T3_*Xma*I. The two amplified products were mixed and further amplified using outside primers *rec8*_exo4F_*Nco*I and T3_*Xma*I. The overlapping PCR product was cloned between *Nco*I and *Xma*I sites of p*Rec8* to create

p*rec8*-A_{65}RZ. For cleavage inactive ribozyme, primers with point mutation were used for PCR with p*Rec8*-A_{65}RZ vector as template resulting in p*Rec8*-A_{65}RZmut vector. The PAS region was deleted from the p*Rec8*-A_{65}RZ vector with primers *rec8*_DPAS_F and *rec8*_DPAS_R. p*Rep1-mmi1* was made by cloning a PCR amplified fragment containing the *mmi1* ORF between the *Xho*I and *BamH*I sites of pJR2-31XL (Moreno et al., 2000).

Fluorescence *in situ* hybridization

Cells were grown in EMM medium to OD600 = 0.5. 5ml cells were collected by certification 2,000 rpm for 2min at room temperature and washed once with 5ml water. Cells were resuspend in 5ml cross-linking solution (4.5ml 0.1M KPO4 pH6.5 and 0.5ml 37% formaldehyde) and incubated at 24°C for 90min. Cross-linked cells were washed with 5ml 0.1M KPO4 pH6.5 twice and resuspend in 0.5ml buffer (0.1M KPO4 pH6.5 and 1.2M sorbitol). To permeabilize the cell wall, cells were digested with 30µl 10mg/ml Zymolyase 100T at 24°C for 30 to 60min, dependents on the strain used. Cells were checked under microscope every 10min after incubation with Zymolyase, and the reaction was stopped before mis-shaped and phase-dark cells appear. To stop the reaction the cells were washed very gently with 1ml 0.1M KPO4 pH6.5/1.2M sorbitol one time and resuspend in 100-250ul (depending on the cell concentration) 0.1MKPO4 pH6.5 /1.2M sorbitol. Cells were placed on ice.

Teflon welled, poly-lysine coated glass slide was used for FISH experiment. 20µl cells were spotted in each well on the glass slide and incubated at 24°C for 10min to allow cells precipitation to the surface of the glass slide and linkage to the poly-lysine residue. Most of the liquid was carefully removed and left a wet layer on the slide. The slide was submerged into freezing-cold methanol (-70°C) for 6min and immediately transferred to freezing-cold acetone (-70°C) for 30sec. The slide was immediately transferred on to a hot flat surface (60°C) to avoid liquid condensation.

The slide was pre-equilibrated in freshly prepared 0.1M triethanolamine pH 8.0 for 2 min at 24°C. The slide was then blocked with 0.25% acetic anhydride in 0.1M triethanolamine at 24°C for 10min and incubated in 2XSSC 24°C for 5min. To further block unspecific probe binding, the slide was pre-hybridized with freshly prepared hybridization buffer (50%formamide, 10% dextran sulfate, 4x SSC, 0.02% polyvinyl

pyrrolidone, 0.02% bovine serum albumin, 0.02% Ficoll-400, 125ug of tRNA/ml and 500ug/ml of denatured and sonicated salmon sperm DNA) at 37°C for 1hr. This hybridization buffer was removed and new hybridization buffer containing 50nM Cy3 labeled DNA probe was added. This hybridization was performed at 37°C for 16hr. Hybridization was performed in a humidified chamber. The slide was washed with 2XSSC at 24°C for 1hr, 1XSSC at 24°C for 2hr, 0.5XSSC at 37°C for 30min and 0.5XSSC at 24°C for 30min.

Cells were examined using anAxioplane2 microscope (Zeiss). Images were obtained and analyzed using Axiovision Rel. 4.7 (Zeiss).

Table 2.1 Strains used in this study. Strain names in parenthesis are the original name from the requested laboratory or from Yeast Genetic Resource Center (YGRC, Japan, FY strains).

Strain Name	Genotype	Reference/Source
F31	*h⁻ leu1-32 ura4-D18*	Lab stock
F277 (FY16057)	*h⁺/h⁺ pat1-114/pat1-114 ade6-M210/ade6-M216*	YGRC
JLP1298	*h⁻ pfs2-11 ade6-M210 his3-D1 leu1-32 ura4-D18*	(Wang et al., 2005)
F259 (MP101)	*h⁻ dhp1-1<<ura4⁺ ade6-M216 leu1-32 ura4-D18*	(Shobuike et al., 2001)
F275 (MY1265)	*h⁺ dis3-54 leu1-32 his2*	(Ohkura et al., 1988)
F306 (JV558)	*h⁻ mmi1+<<kan^r ade6-M210 leu1*	(Harigaya et al., 2006)
F307 (JV564)	*h⁻ mmi1-ts3<<kan^r ade6-M216 leu1*	(Harigaya et al., 2006)
F308 (JV567)	*h⁻ mmi1-ts6<<kan^r ade6-M216 leu1*	(Harigaya et al., 2006)
F327 (JT430)	*h⁻ rrp6-9-GFP <<kan^r ade6-M216 leu1*	(Harigaya et al., 2006)
F319 (YH7a)	*h- rrp6::kanMX6 ade6-704 leu1-32 ura4-D18*	(Huang et al.)
F343 (FBY107)	*h⁻ pab2::kanMX6 ade6-M216 his3-D1 leu1-32 ura4-D18*	(Lemay et al., 2010)
F281 (FY10228)	*h⁻ dsk1::ura4⁺ leu1 ura4-D18*	(Takeuchi and Yanagida, 1993)
F263 (FY9098)	*h⁻ mis11-453 leu1*	(Takahashi et al., 1994)
F271 (FY9616)	*h⁻ dis2-11 leu1*	(Ohkura et al., 1989)
F260 (TS065)	*h- din1::ura4+ ade6-M216 leu1-32 his7-366 ura4-D18*	(Shobuike et al., 2001)
F295 (SWW224)	*h⁻ cid11::ura4+ leu1-32 ura4-D18*	(Wang et al., 2000)
F298 (DS333)	*h⁺ cid14::ura4+ leu1-32 ura4-D18*	(Win et al., 2006)
F258	*h⁻ hrp1::ura4+ ade6-M210 leu1-32 ura4-D18*	(Jin et al., 1998)
JLP1598	*h⁻ rrp6-9-GFP <<kan^r pab2::kanMX6*	This study

	ade6-M210 leu1-32 ura4-D18	
JLP1538	*h⁻ rec8:: ura4⁺ ade6-M210 leu1-32 ura4-D18*	(Parisi et al., 1999)
JLP1548	*h⁻ pat1-114 rec8::ura4⁺ ade6-M210 leu1-32 ura4-D18*	This study
JLP1541	*h⁻ pfs2-11 rec8::ura4⁺ ade6-M210 leu1-32 ura4-D18*	This study
JLP1536	*h⁻ mmi1-ts3<<kan^r rec8::ura4⁺ ade6-M216 leu1-32 ura4-D18*	This study
JLP1545	*h⁻ rrp6-9-GFP <<kan^r rec8::ura4⁺ ade6-M210 leu1-32 ura4-D18*	This study
JLP1594	*h⁻ pab2::kanMX6 rec8::ura4⁺ ade6-M210 his3-D1 leu1-32 ura4-D18*	This study
JLP1543	*h⁻ mmi1-ts3<<kan^r rrp6-9-GFP <<kan^r rec8::Ura4 ade6-M210 leu1-32 ura4-D18*	This study
JLP1278	*h⁻ pfs2-11 ade6-M216 leu1-32*	This study
JLP1483	*h⁻ pfs2-11 mmi1-ts3<<kan^r ade6-M216 leu1-32*	This study

Table 2.2 Primer list. All primers used in Chapter 2.

Splicing Assay		
5' 3 introns	*rec8*_ATG_F	ATGTTTTACAATCAAGATGT
of *rec8*	*rec8*_exo4_R	ACGGTAAAACGTCCTCATCG
4th intron of	*rec8*_3'_F	GGCGCATAACATTTTCAAG
rec8	*rec8*_Stop_R	TCAAATGGCATCGGTGCTTTTTAG
All introns of	*crs1*_SAF_F	CCTTCTATTCTGAATCAAAACATTGC
crs1	*crs1*_exo5_R	TCGTGAAACCGATTTGAGTG
Last intron of	*crs1*_exo4_F	TCCTTGCCTTCTGAAAGCTG
crs1	*crs1*_exo5_R	TCGTGAAACCGATTTGAGTG
All introns of	*mek1*_ATG_F	ATGGACTTTTTATCACATGCCATG
mek1	*mek1*_exo3_R	GCCGGGAATGTTTAAGAGGT
Last intron of	*mek1*_exo2_F	CATGGAGTATAATTCGGAAACTCA
mek1	*mek1*_exo3_R	GCCGGGAATGTTTAAGAGGT
All introns of	*meu13*_exo1_F	TGGCTAAGGCGAAAGAAGTAAA
meu13	*meu13*_end_R	TCCGTTTCAAATCCCAGTTT
Polyadenylation assay		
cDNA primer	P1-T_{16}	GGTCACCTTGATCTGAAGCTTTTTTTTTTTTTTT
		T
Reverse	P1	GGTCACCTTGATCTGAAGC
rec8 F1	*rec8*_3'_F	GGCGCATAACATTTTCAAG
rec8 F2	*rec8*_exo5_F	CACTAGCAACTAAGTCTGCATTTTT
crs1 F1	*crs1*_exo5_F	AGGCCGACGGAAATTTTATG
crs1 F2	*crs1*_RC3m	ATGCGCTTCGTTCTGGGTCTTG
mek1 F1	*mek1*_exo3_F	CGATTTATGGAGCCTTGGAG
mek1 F2	*mek1*_end_F2	GGTTCGCGCGACATAGTAGT
meu13 F1	*meu13*_end_F	CCAAGGAAGCAATGCAAAAG
meu13 F2	*meu13*_+28_F	TGGGAAAAACTGGGATTTGA
Readthrough assay		

Endogenous *rec8*	*rec8*_-42_F	TTGGGAATTAAACCCTTTGTTG
	*rec8*_-263_R	AGTGCTGGACTAACAAGACTCG
rec8-A_{65}RZ	*rec8*_-42_F	TTGGGAATTAAACCCTTTGTTG
	T3_*Xma*I	TCCCCCCGGGATTAACCCTCACTAAAGGGA
Quantitative PCR		
rec8	*rec8*_exo4_F	CAGTTCTTGAAACTCTTCCAGATTC
	*rec8*_exo4_R	ACGGTAAAACGTCCTCATCG
LEU2	LEU2_5'_F	CTGTGGGTGGTCCTAAATGG
	LEU2_mid_R	CCATCACCATCGTCTTCCTT
Cloning		
p*Rec8*	*rec8*_Pro5'_*Sph*IF	GACGCATGCCAACTCAAAGCGATCAATGC
	*rec8*_Ter3'_*Sac*IF	CGAGCTCTTCTTCCATCTCAACCAAAAG
rec8 Intron 4^{th} deletion	*rec8*_int4D_F	AGCCATTTACTGCACTAGCAACTAAGTC
	*rec8*_int4D_R	GACTTAGTTGCTAGTGCAGTAAATGGCT
rec8 Intron 4^{th} mutation	*rec8*_BPmut_F	CTGTGTAAGTATCACAATCAAACCACGAACTCCCAAAAC
	*rec8*_BPmut_R	GTTTTGGGAGTTCGTGGTTTGATTGTGATACTTACACAG
rec8-A_{65}RZ	*rec8*_exo4F_*Nco*I	CATGCCATGGATTGAAAAGCTCAAAC
	*rec8*_-248R_*Sac*IIRZ	AGCAGCCAGATCCTTTGTATAGCCGCGGCATGCTATGTACAACAGCCAAC
	RZ5'_*Sac*II-2	CCGCGGCTATACAAAGGATCTGGCTGCT
	T3_*Xma*I	TCCCCCCGGGATTAACCCTCACTAAAGGGA
RZmut	HHRZmut_F	GTGTTTTCCGGTCTCATGAGTCCGTGAG
	HHRZmut_R	CTCACGGACTCATGAGACCGGAAAACAC
PASΔ	*rec8*_PASD_F	AGATTAATGAATGATAATGCTAGCGGATTTGTTGGCTGTTGTACATAGCATGCCG
	*rec8*_PASD_R	CGGCATGCTATGTACAACAGCCAACAAA

		TCCGCTAGCATTATCATTCATTAATCT
pREP1-*mmi1*	*mmi1*_ATGF_*Xho*I	CCGCTCGAGATGTCAAACACAAACTTCTC
	*mmi1*_StopR_*BamH*I	CGGGATCCTCAACGGTCTCTTCCAATTC
Riboporbe for Northern blot		
rec8	T3	ATTAACCCTCACTAAAGGGAGA
	T7	TAATACGACTCACTATAGGGAGA
	NOTE: Rec8 ORF was cloned into vector and flanked with T3 and T7 primer binding sites.	
mei4	*mei4*_1129_F	CTACGTCCATCATCCCGTTT
	*mei4*_end_T7R	TAATACGACTCACTATAGGGAGAGAAG GATTCCACGGATCTGA
adh1	*adh1*_mid_F	TCACTTGCTATCGTGCCTTG
	*adh1*_-6_T7R	TAATACGACTCACTATAGGGAGAGGAAT TAAAAGTGGATCACATTCTC
LEU2	LEU2_5'_F	CTGTGGGTGGTCCTAAATGG
	LEU2_mid_T7R	TAATACGACTCACTATAGGGAGACCATC ACCATCGTCTTCCTT
THIIB	TFIIB_mid_F	GCAATTAGCTTGCCAAAGGT
	TFIIB_Stop_T7R	TAATACGACTCACTATAGGGAGACTAAG GCTTTGGTAACATAGCATC
SPCC1442.04c	C1442.0c4_mid_F	GCGAGTTTCCAGATCTTTCG
	C1442.0c4_end_T7R	TAATACGACTCACTATAGGGAGAGGTAA TTGGTTCCTGGCTCA
Checking genomic DNA contamination		
7SL	7SL_5'F	GGGTTCGAGTCTCGCTTTCGATCC
	7SL_3'R	GTTGTGTTTATACTTCCATGCACATCC

Table 2.3 mRNA processing factors tested in splicing assay (Figure 2.8). Gene function and homologs in *S. cerevisiae* and *H. sapiens* are listed. HomoloGene (Geer et al., 2010) and Inparanoid (O'Brien et al., 2005) were used to identified homologs. Homologs not found using HomoloGene but found by Inparanoid are marked with *. ?, unknown homolog and --, no homolog.

S. pombe	*S. cerevisiae*	*H. sapiens*	Function
Mmi1	?	?	Selective eliminate meiotic transcripts
Rrp6	RRP6	EXOSC10	3' to 5' exonuclease
Pab2	--	PABPN1	Nuclear polyA binding protein
Pfs2	PFS2	WDR33	Cleavage and polyadenylation
Dhp1	RAT1	XRN2	5' to 3' exonuclease, cleavage, termination
Dis3	DIS3	DIS3	3' to 5' exonuclease
Cid14	TRF4/5	PAPD5/7 *	Non-canonical polyA polymerase
Cid11	--	6 genes*	Non-canonical polyA polymerase
Dsk1	SKY1	SRPK1/2/ 3	SR protein kinase, splicing
Mis11	MUD2*	U2AF2	Member of spliceosome
Din1	RAI1	DOM3Z	Termination
Dis2	GLC7	PPP1CA	Phosphatase, cleavage and polyadenylation
Hrp1	CHD1	CHD1	Termination

V. Unpublished result:

5.1 Hyperadenylation is not a consequence of mRNA nuclear retention

Proper 3' end formation, including proper polyA tail length, is coordinated with RNA export. Defects in 3' end formation lead to nuclear retention of hyperadenylated transcripts that are retained at the site of transcription (Hilleren and Parker, 2001; Jensen et al., 2001). It has been proposed that assembly of the export-competent mRNP displaces the 3' end processing complex. Since it is the 3' end processing complex which recruits (or contains) the polyA polymerase, retention of the 3' end processing complex might result in very long polyA tails due to retention of polyA polymerase (Qu et al., 2009). A riveting possibility is that *S. pombe* utilizes this mechanism to block meiotic transcripts export through Mmi1 activity and hyperadenylation is the consequence of nuclear retention. However, the extended polyA tail observed in export deficient strains of budding yeast is only 50~100nt longer than normal polyA tail and can be readily detected without inactivation of Rrp6 (Hilleren et al., 2001; Hilleren and Parker, 2001; Qu et al., 2009). On the contrary, hyperadenylation of *rec8* exceeds 1 kb and no polyadenylated transcripts can be detected in the presence of Rrp6. With the apparent difference, the hyperadenylation of *rec8* is not likely just a result of nuclear retention. However, we wanted to know if nuclear retention has a role in hyperadenylation of meiotic genes. We used fluorescence *in situ* hybridization (FISH) to detect *rec8* transcripts in *rrp6-9* and *pab2Δ* mutant strains, two conditions that have hyperadenylated *rec8*. The results show that no apparent nuclear retention of *rec8* transcripts in these two strains (Figure 2.17). Thus we think that polyadenylation is actively altered by Mmi1 to achieve hyperadenylation, but is not caused by nuclear retention. These hyperadenylated transcripts are export-competent.

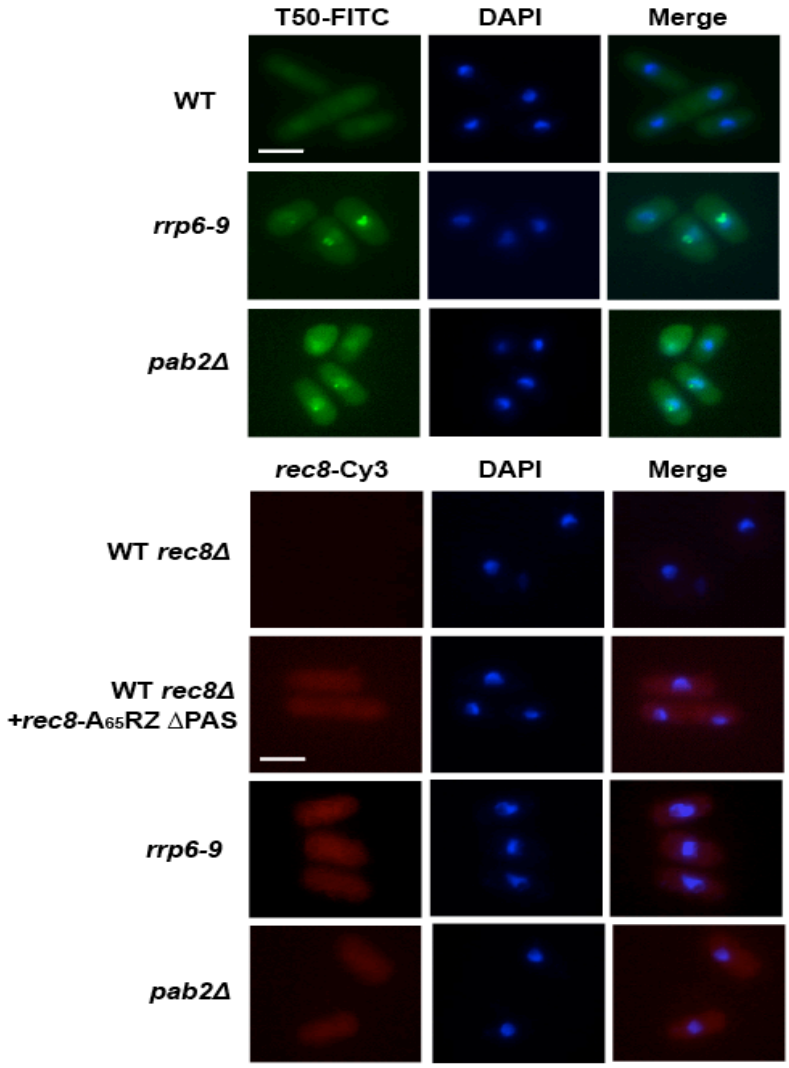

Figure 2.17 Hyperadenylated *rec8* transcripts are not retained in the nucleus. (A) Fluorescence in situ hybridization (FISH) detection of polyadenylated transcripts using FITC-labeled T50 oligo for wild-type (24°C), *rrp6-9* (36°C, 1hr), and *pab2Δ* (30°C) strains. Polyadenylated RNAs accumulate in the nucleolus in the *pab2Δ* strain as previously described (Lemay et al., 2010). Polyadenylated transcripts also accumulate as an irregular nuclear patch in the *rrp6-9* mutants. This patch is distinctly different from the compact single dot observed in *pab2Δ*. (B) FISH detection of *rec8* transcripts using Cy3-labeled antisense *rec8* probe. *rec8Δ* strain (no *rec8* at all) serves as a negative control and *rec8Δ* strain transformed with *rec8*-A_{65}RZΔPAS to express stabilized *rec8* serves as a positive control. Distribution of the wild-type *rec8* transcript was analyzed in both *pab2Δ* (30°C) and *rrp6-9* (36°C, 1hr) mutants (two conditions in which hyperadenylated *rec8* accumulates). There was no obvious nuclear enrichment of *rec8* transcripts in *pab2Δ* or *rrp6-9* suggesting that nuclear retention is not the cause of hyperadenylation and that hyperadenylated transcripts are export competent. FISH was performed as described (Perreault et al., 2008) except that probe concentration was 50nM.

5.2 Cis-regulatory sequences regulate splicing of *rec8, mek1 and meu13*

To determine the importance of the flanking regions, regions before and after the coding sequence, in splicing regulation of *crs1*, Dr. Averbeck cloned *crs1* coding sequence flanked by the *nmt1* promoter and *the nmt1* terminator into a vector. *crs1* transcripts transcribed from the *nmt1* promoter and terminated by the *nmt1* terminator is spliced, suggesting the flanking sequences inhibit splicing of *crs1* (Averbeck et al., 2005). We and collaborators further identified that it is the 3' sequence (part of the last exon and part of the terminator region) of *crs1* that inhibits splicing (McPheteers et al., 2009). Using similar strategy, I found that the terminator sequence is also important for splicing inhibition of *rec8* (Figure 2.18). However, even when the *rec8* terminator is replaced by the *nmt1* terminator some splicing inhibition of *rec8* retained, suggesting that some inhibitory sequence resides in the *rec8* coding sequence. Moreover, the splicing inhibition of *crs1* and *rec8* requires Mmi1, and it is very likely that Mmi1 is bound to *crs1* and *rec8* transcripts at the 3' sequences, which are important for splicing regulation.

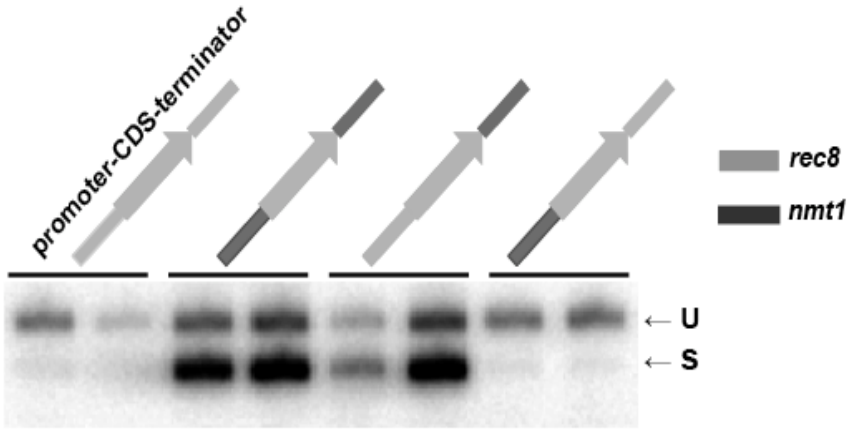

Figure 2.18 Terminator region of *rec8* inhibits splicing. *rec8* was cloned into p*Rep* vector. The promoter and terminator sequence on the vectors were either the endogenous promoter/terminator sequence of *rec8* or replace by *nmt1* sequence. Vectors were transformed into *rec8Δ* WT strain under vegetative growth. Two transformants of each transformation were used for the splicing assay. Splicing assay of the last intron of *rec8* shows that the promoter sequence does not regulate splicing because the *rec8* transcripts were unspliced under both *rec8* and *nmt1* promoter. Splicing of *rec8* is derepressed when the *rec8* terminator sequence was replaced by the *nmt1* terminator, suggesting that *rec8* terminator inhibits splicing.

Several other early meiotic genes are also classified as meiosis specific splicing, and two of them, *mek1* and *meu13* were chosen for further study because their spectrum of splicing responses to the various mutants is different from *rec8* and *crs1*(Figure 2.8), suggesting that the splicing regulation of *mek1* and *meu13* may be different from *rec8* and *crs1*. I used the same strategy mention above (Figure 2.18) to identify the regulatory *cis*-sequence for *mek1* and *meu13*. The results are summarized in Table 2.4.

promoter-gene-terminator (cloned in the vector)	*mek1*	*meu13*
endogenous	U	U
gene-gene-gene	U	S
gene-gene-nmt1	U	S
nmt1-gene-gene (w/o B1)	S	S
nmt1-gene-gene (w/ B1)	U	PS
nmt1-gene-nmt1 (w/o B1)	S	S
nmt1-gene-nmt1 (w/ B1)	U	not detected

Table 2.4 cis-regulator sequences of *mek1* and *meu13*. *mek1* and *meu13* were cloned into vector as mentioned in Figure 2.18, besides that a unique sequence (P1, see Table 2.2 for sequence) was inserted between the coding region and terminator sequence. The primers used for splicing assay were forward gene specific primer before the last intron and a reverse primer complementary to the P1 sequence, so that only the transcript transcribed from the vector can be PCR amplified. These vectors were transformed into WT strain, and two independent transformants were grown in EMM medium with or without B1. The PCR results are summarized above. U: unspliced; S: spliced and PS: partially spliced.

These data indicate that the promoter sequence of *mek1* inhibits splicing. Interestingly, when *mek1* was transcribed from the *nmt1* promoter, the intron was spliced if the *nmt1* promoter is induced (without B1) and the intron was unspliced if the *nmt1* promoter is repressed (with B1). From my tiling array experiments, I noticed that the *nmt1* gene normally associates with antisense RNA in cells grown in B1 containing medium, but not in minus B1 medium. This suggests that under repression condition the *nmt1* terminator function as the promoter for *nmt1* antisense RNA. Therefore, it is

possible that the unspliced *mek1* transcript from the *nmt1-mek1-nmt1* construct growing in B1 containing medium reflects the antisense RNA. However, the *nmt1-mek1-mek1* construct (using *mek1* terminator) growing in B1 containing medium also generated unspliced *mek1* transcripts suggesting that the connection between splicing and promoter induction might be a real connection.

The *cis*-regulatory sequence of *meu13* is enigmatic. It does not seem to reside in the promoter, the coding sequence, or the terminator, because the transcript was spliced even when the entire gene cassette (promoter-gene-terminator all from *meu13*) was cloned in the vector. This result suggests two possibilities: (1) the *cis*-regulatory sequence locates far from the gene loci and (2) the chromosome structure is different between vector cloned *meu13* and genomic *meu13*. The only condition that shown unspliced *meu13* transcripts transcribed from vectors was the *nmt1-meu13-meu13* construct grown in minus B1 medium. This is consistent with the observation with *mek1*, for which splicing correlates with promoter induction.

5.3 Mmi1 represses expression of Mei4

One of the gene repressed by Mmi1 is *mei4*, the meiotic transcription factor for inducing ~500 middle meiotic genes. The responsiveness of *mei4* to Mmi1 is much weaker comparing to *rec8*, who's DSR locates at the 3' end of the gene. In contrast, the DSR of *mei4* locates at the middle of the gene, ~700nt away from the stop codon (Harigaya wt al., 2006). Given the difference of the DSR location, I want to know whether the molecular mechanism of the repression of *mei4* by Mmi1 is similar to or different from *rec8*. Mmi1 represses the expression of *rec8* possibly through inducing hyperadenylation of *rec8* transcripts and the terminator sequence of *rec8* is particularly important for such repression. To test if the terminator sequence is important for the repression of *mei4* by Mmi1, I engineered two constructs: one with wild-type *mei4* (with *mei4* promoter and *mei4* terminator sequence, named *mei4-ter*) and one with *ura4* terminator sequence (named *ura4-ter*). The *ura4* terminator is an efficient terminator (Aranda et al., 1999). Vegetative cells die under Mei4 over-expression. The WT strain transformed with *mei4-ter* grew slightly better than the WT strain transformed with *ura4-*

ter at 28°C, suggesting that the terminator sequence contribute to some of the regulation. More importantly, the *mmi1-ts3* mutant strain transformed with *ura4-ter* was unable to grow under semi-permissive temperature (28°C), while transformed with *mei4-ter* was able to grow. Both *mmi1-ts3* transformants were not viable at restrictive temperature (Figure 2.19). These results suggest that the terminator sequences determine the responsiveness of a gene to Mmi1-mediated repression, even when the DSR locates far from the 3' end.

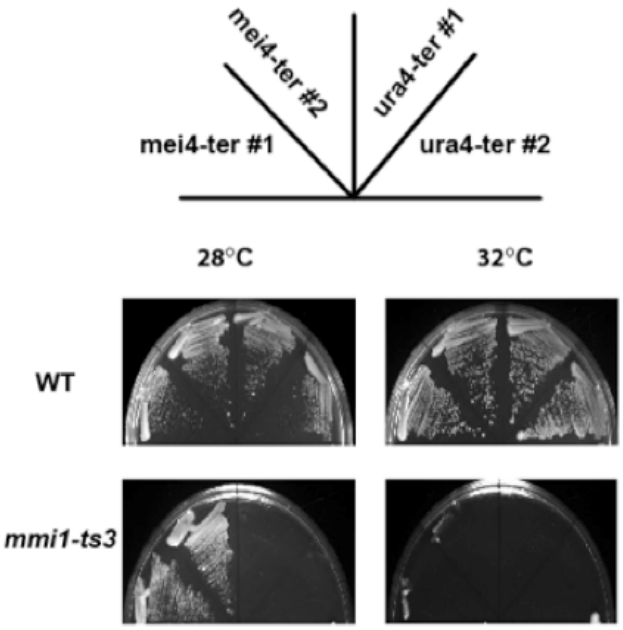

Figure 2.19 Mmi1 does not function well on *ura4* terminator. The two vectors, *mei4-ter* and *ura4-ter*, were transformed into WT or *mmi1-ts3* mutant strain. Two transformants of each transformation were streaked on plate and incubated at 28°C or 32°C for three day before recording the growth phenotype.

Chapter Three: Regulation of Middle Meiotic Genes by Antisense RNA and by Fkh2 Transcription Factor

I. Introduction

Cells divide through two types of cell cycle in sexually reproducing organisms. Somatic (or vegetative, for single cell organisms) cells divide by the mitotic cell cycle, which consists of one round of DNA replication and one round of chromosome segregation followed by cell division. In contrast, germ cells divide by meiosis, which is a specialized cell cycle that generates haploid gametes from a diploid cell. Meiosis consists of one round of DNA replication and two rounds of chromosome segregation followed by gamete maturation. There are notable similarities between mitotic and meiotic transcription factors in the fission yeast *Schizosaccharomyces pombe*. For example, factors belonging to the forkhead transcription family control both vegetative and meiotic M phase genes. Fkh2 and Sep1 are the forkhead transcription factors that control mitotic M phase, whereas Mei4 is the major meiotic forkhead factor that controls meiotic M phase (Buck et al., 2004; Bulmer et al., 2004; Szilagyi et al., 2005). Nevertheless, the transcription profiles of mitosis and meiosis are distinct; meiosis-specific genes are not expressed in vegetative cells. This suggests that some mechanisms prevent the mitotic transcription factor from activating meiotic genes in vegetative cells. Recent studies reveal that almost the entire *S. pombe* genome is transcribed, including regions previously considered to be transcriptionally inert (Dutrow et al., 2008; Wilhelm et al., 2008). This suggests that mis-activation by transcription factors may occur frequently or transcription may happen spontaneously. To keep a gene off, cells may need to invest energy to repress transcription possibly by the mechanisms including heterochromatin formation, transcription interference or other yet to be identified mechanisms.

A simple view of gene expression is that only the sense DNA strand that contains genes is transcribed, where as the opposite strand (antisense) does not yield RNA. This view has been challenged in recent years due to the finding of many antisense RNAs from yeast to mammals (Ge et al., 2008; Huber et al., 2006; Jia et al., 2010; Numata et al., 2007; Yassour et al., 2010). Transcription of the antisense strand produces antisense

RNA that may hybridize with the sense DNA strand, or the sense RNA, to influence transcription or sense RNA stability.

S. pombe also makes antisense RNAs. Depending on the experimental methods and arbitrary cut-off thresholds for the length and intensity of the RNA, the number of identified antisense RNAs range from 37 to ~2000 (Dutrow et al., 2008; Wilhelm et al., 2008). Despite the identification of antisense RNAs, it is still unclear whether these antisense RNAs are beneficial to the cells or are simply transcription by-products.

A few antisense RNAs that overlap with important genes have been shown to play regulatory roles in budding yeast. The sequence encompassing *IME4,* a key meiotic regulator in *S. cerevisiae*, encodes a long antisense RNA, which represses *IME4*. This ~2.5kb antisense RNA spans the entire length of *IME4,* including the promoter region (Hongay et al., 2006). The antisense–mediated *IME4* repression mechanism is most consistent with transcription interference in which one transcription process directly suppresses the other (Hongay et al., 2006). Long antisense RNAs were also found for *PHO84* (Camblong et al., 2007). These 2-3kb antisense RNAs do not function through transcription interference; rather they repress the activity of the *PHO84* promoter by histone deacetylation, a suppressive chromatin mark that can be passed onto the next generation (Camblong et al., 2007). These pioneering studies of individual genes reveal a variety of molecular mechanisms (reviewed in (Wilusz et al., 2009).

In this study, we used a genome-wide approach and determined that long antisense RNAs were formed in vegetative cells at the loci of middle meiotic genes. This observation led to the central hypothesis that antisense RNAs prevent middle meiotic genes from incidental activation in vegetative cells in *S. pombe*.

Meiosis-specific splicing has been proposed to be a mechanism to maintain tight repression of meiotic genes during vegetative growth, but antisense transcripts can generate misleading results in the assays most often used in splicing analyses. In light of the abundant antisense transcripts found in our study, we re-investigated splicing regulation using stringent strand-specific methods. Our results suggest that most "splicing-regulated" middle meiotic genes are not regulated by splicing, but are instead potential targets of antisense-mediated regulation. Since the transcription factor Fkh2 is proposed to be the key repressor of splicing for a dozen middle meiotic genes (Moldon et

al., 2008), we investigated whether Fkh2 is instead a key player in the balance between sense and antisense transcription.

II. Results

2.1 Definition of antisense RNA and the origin of antisense RNA

To study transcription in *S. pombe*, we used Affymertix tiling array to analyze transcripts isolated from vegetative cells and meiotic cells. This *S. pombe* 1.0 array has 25nt oligos that represent the entire genome on both DNA strands. RNA for analysis was first converted to cDNA primed with anchored oligoT primer and then size selected to remove fragments smaller than 70nt, as a result, this cDNA represents long polyadenylated RNA species. Because various reverse transcriptases used for first-strand cDNA synthesis can take both RNA and DNA as template, spurious second-strand cDNA can be made during the reverse transcription reaction (Muller et al., 1971; Spiegelman et al., 1970). On the strand specific tiling array, second-strand cDNAs would generate artifact appearing as spurious antisense transcripts. To prevent second-strand cDNAs synthesis actinomycin D (Act D) was added to the reverse transcription reaction. Act D largely reduces second-strand cDNA synthesis and shows no effect on first-strand cDNA formation (Perocchi et al., 2007). The hybridization signals were normalized and partitioned into segments with constant probe hybridization intensity (see method). The antisense segments were defined based on a single criterion that these segments overlap with a CDS (coding sequence) on the opposite strand. Under this definition, every CDS overlapped with at least one sense segment on the same strand and at least one antisense segment on the opposite strand (Figure 3.1).

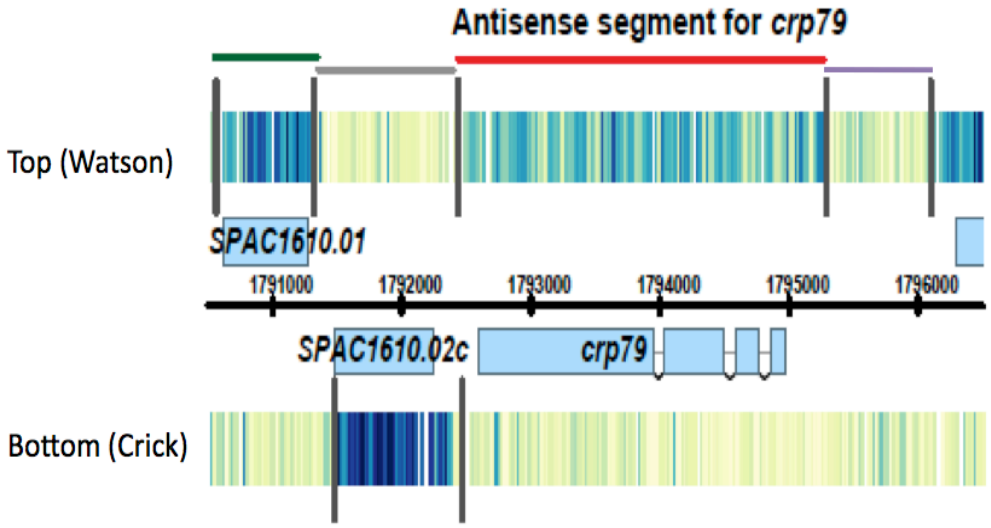

Figure 3.1 Example of high-resolution tiling array data. The black horizontal line in the middle shows the chromosomal coordinates. Genes drawn above the line are encoded on the top (Watson) strand and below the line are encoded on the bottom (Crick) strand. Exons are represented as light blue boxes. For gene with multiple exons, such as *crp79*, the exons are linked by thin lines representing the introns. Signal intensity for each probe is shown as a vertical line with color ranges from light yellow (low signal) to dark blue (high signal). The black vertical line is the calculated boundary; separating two regions of different constant probe hybridization intensities. A segment is the region between two boundary lines. Based on the location of the segments, they can be broadly assigned into three groups: sense segment, antisense segment, and non-annotation segment. The segments on the top strands are color-coded for demonstration. The green segment is on the same strand as SPAC1610.01, thus it is the sense segment for this gene. The grey segment overlaps SPAC2610.02c on the opposite strand, and is defined as the antisense segment for this gene. Note that the grey segment has very low signal intensity as most antisense segments do. The red segment overlaps with *crp79* on the opposite strand, and it is the antisense segment to *crp79* with relatively high signal intensity. The purple segment did not overlap with any feature and has very low signal intensity.

We defined the antisense segments with average intensity above 0.5 as antisense RNAs. These antisense RNAs were divided into two major groups based on their origins. One group of antisense RNAs was composed of discrete transcription units that did not connect with other features (Figure 3.2 A, antisense RNAs for *spo4* and *crp79*). The other group of antisense RNAs was composed of transcripts that originated from the long 3'UTRs (untranslated region) of annotated genes on the opposite strand (Figure 3.2 B, antisense RNAs for *spo6* and *mug28*). The gene carrying long 3'UTR and the gene on the opposite strand overlapping with the long 3'UTR were convergently oriented (tail to tail). Given the compactness of the *S. pombe* genome, it might not be surprising to have some overlapping transcription. Using the same tiling array, Wilhelm et al. estimated the mean 3' UTR length to be 152nt (Wilhelm et al., 2008). Notably, many of these 3'UTR antisense RNAs were extremely long, as long as several kilobases in some cases. Most antisense RNAs from both groups covered the entire CDS of the sense genes (Figure 3.2 A and B). We did not find antisense RNAs originating from 5'UTRs of neighboring divergent genes. In summary, we found around 500 long polyadenylated antisense RNAs and two major sources for these antisense RNAs: discrete transcription units and long 3'UTRs.

2.2 Many middle meiotic genes have abundant antisense RNAs in vegetative cells

Do cells benefit from antisense RNAs? Or are antisense RNAs simply products of random transcription with no function? To probe these questions, we first asked what genes have antisense RNAs in vegetative cells. We calculated two values for each annotated CDS: one for the sense strand and one for the antisense strand. The value is the average probe intensity of all the probes in the CDS on the sense or on the antisense strand. Visual inspection of antisense RNAs in vegetative cells revealed that most antisense RNAs overlap with a large portion of the sense gene CDS.

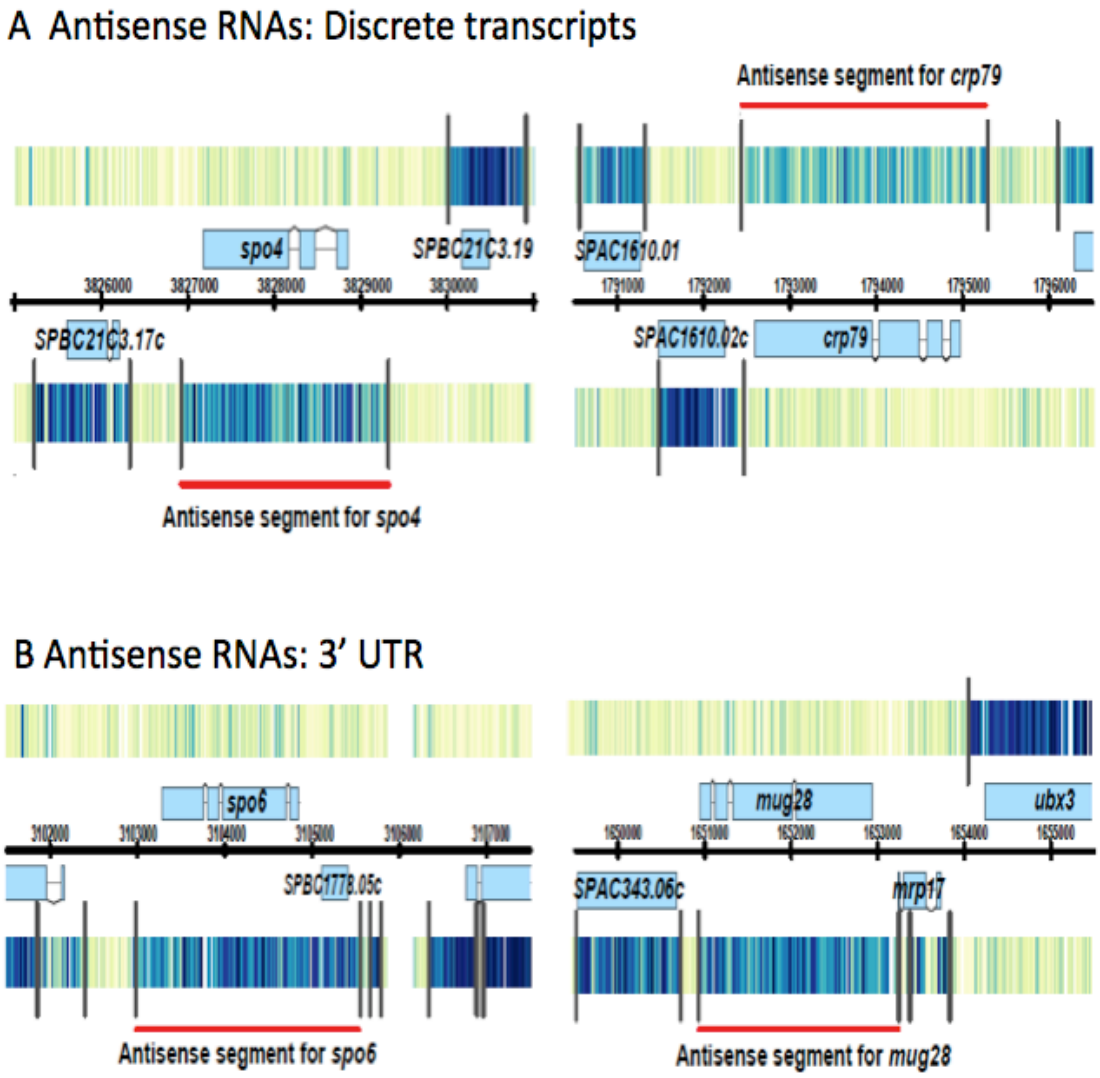

Figure 3.2 Origins of antisense RNAs. 6kb window view for each of four genes that associate with abundant antisense RNAs in vegetative cells. The antisense RNAs are labeled with red lines. (A) The antisense RNAs of *spo4* and *crp79* are discrete transcript units that do not connect with other features (note: *spo4* located on the top strand and *crp79* located on the bottom strand). (B) The antisense RNA of *spo6* and *mug28* are 3' UTR of the adjacent genes SPBC1778.05c and *mrp17,* respectively. These 3' UTR are unusually long.

However, there were exceptions in which antisense RNAs were shorter than their overlapping CDSs on the opposite strand and the level of these short antisense RNAs were underestimated using this average probe intensity method (see below, Figure 3.5). The sense and antisense values were viewed using a dot plot in which the x-axis represented sense and y-axis represented antisense signal intensity. This plot shows the majority of genes have much stronger sense signal than antisense signal in vegetative cells as expected (Figure 3.3 A).

A small group of genes in vegetative cells displayed the opposite behavior and showed low sense signal (<1, average sense = 2.93, mean= 2.98) and relatively high antisense signal (>0.5, average antisense = 0.42, mean= 0.28). GO term analysis of this special group of 117 genes found a significant enrichment of meiotic genes (30%, $p<e^{-6}$), especially genes annotated as meiotic M phase (Princeton, GO). Although 70% of the genes were not annotated as meiotic genes, many of them were also induced during meiosis (data not shown). Only 10 out of the 117 genes did not increase at the transcript level during meiosis. We concluded that in vegetative cells the genes that associate with abundant antisense RNAs are mainly genes for meiosis.

We excluded those genes that had high antisense (>0.5) and also high sense (>1) levels from the GO term analysis. This is because it has been shown that increased chromatin accessibility or high local concentrations of transcription apparatus due to sense RNA transcription permits transcription of spurious antisense RNA (Dutrow et al., 2008). Moreover, Rdp1, the RNA dependent RNA polymerase, can synthesize antisense RNA using the sense RNA as template. Consistent with this, we found that some antisense RNAs decreased in the *rdp1Δ* strain (data not shown).

2.3 Antisense RNAs that overlap with middle meiotic genes decrease during meiosis

We wanted to track how the antisense RNAs behave during meiosis. Antisense RNA changed in the RNA level and in the transcript boundaries in meiotic conditions. For some genes, the antisense RNA level dropped dramatically during meiosis and made it difficult to call the transcript boundary. As an example, the antisense RNA of *crp79* was largely reduced at 4hr meiosis and reappeared at 6hr meiosis with different transcript boundaries (Figure 3.4).

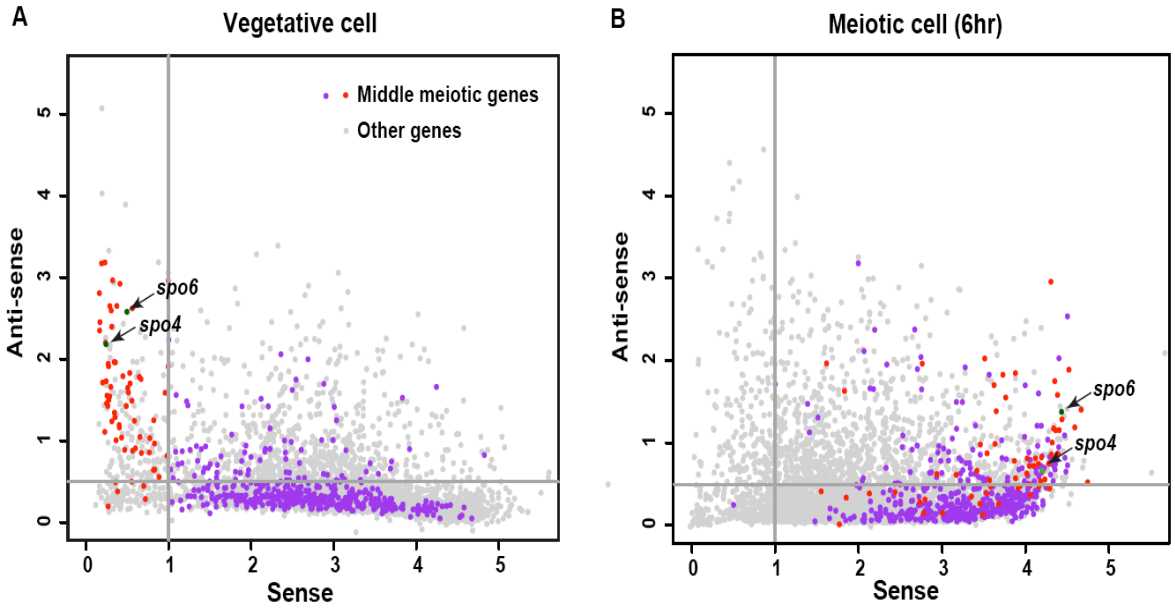

Figure 3.3 Middle meiosis-specific genes are associated with high antisense RNAs in vegetative cells. Each dot represents one gene; the x-axis and y-axis indicated the sense and antisense RNA level, respectively. Previously identified Mei4-dependent middle meiotic genes are shown as blue or red dots. Blue genes had sense RNA levels above 1 in vegetative cells, while red genes had very low sense RNA levels. The two meiotic genes, *spo4* and *spo6,* that were studied in detail in this work are labeled. Other genes are shown as grey dots. (A) Asynchronous vegetative cells. Sense expression levels distributed across a wide range. Antisense RNA level was generally much lower than the sense RNA for a given gene. Mei4-dependent middle meiotic genes were over-represented in the group that had high antisense (>0.5) and low sense (<1) RNA. (B) Middle meiotic cells (6hr). At middle meiosis, these middle meiotic genes were highly induced (as the blue and red dots shifted extensively toward the right). The antisense RNA level for meiosis-specific middle genes had a decreased level (as the red dots shifted toward the bottom).

This reappearance of antisense RNA at the time that the sense RNA was highly transcribed is consistent with the previously suggested connection between spurious antisense RNA transcription and open chromatin. Because the boundary of antisense RNAs often change or do not exist during meiosis, it is technically challenging to track which antisense RNA in vegetative cells corresponds to which antisense RNA in meiotic conditions. To present the changes of sense and antisense RNA levels during meiosis, we used the average probe intensity method described above (Figure 3.3 B). Overall, we observed a negative correlation for the changes between sense and antisense RNA level for all genes during meiosis (-0.221). This suggests that sense and antisense transcription are, to some extent, mutually suppressive. Because the action of sense transcription and the action of antisense transcription compete for the common DNA template, transcription interference is one likely reason for this mutual suppression (see discussion).

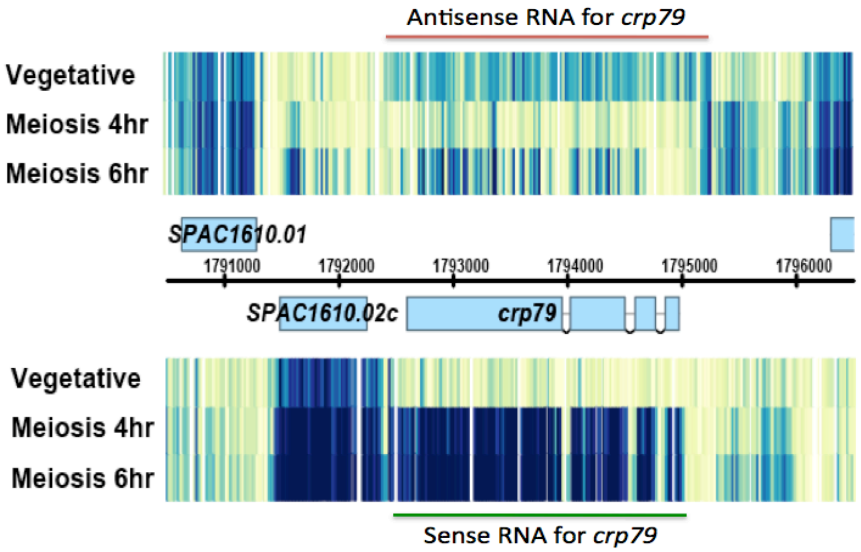

Figure 3.4 Behavior of sense and antisense RNAs of *crp79*. In vegetative cells, *crp79* had abundant antisense RNA but no sense RNA. At 4hr meiosis, the antisense largely decreased and sense RNA appeared. At 6hr meiosis, the antisense RNA reappeared.

About 500 genes that are induced above 4-fold during middle meiosis and are classified as middle meiotic genes (Mata et al., 2002). Mei4, the meiotic forkhead transcription factor, is essential for induction of almost all middle meiotic genes (Mata et al., 2007). In the scatter plots (Figure 3.3 A and B) all the Mei4-induced middle meiotic genes are colored blue or red (*spo4* and *spo6* are colored green). Although designated middle meiotic genes, the blue-colored genes have substantial expression level (sense RNA >1) in vegetative cells. This blue group contains genes required for mitosis, including mitosis activators, condensin complex, spindle pole body complex and mitotic kinases (Mata et al., 2007). These genes are shared genes for nuclear division event during mitotic and meiotic M phase. The red-colored genes had very low expression level in vegetative cells. This red group contains "meiosis-specific" genes, such as s*po4* and *spo6*, the meiotic Cdc7-like kinase and regulatory factor (Nakamura et al., 2002), *mug28* and *crp79*, two meiotic RNA-binding proteins. These genes have extremely low sense RNA in vegetative cells (see Figure 3.2 and 3.3 A). After separation the two groups of middle meiotic genes it became apparent that the meiosis-specific middle meiotic genes have the most abundant antisense transcripts in vegetative cells. For the meiosis-specific genes, the negative correlation between sense and antisense RNA level was more pronounced (6hr = -0.453), reflecting the drastic increasing of sense RNA level and decreasing of antisense RNA level during meiosis.

2.4 Genes for spore wall synthesis have internal bi-directional transcription

As mentioned earlier, some antisense RNAs do not encompass the entire genes on the sense strand in vegetative cells. Using the average probe intensity method, these genes did not pass the antisense >0.5 threshold and were not included in the above analysis. An interesting subset of these genes was also induced highly at middle meiosis and was required for spore wall synthesis. In particular, these genes were important for carbohydrate metabolism, including *bgs2*, (meiosis-specific 1,3-β-glucan synthase) (Liu et al., 2000; Martin et al., 2000), *aah2* (α-amylase) and SPAC1039.11c (predicted α-glycosidase). In vegetative cells, these genes had internal bi-directional transcription that produced two non-overlapping RNAs, one on the sense strand and one on the antisense strand (Figure 3.5). The sense transcripts of these meiotic genes in vegetative cells were

truncated, lacking a big portion of the 5' ORF. At middle meiosis the internal bi-directional transcription was inactivated. Moreover, the functional promoters for these meiotic genes were activated and full-length sense transcripts were made. Notably, the meiotic promoter of SPAC1039.11c also induced bi-directional transcription during meiosis and generates new ncRNA (Figure 3.5 C). The meiotic promoter of *aah2* seemed to activate *aah2* together with the adjacent gene *mok11*, in the divergent direction (head to head). *mok11* is an alpha-1,3-glucan synthase, which also functions in spore wall formation (Garcia et al., 2006). This sharing of meiotic promoter rendered identical transcription induction timing for *aah2* and *mok11*.

We wondered what causes the internal bi-direction transcription. One straightforward possibility is that a DNA motif located inside of these genes induced bi-directional transcription. To test this idea, we retrieved 400nt of DNA sequence, centered at the middle position of the 5' starts of the two divergent transcripts, from each of these three genes that have clear internal bi-directional transcription. These sequences were the input data set for motif search program MEME and one hexamer motif (ACGCTC) was found in all three input sequences, with no base substitution ($p=1.33e^{-4}$) (This motif was marked as intP, internal promoter, in Figure 3.5). This motif was further analyzed using GOMO (Gene Ontology for MOtifs), which took the input motif and scored only the promoter region of every gene in the *S. pombe* genome and determined which GO terms were associated with the input motif. This search returned a highly significant GO term for ribosomal component (GOMO score=7.379 e^{-10}).

In mitotic cell cycle, cells need to produce large quantity of proteins for dividing into daughter cells. Meiotic cells might demand less protein synthesis and therefore less ribosome synthesis. We analyzed our meiotic time course data and found that indeed the majority of ribosomal subunits had a decreasing RNA levels during meiosis (data not shown).

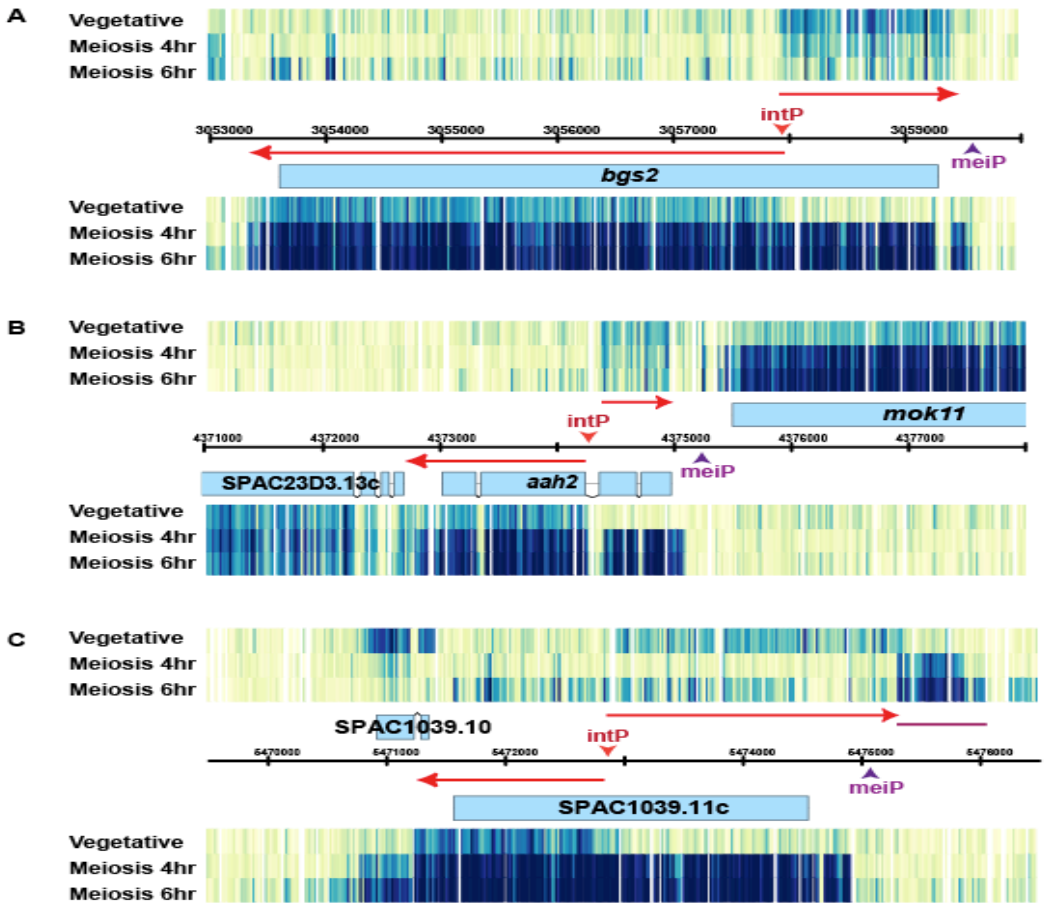

Figure 3.5 Meiotic genes for spore wall synthesis have internal bi-directional transcription in vegetative cells. 7kb window views for each of the three meiotic genes are shown: (A) *bgs2,* (B) *aah2* and (C) SPAC1039.11c. For each gene, transcription initiated from an internal start site generated a 5' truncated sense RNA and a divergent non-coding antisense RNA in vegetative cells. The motif (ACGCTC) that might drive the bi-directional transcription was labeled as intP, internal promoter. During meiosis, the internal promoters seemed to be inactivated and the meiotic promoters, marked as meiP, were activated. This resulted in decreasing of antisense RNAs and transcribing of full-length sense RNAs. The meiotic promoter of SPAC1039.11c (C) possibly induced bidirectional transcription that generated new non-coding RNAs (underlined by a violet line) during meiosis. Similarly, the meiotic promoter of *aah2* (B) also induced bi-directional transcription that induced sense transcription of two meiotic genes, *aah2* and *mok11*.

We hypothesize that this hexamer motif in vegetative cells recruits trans-factor(s) for double functions: transcribing ribosomal genes and inhibiting a set of meiotic genes. In meiosis, this trans-factor(s) is inactivated, and thus reduces ribosome synthesis and also removes the inhibition for this group of meiotic genes.

2.5 Disruption of antisense RNA allows sense RNA expression

Given that many middle meiotic genes are associated with high level antisense RNAs in vegetative cells and that many of these antisense RNAs decrease during meiosis (see Figure 3.3 for genome-wide analysis and Figure 3.6 for Northern blot analysis on individual genes), it seems likely that these antisense RNAs regulate meiotic genes. To test if antisense RNAs prevent transcription of middle meiotic genes in vegetative cells, we planned to disrupt antisense transcription by insertion of an effective terminator derived from *ura4* (Aranda and Proudfoot, 1999). Insertion of the *ura4* terminator will block antisense transcription only if the antisense RNA seen on the tiling array is a continuous RNA and is made by RNA polymerase II. Northern blot analysis shows that the antisense RNA for *spo6* (Figure 3.7 B) and other middle meiotic genes (Figure 3.6) are long RNAs with sizes corresponding to the tiling array segmentation results. To make the antisense disruption strain we inserted the *ura4* terminator into SPBC1778.05c, the neighbor gene to *spo6* and the source of antisense RNA for *spo6* (see Figure 3.2 B for tiling array data and Figure 3.6 A for strain construction). This strain was named *spo6*-AS-KO1 (KO1 in short). We analyzed the *spo6* sense and antisense RNA level from WT vegetative cells, meiotic cells and the KO1 vegetative cells using radioactive PCR (Figure 3.6 C). A decreased antisense RNA level was observed in the KO1 strain, indicating that the terminator blocked some antisense transcription. Importantly, the sense RNA for *spo6* appeared in the KO1 strain, where in the WT vegetative cells the sense RNA was below the detection limit. However, the *spo6* sense RNA level in the KO1 strain was very low compared to meiotic cells. This suggests that the maximum *spo6* sense RNA expression depends on meiosis-specific transcription induction and the antisense RNA in vegetative cells is to prevent the basal expression of *spo6*.

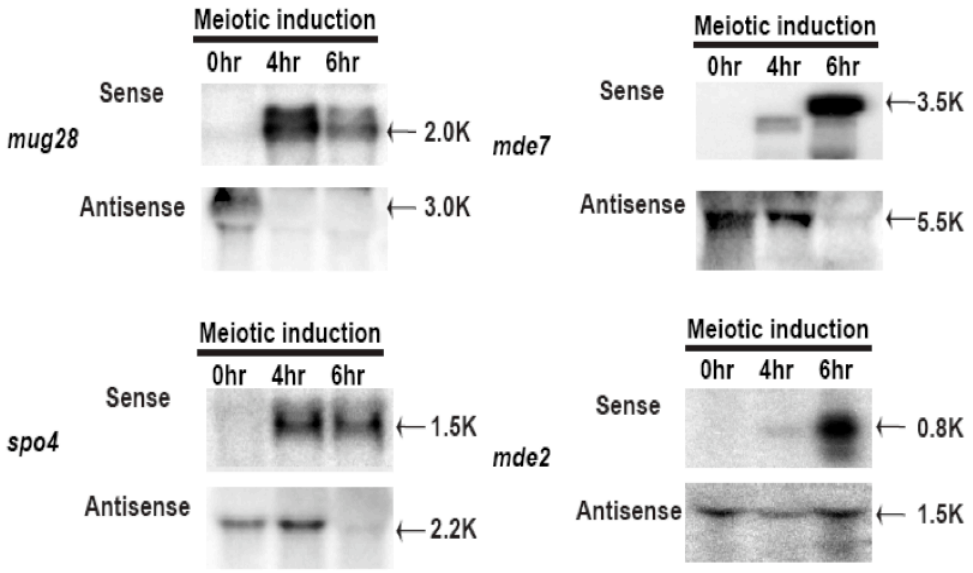

Figure 3.6 Antisense RNAs of middle meiotic genes decrease during meiosis. Northern blot shows that antisense RNAs of four genes are long RNAs and are longer than the corresponding sense RNAs. These antisense RNAs generally decreased during meiosis. One exception, the antisense RNA for *mde2* remained through out middle meiosis. The sense RNAs for these four genes showed different induction timing: *mug28* was induced earlier; *mde7* and *mde2* were induced later. This suggests that even these genes are all classified as "middle" meiotic genes and are all induced by Mei4, they are likely be regulated by other mechanisms (or combinational of mechanisms) for sequential expression timing. Also note that the sense RNA for *mug28* had two major forms in meiosis and the sense RNA for *mde7* was longer in 6hr meiosis than in 4hr meiosis, reflecting alternative 3' end processing during meiosis.

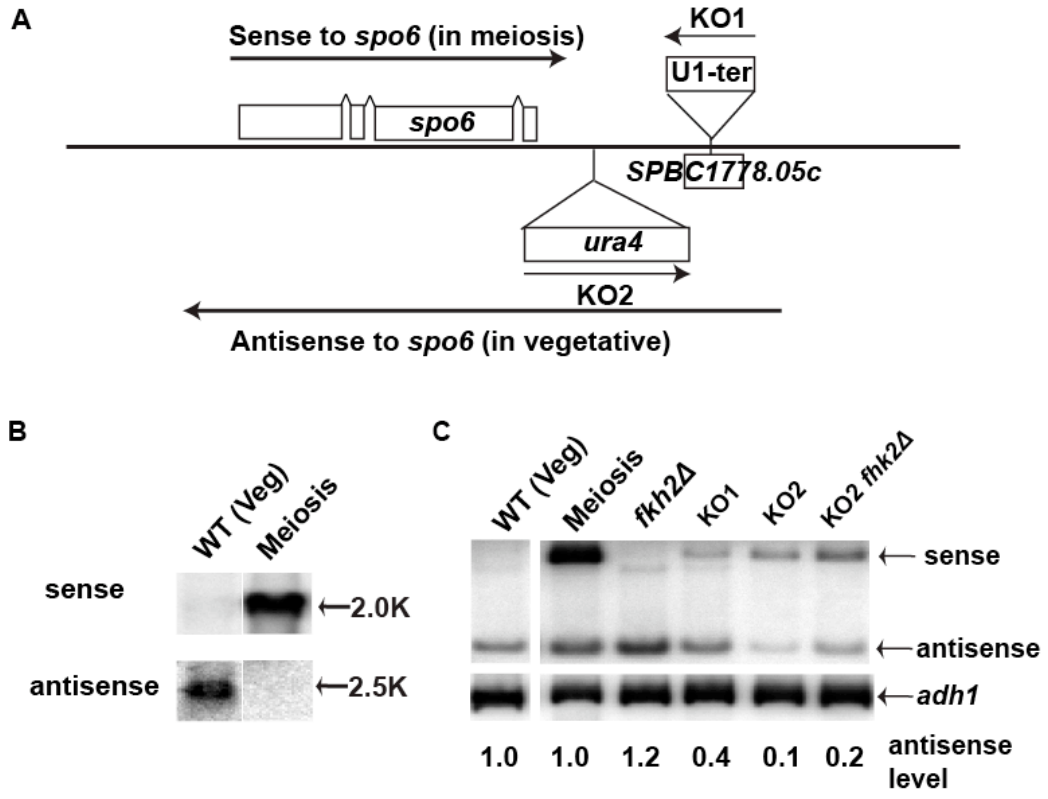

Figure 3.7 Disruption of antisense transcription allows *spo6* sense transcription in vegetative cells. (A) Illustration of *spo6* antisense disruption strains. Arrow above *spo6* represented the sense RNA (arrow was aligned to the transcript start and stop positions shown by Affymetrix tiling array. Figure 3.2). Arrow below *spo6* represented the antisense RNA, which originated from the 3'UTR of SPBC1178.05c. Two antisense knockout strains were constructed. KO1: insertion of the U1 terminator into SPBC1778.05c and the RNA of SPBC1778.05c would terminate at the U1 terminator. KO2: insertion of *ura4* cassette (promoter-*ura4*-terminator) between *spo6* and SPBC1778.05c in the same transcription direction as s*po6*. This transcription of *ura4* would interfere with transcription of SPBC1778.05c and decrease the antisense RNA. (B) Northern blot showed that *spo6* sense RNA is absent in vegetative cells and highly expressed in meiotic cells (6hr), whereas the antisense RNA have the opposite expression pattern. (C) Radioactive PCR detection of sense and antisense RNA. *adh1* was included as internal control. Antisense RNAs decrease in both antisense KO strains and sense RNAs appears. Fkh2 has minimum effect on *spo6* sense and antisense transcription. The antisense RNA level was quantified and Normalized to *adh1* to show the fold change. The fold change was not shown for sense RNA because there was no detectable sense RNA in vegetative cells.

A potential complication in the interpretation of this result is that inserting a terminator might change the chromatin structure at the 3' end of *spo6* and consequently alter the expression of *spo6.* Therefore, the increased sense RNA could be unrelated to the antisense disruption. Taking this into account, the terminator insertion in the KO1 strain was far from the mature 3' end of s*po6*. Moreover, a second antisense disruption strain (*spo6*-AS-KO2) was constructed with the whole *ura4* cassette (promoter-*ura4*-terminator) inserted downstream of *spo6* in the convergent orientation to the antisense RNA. Rather then causing early termination of antisense RNA in the KO1 strain, this KO2 strain was expected to decrease antisense RNA by transcription interference. As the KO1, the antisense RNA level decreased and sense RNA level increased in the KO2 strain comparing to WT strain. Some antisense production remained in the antisense disruption strains. It is likely that the U1 terminator did not terminate efficiently in the KO1 context and/or that cryptic transcription initiation sites were activated in the disruption constructs.

The same antisense disruption strategies were used to block antisense RNA for two other middle meiotic genes, *spo4* and *mug28* (Figure 3.8). For both genes, the antisense RNA decreased in the AS-KO strains and some low level of sense RNA became apparent. Based on these results, we concluded that these antisense RNAs prevents basal level transcription of middle meiotic genes in vegetative cells.

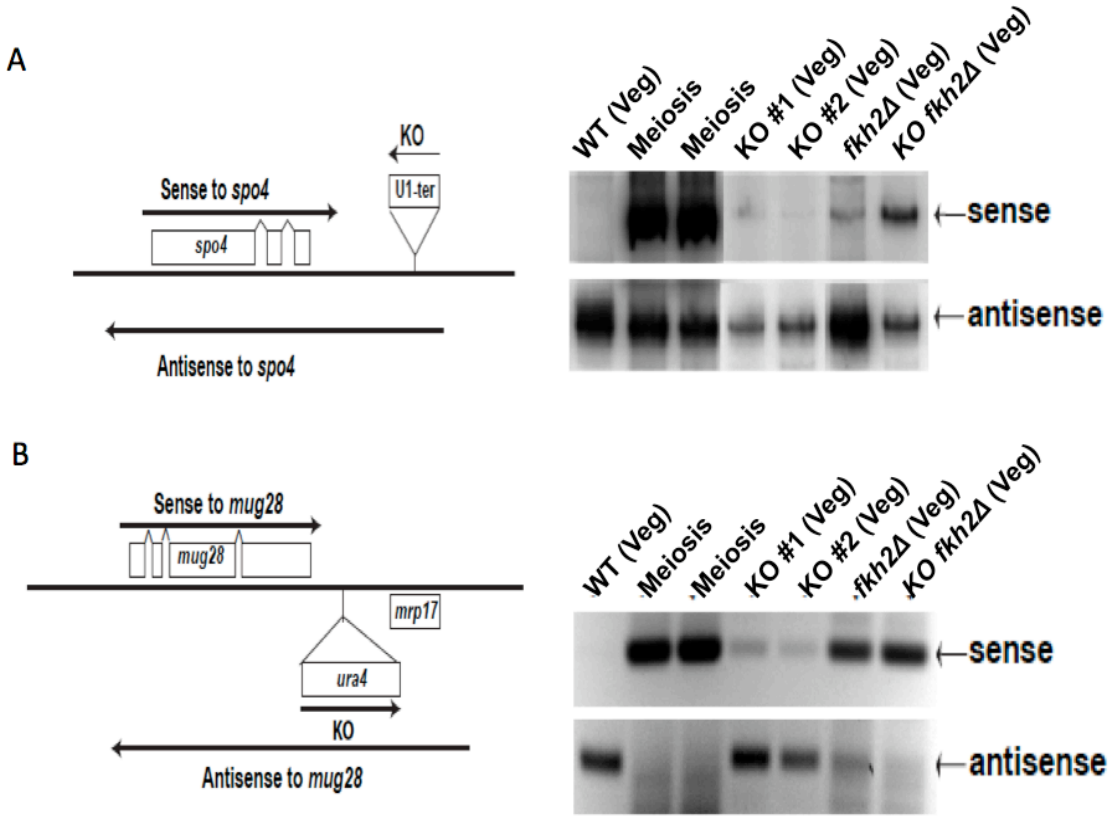

Figure 3.8 Disruption of antisense transcription allows *spo4* and *mug28* sense transcription in vegetative cells. (A) Left: illustration of *spo4* antisense disruption strain. U1 terminator was inserted in the same orientation as *spo4* antisense transcription at the 5' of the antisense coding region (same as *spo6*-AS-KO1). Right: RNA from two independent KO transformants was analyzed (KO #1 and KO #2). Antisense RNA decreased and sense RNA increased in the KO strains. Deletion of *fkh2* also allowed low level of *spo4* sense RNA expression. Sense RNA level became more abundant in the strain with both antisense disrupted and *fkh2Δ*. (B) Left: illustration of *mug28* antisense disruption strain. The *ura4* cassette (promoter-*ura4*-terminator) was inserted between *mug28* and *mrp17* in the same transcription direction as *mug28* (same as *spo6*-AS-KO2). The results of *mug28* were very similar to the results of *spo4* besides that *mug28* sense transcription was much apparent in the *fkh2Δ*.

2.6 Meiotic antisense RNAs generate "unspliced-like" signal in splicing assay

Many intron containing meiotic genes have been categorized as undergoing "meiosis-specific splicing" (Averbeck et al., 2005; Kishida et al., 1994; Moldon et al., 2008). That is, these genes are transcribed in vegetative cells, however, their introns remain unspliced. In meiosis, these introns are spliced corresponding to their functional timing. Most of the splicing studies in yeast applied non-strand specific RT-PCR based splicing assays with primer pair across the intron of interest, including the report from our laboratory. The spliced product is smaller than the unspliced product on the gel. However, antisense RNAs that do not have matching introns (some antisense RNAs have introns, but not at the same position as introns on the sense strand) can generate unspliced-like PCR product in the RT-PCR based splicing assay. Another method, high-throughput sequencing was used to assay genome-wide splicing efficiency in S. pombe (Wilhelm et al., 2008). In that research, the authors found a large number of differentially spliced introns, among these 254 introns were spliced more efficiently in meiosis and 478 introns were spliced less efficiently in meiosis. However, the sample preparation for this sequencing also involved PCR amplification and lost the strand specificity information. The unspliced signal from RT-PCR and sequencing can be originated from either unspliced sense RNA or from antisense RNA.

Spo6 was reported to undergo meiosis-specific splicing using both assays (Averbeck et al., 2005; Wilhelm et al., 2008). Notably, using the non-strand specific splicing assay the unspliced signal for *spo6* in vegetative cells was very intense (Figurer 3.9, right panel). However, inspection of strand specific tiling array (Figure 3.2) and Northern blot data (Figure 3.7) indicates that there was no detectable *spo6* sense RNA, while the antisense RNA was expressed in vegetative cells. Thus, the "unspliced" signal from *spo6* in vegetative cells must originate from the antisense RNA. Similar results were obtained for other middle meiotic genes: *spo4, mug28, crp79, mde6* and *meu31* (Figure 3.9, right panel). These results do not entirely refute meiosis-specific splicing, because the sense RNA in vegetative cells can be very scarce and unspliced. To detect the sense RNA in vegetative cells, we devised a strand specific RT-PCR splicing assay (see method) that only amplifies the sense strand. Using this method, we do not detect unspliced sense RNA in vegetative cells for all six genes tested, and for some genes

(*spo6, mug28, crp79* and *mde6*) there was a low level of the spliced form (Figure 5, left panel 0hr). Mei4, the meiotic forkhead transcription factor, transcriptionally induces these middle meiotic genes during meiosis (Mata et al., 2007). In vegetative cells Mei4 is absent. This suggests that under both low and high transcription levels these middle meiotic genes were spliced efficiently. Our data contradicts the previously suggested linkage between transcription and splicing efficiencies (Wilhelm et al., 2008).

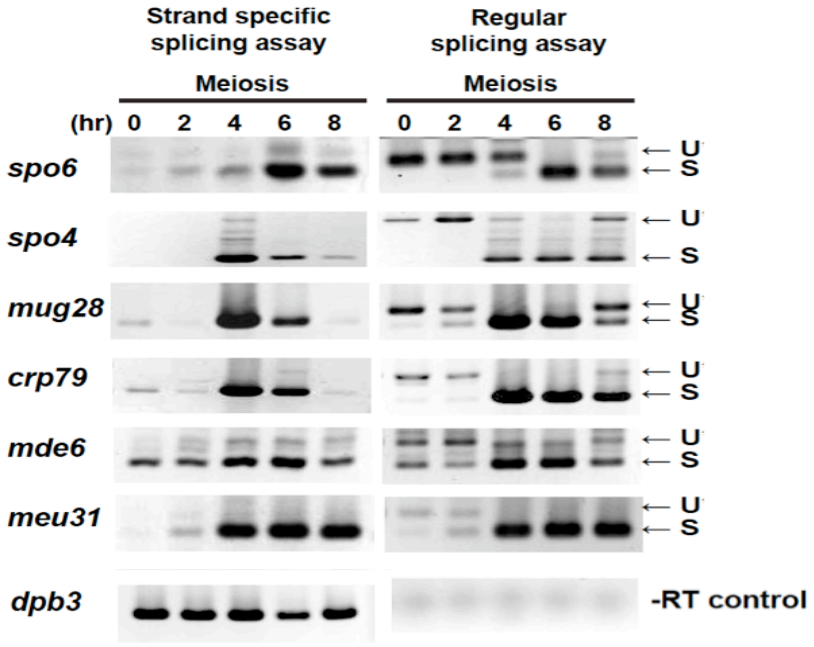

Figure 3.9 Meiosis-specific splicing does not apply to middle meiotic genes. Left: strand-specific splicing assay. Right: regular (non-strand specific) splicing assay. RNA was isolated from vegetative cells (0hr) and cells under meiotic induction for 2-8hr. The same RNA was used in both splicing assays. Six middle meiotic genes and one internal control, *dpb3*, were analyzed. Dpb3 level indicated equal loading and –RT (minus reverse transcriptase) indicated that samples were not contaminated with genomic DNA. The regular splicing assay shows the unspliced form for all six genes in vegetative cells and early meiotic cells (2 and 4hr), while there was no unspliced form detected on the same RNA samples using the strand specific splicing assay.

We examined the sense and antisense RNA levels in vegetative cells for all meiotic genes that had been reported as splicing regulated. In fact, all "splicing regulated" middle meiotic genes have predominant antisense RNA in vegetative cells (Figure 3.10). For these genes the "unspliced" signal in the non-strand specific splicing assay reflects the presence of antisense RNA and the "spliced" signal reflects the sense RNA. On the other hand, half of the splicing regulated early meiotic genes were not associated with abundant antisense RNAs in vegetative cells. We confirmed meiosis-specific splicing for four early meiotic genes and examined the splicing regulation mechanism (McPheeters et al., 2009; Chapter 2, and unpublished results).

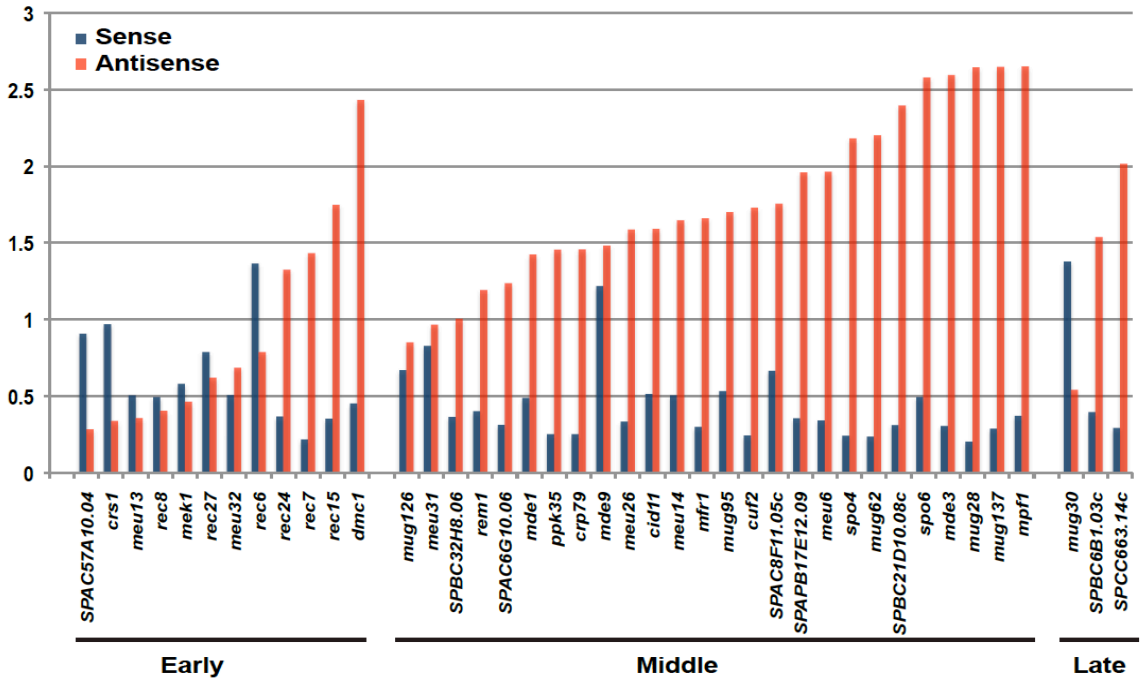

Figure 3.10 Most "splicing regulated" genes associate with abundant antisense RNA in vegetative cells. All genes that were classified as meiosis-specific splicing regulated were shown here (Averbeck et al., 2005; Kishida et al., 1994; Moldon et al., 2008; our unplublished data). Genes were separated into three groups, early, middle and late, according to their expression time. Each gene had two values, one for sense RNA (blue bar) and one for antisense RNA (red bar). The values were calculated using average probe intensity method on vegetative data. All of the middle meiotic genes had higher antisense RNA level than the sense RNA in vegetative cells. For these genes, the splicing results acquired from non-strand specific splicing assay were significantly complicated by the presence of antisense RNA.

2.7 Fkh2 suppresses sense transcription of middle meiotic genes in vegetative cells

Four genes code for forkhead transcription factors in S. pombe: *mei4* is expressed only in meiosis, while *fkh2*, *sep1* and *fhl1* are expressed in vegetative cells. The core DNA binding motif (GTAAAYA) for forkhead transcription factors is well conserved in fission yeast (Horie et al., 1998; Oliva et al., 2005) and likely across species (Kaufmann et al., 1994; Pierrou et al., 1994). *Fhl1* is different from the other three forkheads in that it is most similar to S. cerevisiae *FHL1*, a gene that regulates mainly and possible solely ribosomal proteins (Rudra et al., 2005; Wade et al., 2004). Mei4 induces genes that are expressed at meiotic M phase (MI and MII). Sep1 and Fkh2 seem to function together to regulate expression of genes for mitotic M (Oliva et al., 2005; Rustici et al., 2004). Some genes are shared between mitotic and meiotic M phase (like the blue-colored genes in Figure 3.3), but there are many meiotic M phase genes that are specifically expressed in meiosis (like the red-colored genes). An apparent dilemma is that how Sep1 and Fkh2 selectively activate genes function in mitotic M phase but leave meiosis-specific M phase genes, which may have similar forkhead binding motifs, inactivate in vegetative cells. Little is known about how forkhead transcription factors choose among similar binding motifs. Nevertheless, some forkheads can function as transcriptional repressors, rather than activators. For example, in *S. pombe* deletion of *fkh2* allows higher expression levels of *sep1*-dependent M phase genes (Rustici et al., 2004) and in *S. cerevisiae FKH2* null rescues the lethality of an *NDD1* mutant, a positive regulator for mitotic M phase genes (Koranda et al., 2000). Based on these observations, we hypothesized that in vegetative cells the forkhead transcription factors, especially Fkh2, may prevent untimely transcription of Mei4-induced middle meiotic genes.

A study on the relationship between transcription factors and splicing efficiency incidentally shed light on our hypothesis (Moldon et al., 2008). In the report, the authors found that deletion of *fkh2*, but not *sep1* or *fhl1*, allowed accumulation of spliced forms of several middle meiotic genes in vegetative cells. We now know that many of these genes associate with antisense RNAs, which appear as the unspliced form in the non-strand specific splicing assay. It is likely that the appearance of spliced PCR products in the *fkh2Δ* strain reflects the fact that Fkh2 represses sense transcription of these genes rather than splicing, in vegetative cells.

To study which repression mechanism *fkh2* employs, we generated tiling array data using an *fkh2Δ mei4Δ* mutant strain. The reason for deleting *mei4* in this experiment is that *mei4* has two forkhead binding motifs in the promoter region (Abe and Shimoda, 2000). If Fkh2-mediated repression involves forkhead binding motifs, *mei4* is likely to be one of the genes influenced by Fkh2. Microarray analysis shows 229 genes had increased sense RNA level in *fkh2Δ mei4Δ* mutant (cutoff: *fkh2Δ mei4Δ* -WT >1) and many of these genes were also induced during middle meiosis (Figure 3.11). For example, *crp79* and *mug28*, the two genes that encode meiosis-specific RNA binding proteins, showed no sense RNA in vegetative cells and evident expression in the *fkh2Δ mei4Δ* strain (Figure 3.12 B). This supports our hypothesis that *fkh2* represses sense transcription of middle meiotic genes as opposed to repressing splicing.

Having found that both disruption of antisense RNA and deletion of *fkh2* allow some sense transcription of middle meiotic genes, we wondered if the two mechanisms work together to achieve the maximum repression on the same gene. To test this, we generated strains that carrying the antisense KO allele and *fkh2Δ* allele and assayed the sense and antisense RNA levels. For all three genes tested, the sense RNA level was higher in the double mutant strain comparing to either antisense KO or to *fkh2Δ* alone (Figure 3.7 and 3.8, last lane). We conclude that antisense RNA and Fkh2 work in concert, but likely through unrelated mechanisms, to repress middle meiotic genes in vegetative cells.

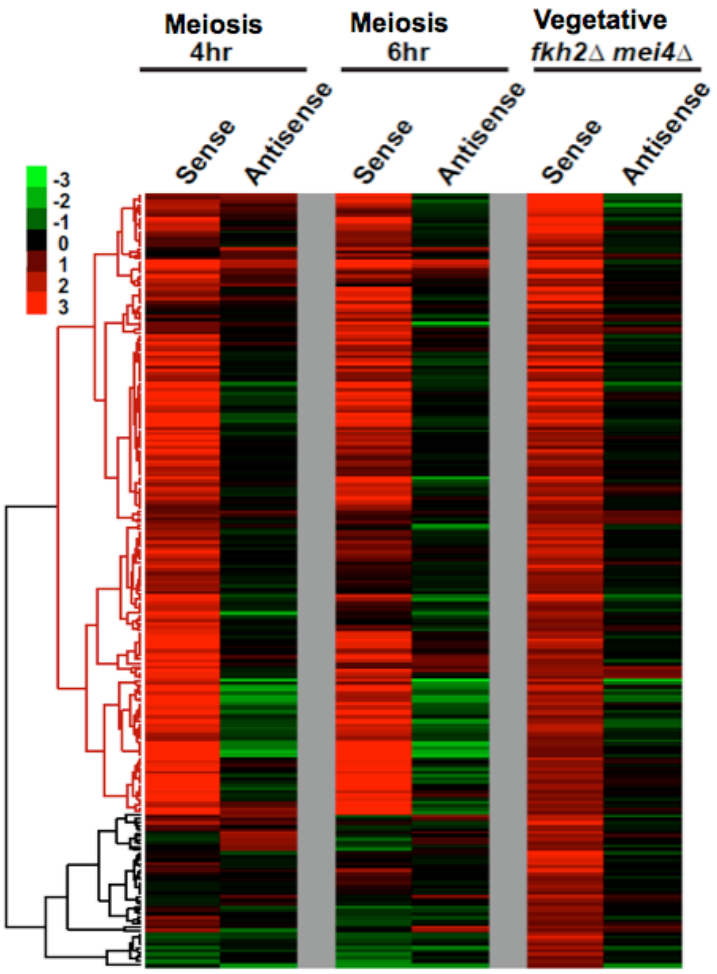

Figure 3.11 Fkh2 represses expression of middle meiotic genes. Expression level for sense and antisense RNA was calculated using the average probe intensity method mentioned above. The data are the difference between sample and vegetative cell (e.g., meiosis 4hr sense level – vegetative sense level). 229 genes that were induced in the *fkh2Δ mei4Δ* strain are shown (cutoff: *fkh2Δ mei4Δ* -WT >1). Data from meiosis 4hr, 6hr and *fkh2Δ mei4Δ* strain was hierarchical clustered. Over 75% of these genes were also induced in middle meiosis.

2.8 RNAi pathway and heterochromatin formation are not involved in antisense-mediated repression

We next investigated the molecular mechanism of antisense-mediated repression. One possibility is that these antisense RNAs are processed into small RNAs by the RNAi pathway. Subsequently, the small RNA can repress sense RNAs level by directly interacting with sense RNA (post-transcriptional gene silencing or PTGS) and/or by inducing heterochromatin formation and then repressing sense transcription (RNA induced gene silencing or RIGS) (review in (Almeida and Allshire, 2005)). To examine the involvement of the RNAi pathway in this antisense-mediated regulation, we assayed the sense and antisense RNA level of four middle meiotic genes that have abundant antisense RNA in the mutants that affect major components of the RNAi pathway. These mutants were *ago1Δ* (Argonaute), *dcr1Δ* (Dicer) and *rdp1Δ* (RNA-dependent RNA polymerase). The four genes tested were *spo4*, *spo6*, *mug28* and *crp79* (Figure 3.12). None of the RNAi mutants affected the sense RNA level for *spo4*, *mug28* and *crp79*. Notably, the sense signal was elevated only for *spo6* and only in the *rdp1Δ* strain. This suggests that the general RNAi pathway is not the main mechanism for this antisense-mediated repression. Consistent with this view, a recent report identifying Ago1-associated small RNAs by high through-put sequencing did not find any small RNAs derived from these four genes and did not show an enrichment for antisense RNA-associated middle meiotic genes (Buhler et al., 2008). The effect of *rdp1* on *spo6* repression is likely to be independent of the RNAi pathway (see discussion).

The RNAi pathway is essential for heterochromatin formation and gene silencing at centromeres, but is dispensable at other heterochromatic loci such as telomeres or silent mating-type loci (reviewed in (Grewal and Elgin, 2007)). Hence, the antisense-mediated repression could cause heterochromatin formation on middle meiotic genes independent of the RNAi pathway. This would predict that an enrichment of heterochromatin landmarks would be present at these middle meiotic gene loci. Cam et al. published a comprehensive mapping of heterochromatin landmarks, including H3K9me and its interacting chromodomain protein Swi6, using ChIP-on-chip of vegetative cells provides answers to this prediction (Cam et al., 2005). They observed that H3K9me and Swi6 associate mainly with major heterochromatic loci including

centromeres, subtelomeres, the *mat* locus and ribosomal DNA repeats. They also detected a few heterochromatic 'islands' corresponded to meiotic induced genes, including Mei4 (see discussion). However, none of these heterochromatic 'islands' associates with notable antisense transcripts in vegetative cells. We concluded that the antisense-mediated repression of middle meiotic genes is largely independent of heterochromatin formation.

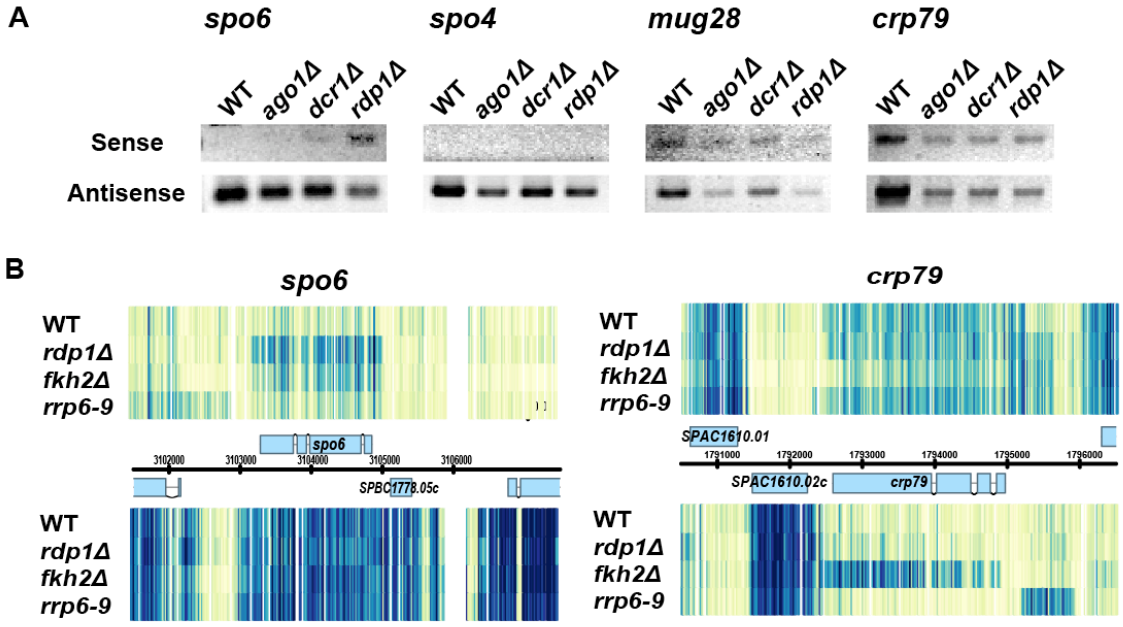

Figure 3.12 RNAi machinery is not involved in antisense-mediated repression. (a) Testing the sense and antisense RNA level in RNAi mutants, a*go1Δ*, *dcr1Δ* and *rdp1Δ,* using radioactive PCR. These mutants did not affect the sense RNA level for *spo4*, *mug28* and *crp79*. Only *spo6* sense RNA was induced in *rdp1Δ* strain. (B) Tiling array data confirmed that *spo6* was induced in the *rdp1Δ* (left panel), and *crp79* was not affected by *rdp1* (right panel). In the *fkh2Δ mei4Δ* strain (shown as *fkh2Δ* in the figure), the sense RNA for *spo6* was only slightly elevated, whereas *crp79* sense RNA was clearly induced. Note that sense RNA for both genes did not accumulate in *rrp6-9 mei4Δ* strain (shown as *rrp6-9* in the figure, *rrp6* codes for the major nuclear 3' to 5' exosomal exonuclease).

2.9 New antisense RNAs appear during meiosis

During meiosis, the antisense RNAs for meiotic genes generally decreased. On the contrary, many new antisense RNAs for non-meiotic genes emerged. We inspected the new antisense RNA that had the induction levels in our 6hr meiotic sample (cutoff: 6hr-veg >2, 48 genes). The sense and antisense RNA level for the genes associated with meiosis-induced antisense RNA also showed a strong inverse correlation (-0.399), suggesting that meiosis-nduced antisense RNA may interfere with sense transcription. The antisense RNAs in meiosis were generally long RNAs and overlapping with the entire ORF of the gene on the sense strand, similar to the antisense RNAs observed in vegetative cell. The source of the antisense RNA in meiosis can be divided into two categories: Mei4 motif related (41/48, 85.4%) and non-related (7/48, 14.6%) (Figure 3.13). The Mei4 motif related antisense can be sub-divided into 5 groups: (1) the motif induced bi-directional transcription, in one direction made into meiotic RNA and in the other direction made into antisense RNA; (2) the motif induced only antisense RNA; (Liu et al.) Mei4 induced gene with long 3'UTR; (4) Mei4 induced gene with long 5'UTR and (5) meiotic gene overlapping with the other gene. The unique features of meiosis-induced antisense RNA argues that Mei4 plays dual roles in meiosis: to activate middle meiotic genes and to repress a selective subset of non-meiotic genes, located close to the meiotic genes, by inducing antisense RNA expression. In addition, some meiosis-induced antisense RNAs might have been scored as "unspliced" sense RNA (see Figure 3.13 A3) and mistakenly lead to the conclusion that splicing efficiency of these genes decreases during meiosis (Wilhelm et al., 2008).

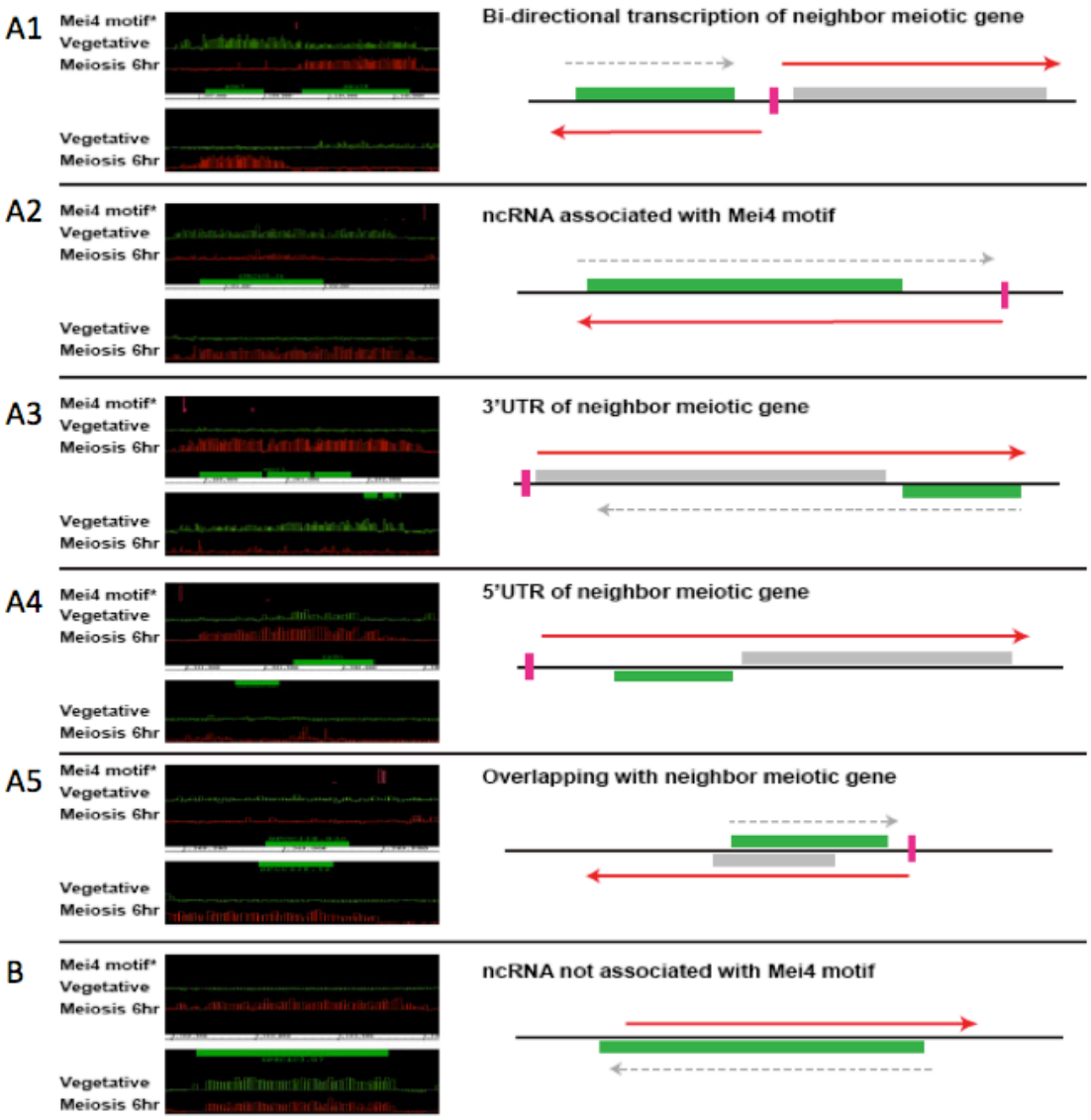

Figure 3.13 Origins of antisense RNAs in meiotic cells. A1 to A5: antisense RNA associates with predicted Mei4 binding motif. B: antisense RNA not associates with Mei4 motif. Left panel: Tiling array data of vegetative cells (shown in green) and meiotic cells (shown in red). The predicted Mei4 binding site was shown in the top row. Right: cartoon presentation of the tiling array data. Gene that associates with antisense RNA in meiosis (green box), meiotic gene (grey box), predicted Mei4 binding site (pink bar), RNA in vegetative cells (grey dash arrow) and RNA in meiotic cells (red arrow). The consensus forkhead binding motif GTAAAYA was used to predict Mei4 binding sites. The motif was scored between 0 to 4; no match to perfect match.

III. Discussion

Cells perceive and respond to external signals in order to make decisions for their fates, whether the decision is to divide mitotically, to form gametes, to develop into a different cell type or to die. Each decision relies on appropriate gene expression profiles, which involves activation of some genes and repression of other genes. To this end, cells employ a variety of transcriptional activation and repression mechanisms. The simplest form of repression is not to make activators, than the genes are not activated and energy is conserved. However, widespread transcription (Wilhelm et al., 2008) suggests that transcription can be rather spontaneous (i.e., activator is not required) or that activators sometimes activate off-target loci. Therefore, to prevent genes that are deleterious for current cell fate decision from expression, more vigorous repression mechanisms are evolved. In this report, we provided the first genome-wide evidence that *S. pombe* utilized two repression mechanisms to keep meiotic genes off in vegetative cells.

Repression by antisense transcription

We observed that many meiotic genes had predominant antisense RNA in vegetative cells and the level of these antisense RNAs often decreased during meiosis. This observation led to the idea that antisense RNA keeps meiotic genes off in vegetative cells. Supporting this idea, disruption the synthesis of antisense RNA allowed sense RNA to express. This repression may dependent on the action of antisense transcription, the product of antisense transcription or a combination of both (for recent review, see (Werner and Sayer, 2009). Antisense RNA can repress a gene by directly binding to the sense RNA and reducing its stability. For this to occur, the sense RNA has to be transcribed at the first place. We did not have evidence that any of the four genes tested in this study were transcribed and then repressed by the lack of stability in vegetative cells, since the sense RNA of these genes did not accumulate in the strains carrying mutation alleles of *rrp6* and *dis3*, the two major 3' to 5' exonucleases that degrade unstable RNAs (see Figure 3.12 B for results of *rrp6-9* on two genes. Data not shown for *dis3* mutant.) Because these four genes were likely not transcribed, it is improbable that a duplex of sense and antisense RNA was formed and processed by the RNAi machinery into siRNA (small interfering RNA). Consistent with this view, the repression of these

four genes sustained in *ago1Δ* and *dcr1Δ* mutants (Figure 3.12 A). In addition, there was no apparent correlation between Ago1-associated siRNA identified by genome wide study (Buhler et al., 2008) and antisense RNAs identified by us. Collectively, these data suggests that the RNAi pathway is not involved in the antisense-mediated repression. An exception is that *spo6* sense RNA was elevated in *rdp1Δ* strain. The repression of *spo6* by Rdp1 was independent to the classical RNAi machinery because *ago1Δ* or *dcr1Δ* did not exhibit the same effect as *rdp1Δ*. Rdp1 functionally divergent from Ago1 and Dcr1 in regulating cell cycle events was reported (Carmichael et al., 2004). *spo6* may provide another example where the components of the RNAi machinery function differently. An important next step is to understand how Rdp1 represses *spo6* and if the repression depends on antisense RNAs.

We also evaluated the involvement of heterochromatin-mediated gene silencing. Genome-wide association analysis between heterochromatic markers, H3K9 methylation and its interacting protein Swi6/HP-1 (Cam et al., 2005), and antisense RNAs did not reveal any correlation, suggesting that these antisense RNAs do not induce heterochromatin formation. Antisense RNA induced epigenetic modification was the strategy of choice to suppress *PHO84* in aged *S. cerevisiae* cells, where the antisense RNA is required for recruiting histone deacetylase, HDAC, to the promoter of *PHO84* (Camblong et al., 2007). In the case of *PHO84*, the antisense-mediated histone deacetylation is to turn off transcribing gene that associated with acetylated histone. For non-transcribing meiotic genes in vegetative cells, such mechanism is less likely to be involved.

The action of transcription can directly influence another transcription of a neighbor or overlapping DNA locus in *cis* by a mechanism termed transcription interference. This mechanism is utilized by *S. cerevisiae* in regulating meiotic entry in a cell-type specific manner (Hongay et al., 2006). In haploid cell the meiotic gene *IME4* is repressed by antisense transcription, where in diploid cell the diploid-specific repressor represses *IME4* antisense and allows *IME4* expression (Hongay et al., 2006). The antisense RNA is not required since transcription of *IME4* antisense RNA in *trans* did not repress *IME4* expression. The ~2.5kb polyadenylated antisense RNA starts at the 3' UTR and terminates at the promoter region of *IME4* (Hongay et al., 2006). There are many

similarities between *IME4* antisense RNA and antisense RNAs identified in our research. Meiotic antisense RNAs in *S. pombe* are polyadenylated long RNA, and many of them encompass the entire CDS and promoter of the corresponding sense genes. The polyA tail suggests that these antisense RNA are products of RNA pol II. In fact, half of these long antisense RNAs are 3' UTR of convergent genes that are transcribed by RNA pol II. The feature of these antisense RNAs suggests two repression schemes. First, the antisense transcription may prevent the transcription activator from recognizing the sense promoter (promoter occlusion model, (Adhya and Gottesman, 1982). Second, if sense transcription was initiated, collision between converging RNA polymerases would lead to premature termination (collision model, (Prescott and Proudfoot, 2002). Depending of the promoter strength of each pair of sense and antisense, these two schemes may occur separately or in combination on different genes.

Many new antisense RNAs appear in meiosis and Mei4 possibly induces most of them. An interesting pair of genes is *mug28* and *mrp17*, which encode meiotic RNA-binding protein and mitochondria ribosomal subunit, respectively. In vegetative cells, the 3'UTR of *mrp17* was the antisense RNA to *mug28* (Figure 3.2) and repressed *mug28* expression (Figure 3.8). When *mug28* was induced in meiosis, the 3'UTR of *mug28* covered *mrp17* (data not shown) and possibly also represses transcription of *mrp17*. This observation suggests that the organization of genes on the genome may provide yet another level of regulation. The abundance of antisense RNA for meiotic genes has been recently reported in other yeast species (Yassour et al., 2010). Collectively, these researches suggest that antisense RNAs may be a general mechanism in regulating cell differentiation.

Repression by *Fkh2*

The SPBC16G5.15c gene of *S. pombe* was named as *fkh2* owing to its protein similarity to the *FKH2* gene of *S. cerevisiae*. In both yeasts, forkhead transcription factors regulate cell cycle at the G2/M phase transition (Bulmer et al., 2004; Koranda et al., 2000; Kumar et al., 2000), and in both yeasts, *fkh2/FKH2* has been implicated in negatively regulating some G2/M genes (Bulmer et al., 2004; Koranda et al., 2000). In *S. pombe,* the mRNA expression of two M phase genes*, cdc15* and *spo12*, are very much

increased and lost normal cell cycle periodicity in *fkh2Δ* strain, suggesting that Fkh2 is required for their repression in order to maintain the periodicity (Bulmer et al., 2004). In this report, we identified that the RNA level of 229 genes accumulated significantly in *fkh2Δ* and many of these genes also accumulated during meiosis, suggesting that Fkh2 represses these meiotically up-regulated genes in vegetative cells (Figure 3.11).

Fkh2 contains two signature domains, the FKH domain for DNA binding and the FHA (forkhead-associated) domain for protein-protein interaction. One possible scheme for Fkh2-mediated repression is that Fkh2 binds to the target genes through the interaction between the FKH domain and a "DNA motif" on the target genes. We attempted to identify such motif in two ways; search specifically for a motif in the promoter region of genes that accumulated in *fkh2Δ* using MEME and search for motif, anywhere in the gene, that correlates with gene expression level in *fkh2Δ* using FIRE. None of these approaches returned significant result, not even the conserved forkhead-binding motif (GTAAAYA). We currently do not know if Fkh2 exerts its function through binding to the target promoter. Whether or not Fkh2 binds to the promoter region of its target genes, such as *cdc15* and *spo12*, is under debate (Bulmer et al., 2004). Genome-wide Fkh2 binding experiment might be a good way to settle this debate and provide insight into Fkh2-mediated repression. With current technologies, we expect such data set will soon emerge.

The FHA domain interacts with phosphorylated proteins (Mahajan et al., 2008). In budding yeast the Mcm1-Fkh2 complex at target promoter of G2/M genes does not trigger transcription. Transcription is activated when the co-activator, Ndd1, is phosphorylated and recruited to the Mcm1-Fkh2 complex in a cell cycle-dependent manner (Darieva et al., 2006; Reynolds et al., 2003). It is hard to classify Fkh2 as either activator or repressor; the net function of Fkh2 possibly depends on the proteins it is bound to, its post-translational modification and other factors. We expect that the FHA domain has a role in the Fkh2-mediated repression in *S. pombe*. However, the detail underlying such repression remains to be answered.

Besides cell cycle regulation in yeasts, forkhead transcription factors in higher eukaryotes have been linked with a number of cellular processes including cell cycle, embryogenesis and cell differentiation (Cirillo and Barton, 2008). Therefore, it is likely

that understanding the molecular mechanism of Fkh2 in *S. pombe* will yield insight into the regulation of this important transcription family in mammals.

Transcription repression in gene expression timing control

The meiotic genes are classified by the peak induction time into three temporal classes: early (2-4hr after meiotic induction, premeiotic S phase and recombination), middle (4-6hr, meiotic divisions) and late (6hr and later, spore formation). There are many steps that occur in each stage. For example, the sequential (and partially overlapped) chromosome morphologies in middle meiosis are: chromosome condensation, chiasmata formation between non-sister chromatids, microtubules attachment to the kinetochore, first round of chromosome separation, and repeat most of the steps with some modifications for second round of division. The genes that instruct these events need to be expressed in correct sequence for proper meiosis. Surprisingly, Mei4 is the only transcription factor required to induce almost all middle meiotic genes (about 500 genes); deletion of *mei4* impaired the up-regulation of almost all middle meiotic genes during meiosis and over expression of Mei4 induced more then 60% of these genes in vegetative cells (Mata et al., 2007). How does a single transcription factor manage the sequential expression of middle meiotic genes? We now can image several possibilities. First, the promoter sequence of each gene is different, and depends on the DNA sequence it may attract Mei4 with different kinetics. Second, like Fkh2, Mei4 may interact with different co-activators at different promoters, and the interaction timing with the co-activators decides expression timing of different genes. Third, antisense transcription may help fine-tune gene expression timing through promoter occlusion or collision. In fact, the expression timing of the four genes that we studied was different (Figure 3.14). *crp79* and *mug28*, which encode RNA biding proteins that may regulates the RNA stability of other middle meiotic genes (Amorim et al., 2010; Shigehisa et al., 2010) were expressed earlier then *spo4* and *spo6*, the meiotic kinase and its regulatory partner, that are required for second meiotic division. Interestingly, the induction timing for sense RNA was parallel with the decline of antisense RNA; the antisense RNA for *crp79* and *mug28* declined earlier then *spo4* and *spo6* (Figure 3.14). This observation implies that regulation of antisense RNA transcription may in turn regulate the sense

RNA transcription timing. However, we cannot exclude the possibility that the decline of antisense RNA is a result of induction of sense RNA transcription. Fourth, transcriptional repression by Fkh2 for each gene may be de-repressed with different kinetics during meiosis. Consistent with this, the accuracy of meiotic division is compromised in *fkh2Δ* strain, where aberrant asci with two spores are often observed (Szilagyi et al., 2005). Two-spored asci can be generated through several ways, such as proceeding second meiotic chromosome division without the first division (Klapholz and Esposito, 1980). Notably, the mRNA level of *fkh2* accumulates during meiosis, suggesting a role in meiotic M phase progression. However, what the role is in general or what the roles are for specific genes needs further investigation.

It is interesting to note that the mRNA expression of *mei4* is regulated by very different mechanisms compared to the genes regulated by Mei4. First of all, unlike many meiosis-specific middle genes, there was no detectable *mei4* antisense RNA in vegetative cells. We speculated that Fkh2 might repress *mei4* in vegetative cells and that deletion of *fkh2* might allow *mei4* mRNA accumulation. However, *mei4* expression seemed to be irrelevant to Fkh2-mediated repression since tiling array analysis of *fkh2Δ* strain (not *fkh2Δ mei4Δ* strain) did not show accumulated *mei4* mRNA level. Mei4 is regulated at least by three mechanisms. In vegetative cells the *mei4* gene locus is coated with heterochromatic markers, H3K9me and Swi6, suggesting that the transcription of *mei4* is repressed by condensed chromatin structure (Cam et al., 2005). *mei4* is not entirely shut off by heterochromatin. Some *mei4* mRNAs are transcribed in vegetative cells, but these RNAs are rapidly degraded by exonuclease Rrp6 through a mechanism involving aberrant polyadenylation (Harigaya et al., 2006; Yamanaka et al., 2010). The target genes for this polyadenylation-mediated mechanism are mostly early meiotic genes, and this mechanism is removed at early meiosis (Harigaya et al., 2006). This is consistent with the observation that the expression of *mei4* occurs before the expression of the majority of middle meiotic genes. Finally, Mei4 positively auto regulates itself (Abe and Shimoda, 2000) which might generate a Mei4 protein gradient (from low to high) along the mid meiosis time line (from early to late). One can image that the gradient of Mei4 can cooperate with the promoter sequences of different Mei4-target genes and the combinatorial effects will help define the sequential gene expression patterns.

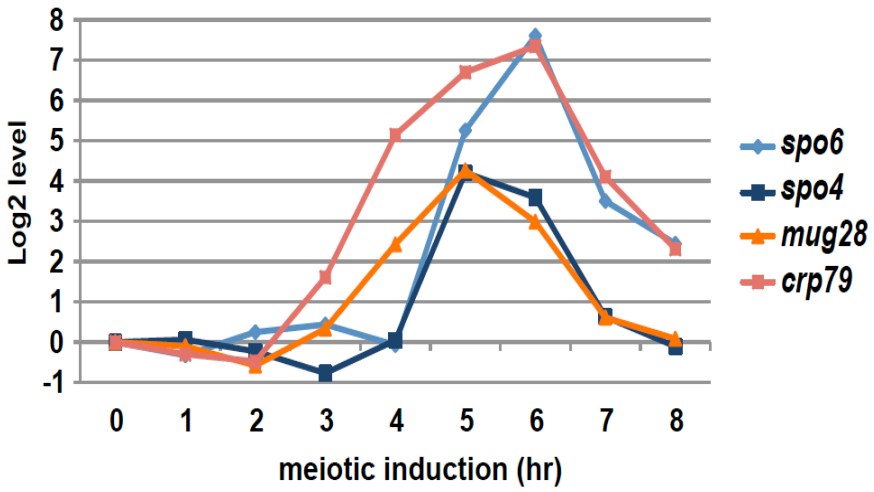

Figure 3.14 Meiotic genes are induced at different kinetics. Expression microarray data of the four meiotic genes studied in this chapter were shown. 0hr was the vegetative cells. The y-axis presented the log2 scale. *crp79* and *mug28* were induced earlier that *spo4* and *spo6*.

Concluding remarks

Ironically, I started this research with the meiosis-specific splicing story in mind. I analyzed the splicing status of 650 genes by RT-PCR in many conditions. RT-PCR based splicing assay was chosen over microarray-based splicing assay because the level of these meiotic genes is very low in vegetative cells, and this low signal intensity will be significantly influenced by microarray-related noise. Using various approaches, I and others had found many meiotic genes are "splicing regulated". However, with the new tiling array data and strand-specific splicing assay, we now believe that these once called "splicing regulated" genes are regulated by antisense transcription. Unexpectedly, this "hypothetical splicing regulation" led me to investigate novel gene repression mechanisms of meiotic genes using genome-wide approach.

It is increasingly clear that cells rely on multiple repression mechanisms to control gene expression. Various reports from yeasts to plants to mammals had linked transcriptional repression with cell growth, cell differentiation and many diseases (for reviews, see (Krogan and Long, 2009; Perissi et al., 2010). Future challenges lie in understanding the molecular details of each repression mechanism and the interplay of

these mechanisms. We suggest that using a genome-wide approach will be a crucial tool to understand the complex transcription network. Simple eukaryotic organisms, such as *S. cerevisiae* and *S. pombe*, may provide the most suitable research environments.

Table 3.1 Strains used in Chapter 3. Strain names in parenthesis are the original name from the requested laboratory or from Yeast Genetic Resource Center (YGRC, Japan, FY strains).

Strain Name	Genotype	Reference/Source
JLP988	*h⁻ ade6-M216 leu1-32 his7-366 ura4-D18*	Lab stock
F277 (FY16057)	*h⁺/h⁺ pat1-114/pat1-114 ade6-M210/ade6-M216*	YGRC
JLP1486	*h⁻ spo6*-AS-KO1 *ade6-M216 leu1-32 his7-366 ura4-D18*	This work
JLP1673	*h⁻ spo6*-AS-KO2 *ade6-M216 leu1-32 his7-366 ura4-D18*	This work
JLP1675	*h⁻ spo4*-AS-KO *ade6-M216 leu1-32 his7-366 ura4-D18*	This work
JLP1677	*h⁻ mug28*-AS-KO *ade6-M216 leu1-32 his7-366 ura4-D18*	This work
JLP1674	*h⁻ spo6*-AS-KO2 *fkh2::ura4⁺ ade6-M216 leu1-32 his7-366 ura4-D18*	This work
JLP1676	*h⁻ spo4*-AS-KO *fkh2::ura4⁺ ade6-M216 leu1-32 his7-366 ura4-D18*	This work
JLP1678	*h⁻ mug28*-AS-KO *fkh2::ura4⁺ ade6-M216 leu1-32 his7-366 ura4-D18*	This work
JLP1501	*h⁻ fkh2::ura4⁺ ade6-M210 leu1-32 ura4-D18*	This work *
JLP1500	*h⁻ fkh2::ura4⁺mei4::ura4⁺ ade6-M210 leu1-32 ura4-D18*	This work
JLP1503	*h⁻ rrp6-9-GFP <<kan^r mei4::ura4⁺ ade6-M210 leu1-32 ura4-D18*	This work **
F322 (yFS316)	*h⁺ ago1::kanMX leu1-32 ura4-? ade6-210 adh1:gfp*	(Sigova et al., 2004)

F323 (yFS317)	*h⁻ rdp1::kanMX leu1-32 ura4-? ade6-210 adh1:gfp*	(Sigova et al., 2004)
F324 (yFS318)	*h⁻ dcr1::kanMX leu1-32 ura4-? adh1:gfp*	(Sigova et al., 2004)

* The original *fkh2::ura4*$^{+}$ allele was requested from Dr. Gould.

** The original *rrp6-9-GFP <<kan*^{r} allele was requested from Dr. Yamamoto (Harigaya et al., 2006).

Supplemental Table 3.2 Primers used in Chapter 3.

AS-KO strains construction		
pSC-*ura4*	*ura4*_Pro_*Hind*III	CCCAAGCTTAGCTACAAATCCCACTGGCTA
	*ura4*_Ter_*EcoR*I	GGAATTCGTGATATTGACGAAACTTTTTGAC
pSC-ter-*ura4*	*ura4*-Ter-U15'-*BamH*I	CGGGATCCGGGAATAAAAAGTAATTTGCTATAG
	ura4-Ter-U13'-*HindIII*	CCCAAGCTTGTGATATTGACGAAACTTTTGAC
spo6-AS-KO1	c1778.05c_5'F2_*Xba*I	GCTCTAGATCAGATACCAAACTGCGTAG
	c1778.05c_5'R_*BamH*I	CGGGATCCATCAATTGAAATGGCGGCTA
	c1778.05c_3'_F_*EcoR*I	GGAATTCCCCATTATTATTAGGGATTGTTGG
	c1778.05c_3'_R2_*Xho*I	CCGCTCGAGGTGTGTTGGTGCGTCAAATC
p*Rep41*-c1778.05c	c1778.05c-*Xho*I-ATG	CCGCTCGAGATGTATTCACTTTATACTGCAACCA
	c1778.05c-*BamH*I-Stop	CGGGATCCTTAGACTGGTTTTCCAAGCGTG
spo6-AS-KO2	*ura4*_Pro	AGCTACAAATCCCACTGGCTA
	*ura4*_Ter	GTGATATTGACGAAACTTTTTGAC
	spo6-exo3F	ACCTAATGCCTTCGATGCAG
	spo6-150R-*ura4*P	GCATACATATAGCCAGTGGGATTTGTAGCTACATCATTATATTGTTAATTTTCTCTTC
	spo6-150F-*ura4*T	TTAGATGTCAAAAAGTTTCGTCAATATCACGTTGTAGCATTCTTTTCTTAAAC
	spo6-441R	TTGAGTTTGAAAGGGGGAAA
spo4-AS-	*spo4*-KO5'F-*Xba*I	GCTCTAGAAACGCACGATAGCACCTTTT

KO	*spo4*-KO5'R-*BamH*I	CGGGATCCCGGTCAAATACTAAGTACAG
	spo4-KO3'F-*Sal*I	ACGCGTCGACATTCGCTTTTCTCACGTGCT
	spo4-KO3'R-*Xho*I	CCGCTCGAGAGCCATTGACTTGTTGGACA
mug28-AS-KO	*mug28*-KO5'F	GCATACATATAGCCAGTGGGATTTGTAGC TTCAACCGTTGTTAACGACTCC
	mug28-KO5'R-*ura4*P	CGCCCTCTCTAACAATTCCA
	mug28-KO3'F-*ura4*T	TTAGATGTCAAAAAGTTTCGTCAATATCA CGGACAGCTCTGCGAATATTTTT
	mug28-KO3'R	GCGGTAATACCTCGTTTTTGC

Splicing assay

For each gene, primers were listed in the following order: (1) strand–specific cDNA synthesis, (2) forward primer for both splicing assays and (3) reverse primer for regular splicing assay. P1 primer was used as reverse primer for strand-specific splicing assay.

spo6	SSS-P1-*spo6*	GGTCACCTTGATCTGAAGCCGTCGGATTAGCAAAAA CAAA
	spo6-exo3F	ACCTAATGCCTTCGATGCAG
	spo6-exo4R	CGTCGGATTAGCAAAAACAAA
spo4	SSS-P1-*spo4*	GGTCACCTTGATCTGAAGCGCTGTTTTGGCCTTTACT CG
	spo4-A10L	CCTCCAGAGGGTTACTTGCTAC
	spo4-exo3R	GCTGTTTTGGCCTTTACTCG
mug28	SSS-P1-*mug28*	GGTCACCTTGATCTGAAGCAAATGGATTTGGCAAAG CAG
	mug28-exo1F	GCCAAAGCTCAGATCTTCA
	mug28-exo4R	AAATGGATTTGGCAAAGCAG
crp79	SSS-P1-*crp79*	GGTCACCTTGATCTGAAGCGGCTGGATGATTTTGCT GAT
	crp79-exo1F	GTCCCCGGACAGTATGAAGA
	crp79-exo4R	GGCTGGATGATTTTGCTGAT
mde6	SSS-P1-*mde6*	GGTCACCTTGATCTGAAGCGCGCATTCCAAAATAAA

		GGA
	mde6-exo4F	TGGTTTTGAACAGCGAAACA
	mde6-2RC9	CGTTCCACTAAAAGCATCCAA
meu31	SSS-P1-*meu31*	GGTCACCTTGATCTGAAGCAGAAGGCATCAATCGTGGAC
	meu31-3LC4	GCATAAGTGAAATCGGCAAA
	meu31-3RC4	GAAGAAGGCATCAATCGTGG
dpb3	*dpb3*-5'F	GCAGATTTCCTGTTGCTCGT
	dpb3-3'R	ACGCGGAAGAGGCTTCACTA
P1		GGTCACCTTGATCTGAAGC
Semi-quantitative PCR		
Primer for sense cDNA synthesis (SSS-P1-*gene*) and forward primer for sense strands PCR were list above. Primers were listed in the following order: antisense strand cDNA synthesis and forward primer for antisense strand PCR. P1 and P2 primer were used as reverse PCR primer for sense and antisense strand, respectively.		
spo6	SSS-P2-*spo6*	GCTTCAGATCAAGGTGACCACCTAATGCCTTCGATGCAG
	spo6-exo3F	ACCTAATGCCTTCGATGCAG
spo4	SSS-P2-*spo4*	GCTTCAGATCAAGGTGACCAGCCATTGACTTGTTGGACA
	spo4-exo3R	GCTGTTTTGGCCTTTACTCG
mug28	SSS-P2-*mug28*	GCTTCAGATCAAGGTGACCTGAAAAATTTCACGCCATTG
	mug28-exo4R	AAATGGATTTGGCAAAGCAG
crp79	SSS-P2-*crp79*	GCTTCAGATCAAGGTGACCAGCTTATGGCCTTTCCCATC
	crp79-exo4R	GGCTGGATGATTTTGCTGAT
P2		GCTTCAGATCAAGGTGACC
IVT		
The following PCR products were inserted into pSCA-K vector (Invotrogen) for IVT		

template preparation (see method).		
spo6	*spo6*-exo3F/*spo6*-exo4R (see above)	
spo4	*spo4*-A10L/*spo4*-exo3R (see above)	
mug28	*mug28*-exo1F/*mug28*-exo4R (see above)	
mde7	*mde7*-3'F	AAGTGGAAGCCTATGCCAGA
	mde7-3'R	GGATGCCTTTGCTGAGTAGC
mde2	*mde2*-5'F	AAATGGAGCCGTGAAATCAG
	mde2-3'R	TGCACAACTTTCGTTCCTCA

IV. Materials and Methods

RT-PCR based splicing assay

Total RNA was isolated using the RiboPure™-Yeast kit (Ambion). 20μg of total RNA was treated with 4 U TURBO DNase in 40μl at 37°C for 1hr (Ambion). cDNA was synthesized from 4μg total RNA using SuperScript III reverse transcriptase (Invitrogen) according to manufacturer's instructions and with addition of 50ng actinomycin D to prevent second strand cDNA synthesis (Ruprecht et al., 1973). cDNA for regular splicing assay was primed with 250ng random hexamer, while cDNA for strand specific splicing assay was primed with 100ng anchored gene-specific primer (gsp). The anchor is a unique sequence at the 5' end of each gsp and we named this anchor as P1. Only the cDNA primed with the anchored gsp would have the P1 sequence, and cDNA primed by DNA and RNA fragments that naturally occur in the RNA sample would lack the P1 sequence. cDNA was digested with 0.3μl 10mg/ml RNaseA and 1U RNaseH at 37°C for 30min to hydrolyze RNA template. To remove unused anchored gsp, cDNA was purified using absorption spin column that removes oligo smaller than 70nt (Qiagen, MiniElute). The final volume of cDNA was adjusted to 40μl and 1μl was used for PCR reaction. Forward and reverse primers across the intron were used for regular splicing assay; the same forward and the P1 reverse primer were used for strand-specific splicing assay. Therefore, the regular splicing assay detected signals from both sense and antisense RNAs, while the strand-specific assay detected only the cDNA converted from the sense RNA. The PCR reaction was resolved by agarose gel electrophoresis and stained with ethidium bromide.

Tiling array sample preparation, hybridization and scanning

400μg of total RNA was mix with 30μg dephased oligo(dT) primers (equal molar (dT)16-(dA/dG), (dT)16-dC(dA/dG/dC)) in a final volume of 300μl and incubated for 5min at 65°C, 2 min on ice and 2 min at room temperature. 90μl 5X First Strand Buffer 22.5μl 0.1M DTT, 18μl 10mM dNTPs and 2mM dUTP, 4.5μl 600μg/μl Actinomycin D (Sigma), 3μl RNasin and 12μl Superscript III RT (Invitrogen) were added to 450μl. Reverse transcription was performed at 42°C for 16hr and 2μl 10mg/ml RNase A and 10U RNase H was added to hydrolyze RNA at 37°C for 30min. Sample was purified

using absorption spin column (Qiagen, QIAquick PCR purification kit). The total recovered cDNA for each sample was between 10-15µg in 90ul.

Purified cDNA was fragmented and labeled. Purified cDNA was fragmented and end labeled. 85µl cDNA, 10ul 10X fragmentation buffer (Affymetrix, GeneChip® WT Double-Stranded DNA Terminal Labeling Kit), 2µl UDG (uracil DNA glycosidase) and 3µl APE1 (apurinic/apyrimidinic endonuclease) were incubated at 37°C for 1hr. To stop the fragmentation reaction, sample was heated to 93°C for 10min and cooled on ice. 93µl of fragmented cDNA was incubated in a reaction containing 30µl 5X TdT buffer, 3µl DNA labeling reagent (Affymertix) and 16µl H_2O at 37°C for 1hr to label the cDNA ends. To stop the labeling reaction, sample was heated to 70°C for 10min and cooled on ice.

For every sample, tiling array hybridizations were performed in triplicate. 150µl hybridization cocktail, which contains 5µg of labeled cDNA, 2.5µl Control Oligo B2 (Affymetrix), 75µl 2X hybridization buffer and 10.5µl DMSO, was prepared for each array cartridge9Affymetrix, S. pombe tiling 1.0FR). Hybridization cocktail was denatured at 99°C for 5 min followed by slow cooling in an air incubator set at 45°C for 5min. 130µl of hybridization cocktail was loaded into the array cartridge and hybridized at 45°C for 16hr with constant rotating at 60rpm. Array was washed and stained as manufacturer instructions (Affymetrix. FS450 fluidic station and FS450_0002 protocol). Array was filled with 160µl Array Holding Buffer and immediately scanned on a GeneChip® Array Scanner (Model 3000-7G). Grids were placed and aligned to raw image files with GeneChip Operating System 1.4 (Affymetrix). The resulting cell level summary files (.cel) were used for analysis.

Tiling array analysis

S. pombe Tiling 1.0 array probe sequences were obtained from Affymetrix. Probes were mapped to Sanger *S. pombe* genome sequence (April 2007 version) using xMAN (Li et al., 2008). Probe intensity files (.cel) that contains the raw intensity were normalized to genomic DNA hybridization to correct probe effects and background correction. Probes that mapped the genome perfectly once were used to correct for probe effects, and subset of these probes, which mapped outside of the CDS were used for

background correction. The normalized data was segmented using Change Point Segmentation Model. Bioconductor package "tilingArray" (Huber et al., 2006) were used for these analyses.

Strain construction

The *ura4* terminator as a direct repeats flanking the selectable marker *ura4* to form the ter-*ura4* cassette (teminator-promoter-*ura4*-terminator) was cloned. The promoter-ura4-terminator sequence was PCR amplified with primers *ura4*-Pro-*Hind*III and *ura4*-Ter-*EcoR*I into pSC-AK (Stratagene) between *Hind*III and *EcoR*I sites; this plasmid was pSC-*Ura4*. The terminator was PCR amplified with primers *ura4*-Ter-U15'-*BamH*I and *ura4*-Ter-U13'-*HindIII* and cloned in front of the ura4 promoter a*t BamH*I and *Hind*III sites of pSC-*ura4*; this plasmid was pSC-ter-*Ura4.*

To make the *Spo6*-AS-KO1 strain, we further cloned upstream and downstream regions that will instruct recombination flanking the ter-*ura4*. The upstream and downstream regions were PCR amplified with primers c1778.05c-5'F2-*Xba*I/c1778.05c-5'R-*BamH*I and c1778.05c-3'F-*EcoR*I/c1778.05c-5' R2-*Xho*I, respectively. The upstream and downstream PCR products were sequentially cloned into pSC-ter-*Ura4* between *Xba*I/*BamH*I and *EcoR*I/*Xho*I sites. This plasmid was digested with *Xba*I and *Xho*I and transformed into WT diploid strain (JLP560). The recombinant would disrupted the SPBC1778.05c, who's 3'UTR is the source of the *spo6* antisense transcript, and carried functional *ura4*. Tetra-dissection of recombinant recovered from minus uracil plates shown two to two segregation of *ura*- and *ura*+ phenotype and all the ura^+ colonies (SPBC1778.05c disrupted, *Spo6*-AS-KO1 strains) were consistently smaller then ura^- colonies (data not shown). This suggests that the sequence orphan SPBC1778.05c was responsible for this slow growth phenotype. SPBC1778.05c was PCR amplified with primers c1778.05c-*Xho*I-ATG/c1778.05c-*BamH*I-Stop and cloned into p*Rep41*-XL between *Xho*I and *BamH*I sites; this plasmid was p*Rep41*-c1778.05c. Transformation of p*Rep41*-c1778.05c into *Spo6*-AS-KO1 strains rescued the slow growing phenotype. This *Spo6*-AS-KO1 strain was counter selected by 5-FOA that removes the *ura4* by recombination between the two direct terminator repeats, leaving a single terminator in the correct place and orientation. This strain was confirmed by Southern blot and

sequencing (data not shown). All experiments with *Spo6*-AS-KO1 strain were complement with p*Rep41*-c1778.05c.

To make the *Spo6*-AS-KO2 strain, we cloned different upstream and downstream regions for recombination flanking *ura4* (promoter-ura4-terminator). Two-step overlapping PCR strategy was used for this construction. First PCR involved three fragments: *ura4*, upstream and downstream regions, and they were PCR amplified with primers *ura4*-pro/*ura4*-ter, *spo6*-exo3F/*spo6*-150R-*ura4*P and s*po6*-150F-*ura4*T/*spo6*-441R. 3' of the upstream fragment and 5' of the ura4 fragments overlapped 30nt and 3' of the ura4 fragment and 5' of the downstream fragment overlapped 30nt. 10 cycles of PCR reaction with equal molar of the three segments were preformed followed another 20 cycles of PCR reaction with the two outer-most primers *spo6*-exo3F/*spo6*-441R. This PCR product was transformed into WT haploid cell (JLP988). Colonies recovered from minus uracil plate were sequencing confirmed (data not shown).

Semi-quantitative RT-PCR

Semi-quantitative PCR with α-^{32}p-dCTP was used for measuring the sense and antisense RNA levels. Sense cDNA and antisense cDNA were synthesized with anchored gene-specific primers that complement to sense or antisense RNA, respectively. The anchor sequence for sense-gsp was P1 and for antisense-gsp was P2. Other cDNA synthesis steps were the same as described above. Each 20μl PCR mixture contained 1μl cDNA and 2μCi α-^{32}p-dCTP. 18 cycles PCR reaction were performed and 5μl of sample was resolved on 5% TBE-acrylamide gel. Desiccated gel was exposed to the Phosphor Storage Screen (Molecular Dynamics). Signals were detected and analyzed using the Phosphoimager Storm system (GE) and ImageQuant software (GE).

Chapter Four: Perspectives and Future Directions

Maintaining the appropriate gene expression pattern for any given cell type at any stage is crucial for the organism. To ensure correct gene expression patterns, cells employ a variety of strategies to repress genes. In this thesis, I present three mechanisms that *S. pombe* utilizes to prevent untimely expression of meiotic genes. All of these mechanisms have been reported in other organisms as well. In this chapter, I highlight interesting recent discoveries in yeasts and in other organisms and describe possible future research directions.

1. Regulation of gene expression by mRNA 3' end formation

mRNA 3' end processing consists in the recognition of poly(A) signals of the pre-mRNAs by a large cleavage/polyadenylation machinery. Several complexes, composed of more than forty proteins in total, are involved in this process in yeast (Keller and Minvielle-Sebastia, 1999; Millevoi and Vagner, 2010). Recent studies indicate that regulation of key 3' end processing protein factors are important for proper developmental processes, especially meiosis, from yeast to plants to mammals (Hornyik et al., 2010; Liu et al., 2007; McPheeters et al., 2009; Yamanaka et al., 2010). In fission yeast, I and others described that Mmi1 interacts with core 3' end processing factors, including RNA15 (Yamanaka et al., 2010) and Pfs2 (Chapter Two). These interactions suggest that Mmi1 is an auxiliary factor of the 3' end processing complexes and Mmi1 may exert its function by modulating 3' end processing. Although the role of Pfs2 in regulating meiotic genes is not resolved in my study, Pfs2 certainly has an important role. Interestingly, the homologs of Pfs2 are also involved in regulation of meiotic progression in plants and in mammalians. During spermatogenesis (male animal meiosis), systematic and progressive lengthening of 3' UTR by alternative poly(A) signals usage had been reported (Ji et al., 2009; Liu et al., 2007). This alternative 3' end processing is likely dictated by the meiosis-specific 3' end processing factor, tauCstF-64 in mouse (Dass et al., 2007) or WDR33 in human (Ito et al., 2001), both are homologs of Pfs2 and both show a testis-specific expression pattern. The mechanism by which these tissue specific factors selectively use distal alternative poly(A) signals (or skip proximal signals) is

largely unknown. In plants and mammals, CstF-50 (cleavage stimulatory factor) has also been suggested to be the functional equivalent to Pfs2 (Ohnacker et al., 2000). Both fission and budding yeasts have only one Pfs2 that is important for both vegetative growth and meiosis. In multi-cellular organisms, functional related proteins have evolved that favor usage of different poly(A) signals in different conditions. While in yeasts, 3' end regulation may be mostly carried out through interaction with auxiliary factors, such as Mmi1.

3' end processing factors also control flower development in Arabidopsis (reviewed in (Hornyik et al., 2010)). Flowering timing is controlled by FLC, a potent transcriptional repressor, which is regulated by two factors involved mRNA 3' end formation, FCA and FY. FY is homologous to Pfs2. As these factors are involved in 3' end formation, it is naturally hypothesized that they influence the 3' processing of *FLC* mRNA. However, no differences in *FLC* mRNA have been found in *FCA* or *FY* mutant plants. The identity of the target RNA regulated by FCA and FY was recently reported (Swiezewski et al., 2009; Liu et al., 2010). FCA and FY appear to control *FLC* transcription by mediating alternative cleavage/polyadenylation of non-coding antisense RNAs that are embedded in the *FLC* locus. As co-expressed sense and antisense gene pairs are common in eukaryotes, alternative 3' end processing of antisense RNAs may be a significant form of gene regulation.

Future Directions:

1.1 Examine differential 3' end processing in meiosis

The abundance of microarray data I and co-workers generated in the past few years have much more to offer than what is presented in this thesis. In particular, I observed alternative 3' UTR in meiosis compared to vegetative cells on genes that are particularly interesting to me. One of these genes is *sme2*/meiRNA (shown in Figure 4.1). A visual inspection of tiling array data of vegetative and meiotic samples did not reveal extensive alternative 3' cleavage site usage as reported in mouse spermatogenesis. It seems to me that the changes on transcription start sites are more frequent than changes in 3' processing, and transcripts tend to have longer 5' UTR in meiosis. However, these

observations were not acquired in a systematic way. Computational analysis on 3' UTR and 5'UTR should be carried out on the tiling array data set in the near future.

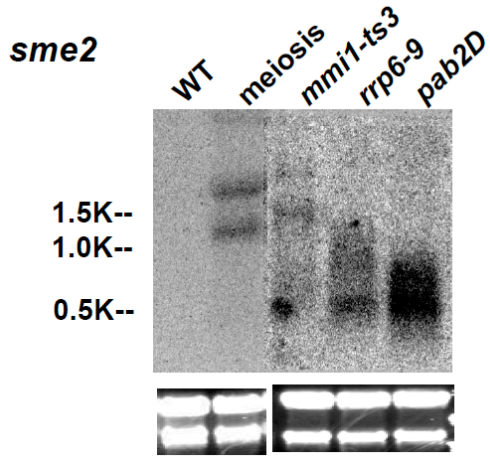

Figure 4.1 Northern blot analysis of *sme2,* the meiRNA. The size of meiRNA changed dramatically during meiosis. In *rrp6-9* mutant meiRNA accumulated comparing to WT strain and the meiRNA in *rrp6-9* mutant seemed to be hyperadenylated. This suggests that Rrp6 degraded meiRNA, possibly through the hyperadenylation-mediated pathway. Similar result was shown in *pab2Δ* strain, indicating that Pab2 involved in this degradation. meiRNA responded to Mmi1 in a very different way since the longer forms of meiRNA, the forms that appeared in meiosis, was the major meiRNA in the *mmi1-ts3* mutant. This suggests that Mmi1 promoted the usage of proximal poly(A) signal in vegetative cells and transcripts ended in the proximal sites were hyperadenylated and degraded. In meiosis, the 3' end of meiRNA was changed in two levels: the site of cleavage/polyadenylation and the quantity of polyadenylation. The regulation of meiRNA is very different from the regulation of *rec8*, even though Mmi1 is involved in regulating both genes. Similar data were obtained from tiling array on vegetative, *rrp6-9* and meiotic samples (data not shown).

1.2 Hyperadenylation-mediated RNA decay

The hyperadenylation-mediated RNA decay that I proposed in Chapter Two invites the possibility that an ideal length of polyA tail exists and mRNAs with polyA tail longer than the ideal length is targeted for degradation. To test if this decay pathway is commonly applied in regulating the abundance of mRNAs, identifying mRNAs with very long polyA tails in exonuclease mutants is the first step. I tested the polyA tail length on

several genes using Northern blot assay and found several early meiotic genes (regulated by Mmi1) and two non-meiotic genes (not regulated by Mmi1) carried hyperadenylation in the *rrp6-9* mutant strain. One should take advantage of microarray technology to find these hyperadenylated mRNAs more efficiently. The method of fractionation of mRNAs by the length of their polyA tail has been well established (Meijer et al., 2007). This method is adopted from oligoT affinity chromatography, in which total RNA is hybridized with biotinylated oligoT_{25} and then bound to streptavidin coated paramagnetic beads and followed by wash and elution with decreasing salt concentration. Unlike hybridization with oligoT-linked on a supportive material, hybridization with saturated oligoT in a solution will lead to continuous duplex formation between oligoT and polyA tail. Longer polyA tail will have higher thermodynamic stability, and will be bound tighter to the beads than short polyA tail. A mixed length of radio-labeled polyadenylated probe (10nt to 500nt) can be used for calibration. Comparison with a radio-labeled marker enables the determination of the polyA length in each fractionation sample. RNA from each fraction, or the fraction with the longest polyA tail, will be concentrated and a portion of the RNA will be run on urea-PAGE to determine the polyA length in the fraction. Also, RNAs will be reverse-transcribed to cDNA for tiling array analysis to determine the mRNA identity and the approximate site of cleavage. Or, alternatively, one can use high-throughput RNA sequencing to determine the cleavage site in a single nucleotide resolution. It will be very interesting to know what genes are regulated by hyperadenylation-mediated decay. Analysis the 3'UTR sequences of these hyperadenylated RNAs may further provide us insight of the regulation of hyperadenylation.

1.3 Genetic screening to identified factors involved in regulating *mek1*

I studied the splicing regulation of four early meiotic genes: *rec8, crs1, mek1* and *meu13.* All of them showed meiosis-specific splicing patterns. Mmi1 repressed splicing of *rec8* and *crs1* in vegetative cells but only had a small effect on *mek1* and *meu13*. Therefore, regulatory factor(s) other than Mmi1 may control splicing and RNA stability of *mek1* and *meu13*. The splicing inhibition imposed on *meu13* seemed to be more complex than those on *mek1*, because *meu13* became spliced in all the mutant strains that

affected *mek1* and in two other mutants that did not affect *mek1* (Figure 2.8). Moreover, the *cis*-regulatory sequences involved in *meu13* splicing regulation were located in both promoter and terminator regions, while only the promoter sequence was important for *mek1* splicing regulation. In summary, I found that *mek1* was regulated through an unknown mechanism(s) that is very different from the mechanism applied on *rec8*. Given that the regulation of *mek1* seemed to be simpler than *meu13,* I decided to continue work on *mek1*.

I attempted to ask if *mek1* is one of the targets of hyperadenylation-mediated decay by Northern blot, and uncovered a surprising feature of *mek1* mRNA (Figure 4.2 A). *mek1* mRNA level was very low (and unspliced) in vegetative cells and accumulated in meiotic cells. The size of *mek1* mRNA in meiotic cells was ~1.5kb. Consistent with results shown in Chapter Two that *mek1* was slightly influenced by Mmi1, only a very low level of mRNA appeared in *mmi1-ts3* mutant by Northern blot. In the *rrp6-9* mutant, *mek1* mRNA was around 3kb, much longer than the size observed in meiosis or in *mmi1-ts3* mutant. The increasing in size did not appear to be hyperadenylation; rather it was caused by readthrough transcription of the upstream gene, *dad3,* into *mek1* locus and formed a fused RNA that contains two genes (similar to the polycistronic RNAs in bacteria). This result was confirmed by tiling array (Figure 4.2 B). Mmi1 did not affect the fused form of *dad3-mek1* mRNA since it remained in the *rrp6-9 mmi1-ts3* double mutant.

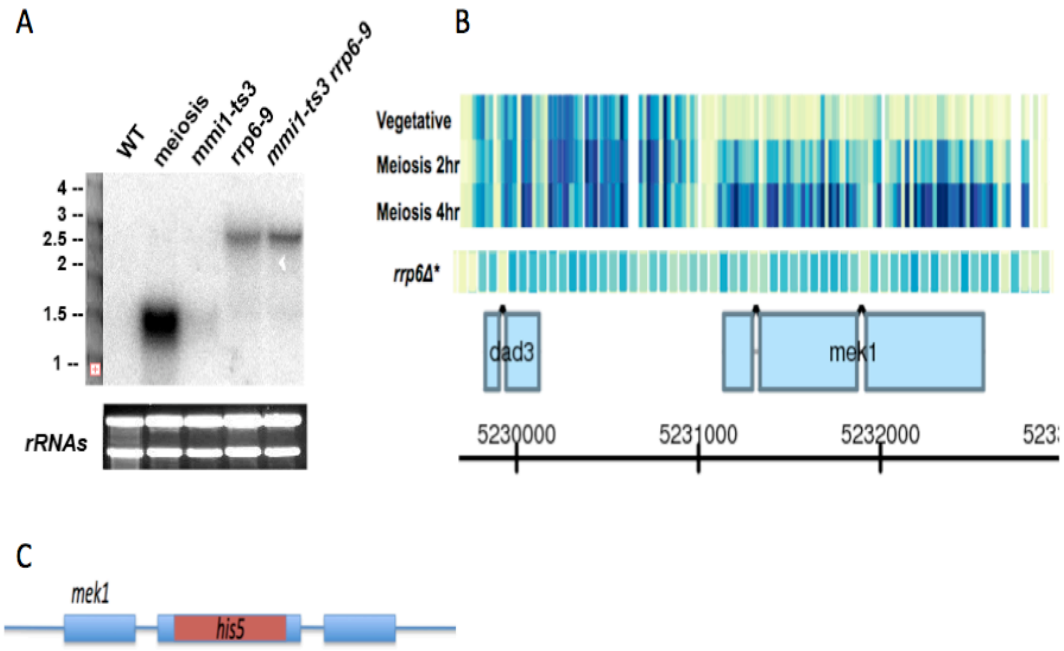

Figure 4.2 Special features of *mek1* mRNA. (A) Northern blot analysis of *mek1*. The mRNA was absent in WT vegetative cells and appeared in meiosis (4hr). In *rrp6-9* mutant the mRNA became much longer comparing to the mRNA in meiosis. (B) Tiling array data were consistent with the Northern blot results. * *rrp6Δ* result tiling array was adapted form (Dutrow et al., 2008.) (C) Illustration of *mek1::his5* strain for genetic screening. Most of the *mek1* exon 2 was replaced by *his5*.

The fused RNA in *rrp6-9* mutant suggests that this form was normally made in vegetative cells. This readthrough of *dad3* may be a novel type of transcription interference that inhibits the promoter usage of *mek1*. This idea is consistent with the fact that the promoter sequence of *mek1* inhibits splicing. *mek1 en*codes an important kinase for meiotic recombination checkpoint that prevent meiotic chromosome segregation if defects in recombination are sensed (Perez-Hidalgo et al., 2003). *dad3* encodes an important protein for mitotic chromosome segregation (Liu et al., 2005), a process that is likely to be inhibited by *mek1*. An attractive model is that cells utilize the *dad3* readthrough to prevent *mek1* from interfering with chromosome segregation in mitosis.

To search for factors that involved in *mek1* regulation, I engineered a strain suitable for genetic screening (Figure 4.2 C). The exon 2 of *mek1* was replaced by *his5* and the genomic copy of *his5* was disrupted by KanMX. This strain would be able to

grow on medium lacking histidine when the factor(s) that inhibits *mek1* expression is mutated. Lab technician Hong Wang treated this reporter strain with EMS to induce mutation and plated on medium without histidine. Around 500 colonies were recovered from minus histidine plate. Fellow graduate student Kaustav Mukherjee is continuing this project.

1.4 Does *pfs2* regulate antisense RNA in *S. pombe*? (Short answer is yes.)

Pfs2 is a core factor in the yeast CPF complex (cleavage and polyadenylation factor), a complex equivalent to mammalian CPSF complex (cleavage and polyadenylation specificity factor) (review in (Millevoi and Vagner, 2010)). This complex contributes to the recognition of poly(A) signals and to the reaction of 3' end cleavage and polyadenylation. The first functional report of Pfs2 in *S. pombe* identified that the *pfs2-11* mutant strain exhibited a chromosome segregation defect, an inability to enter S phase and 3' end processing defects (Wang et al., 2005). The 3' end processing defects were selectively tested on two genes, *cdc18* and *cdt1*, which encode MCM loader and DNA replication licensing factor, respectively. These two genes are essential initiation factors for DNA replication (Yanow et al., 2001). Since Pfs2 was known as a 3' end processing factor in budding yeast by that time, an obvious possibility was that the *pfs2-11* mutant strain fails to synthesize proper mRNAs required for DNA replication. However, RT-PCR (not strand specific) indicated that the level of *cdc18* and *cdt1* in the *pfs2-11* mutant were abundant (Figure 4.3 A). The author than tested the 3' end property of *cdc18* (but not *cdt1*) and found readthrough RNAs of *cdc18* in the *pfs2-11* mutant, suggesting that these RNAs are not functional and result in S phase defects.

I have developed an interest in Pfs2 since the beginning of my research. I found that many meiotic genes had readthrough RNAs in the *pfs2-11* mutant and these readthrough RNAs were partially spliced, not polyadenylated and surprisingly were able to accumulate. In order to study the connection between splicing and 3' end processing, I generated tiling array data on the *pfs2-11* mutant. Because oligo d(T) was used for cDNA priming, transcripts affected by *pfs2-11* that did not carry a polyA tail were poorly primed and didn't show up on the tiling array. Nevertheless, I found another reason, possibly the real reason, to explain the inability of the *pfs2-11* mutant to enter S phase. In

WT cells, *cdt1* sense mRNA was clearly detected by the tiling array. On the contrary, the *cdt1* locus was transcribed in the opposite direction and resulted in antisense RNA of *cdt1* in the *pfs2-11* mutant (Figure 4.3). This change was unexpected and suggested that Pfs2 regulates the expression of *cdt1* by mediating the transcription of *cdt1* antisense RNA, a phenomenon similar to the regulation of FLC by FCA and FY in plants. The *cdt18* mRNA level was normal in the *pfs2-11* mutant compared to the WT strain, suggesting the polyadenylated *cdc18* mRNAs dose exist in the *pfs2-11* mutant (data not shown).

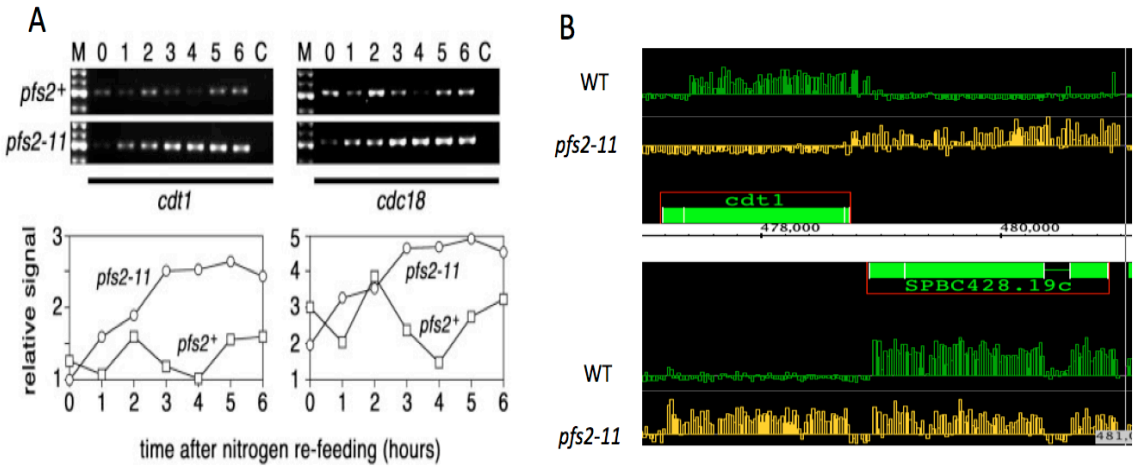

Figure 4.3 Pfs2 regulates the sense and antisense transcription transition of *cdt1*. (A) Analysis of *cdt1* and *cdc18* mRNA level by RT-PCR. Cells were synchronized in G1 by nitrogen starvation and released to enter cell cycle by nitrogen re-feeding. Samples were collect every hour from 0 to 6hr after the nitrogen re-feeding (about two cell cycles). Bottom panel shown the quantification of RT-PCR. (B) Tilling array data of *cdt1* locus expression in the WT strain (green) and *pfs2-11* mutant (yellow). *cdt1* sense RNA was detected in WT strain, while the *cdt1* antisense RNA was expressed in *pfs2-11* mutant.

To understand the mechanism by which 3' end processing factors determine transcription direction is certainly interesting. The first experiment I propose to conduct is to determine if the *cdt1* antisense is regulated by cell cycle since *cdt1* sense RNA fluctuates in a cell cycle dependent manner (Figure 4.3 A, *cdt1* is expressed at G1/S).

Moreover, I propose to test if mutation of other 3' end processing factors, such as RNA15, will influence *cdt1* as *pfs2-11*.

2. Identification of functional non-coding RNAs

The recognition that substantial fractions of the non-coding regions are transcribed has aroused great interest in the potential biological functions of ncRNAs (ENCODE, 2004; Wilhelm et al., 2008). These ncRNAs are categorized into different groups based on their sizes, such as siRNAs (small interfering) are smaller than 25nt and lncRNAs (long non-coding) are more than 200nt. The ncRNAs I discovered belong to the lncRNA category and these RNAs are single-stranded, polyadenylated RNA molecules. In addition, these RNAs are naturally occurring RNAs antisense to meiotic genes. Recent studies also revealed widespread expression of complementary sense-antisense transcription pairs. Several landmark studies have proved that antisense RNA can modulate the expression of the sense gene, at the transcription level or post-transcription level (see below for these studies).

Genome wide association (GWA) analysis of the antisense RNAs identified in Chapter Three suggested that these antisense RNA did not utilize the RNAi pathway (Ago1-assocotaed siRNAs were not derived from these antisense RNAs) and did not correlate with heterochromatic markers, H3K9me and Swi6. However, these genome wide studies were limited by the depth of sequence coverage (i.e. RNAs of low abundance would not be sequenced) or by detection sensitivity (i.e. ChIPped-DNA of low abundance would be under detection limit). Therefore, lack of GWA correlation may be a result of technology restraints. The *ago1Δ, dcr1Δ* and *rdp1Δ* did not affect these antisense RNAs and their corresponding sense RNAs tested by strand specific RT-PCR strengthen the conclusion that RNAi pathway was not relevant. In the following section I highlight recent advances in the ncRNA-mediated, but not siRNA related, gene regulation mechanisms at the level of transcription. These mechanisms may also apply on the antisense-mediated repression of meiotic genes in *S. pombe.*

ncRNA-mediated chromosome modification

- **Fission yeast - Nucleosome remodeling** (Hirota et al., 2008)

  fbp1, a gene responsive to carbohydrate source, is regulated by upstream ncRNAs in a carbohydrate-dependent manner. The transcription of these upstream ncRNAs by RNA pol II is required for activation of *fbp1* transcription. The chromatin of the *fbp1* promoter region is progressively remodeled to an open configuration, as the upstream ncRNAs are transcribed, that may increase accessibility for transcription factors.

- **Budding yeast - Histone deacetylation** (Camblong et al., 2007)

  PHO84, a gene that regulates phosphate metabolism, is repressed by long polyadenylated antisense ncRNA in *RRP6* mutant strains and in aged cells, which may have a decreased Rrp6 activity. The loss of Rrp6 function leads to accumulation of *PHO84* antisense RNA and subsequently represses *PHO84* gene expression. This antisense ncRNA-mediated repression is not due to transcription interference. The correlation between antisense ncRNA and histone deacetylation by histone deacetylase HDAC complex suggests that ncRNA is important for recruiting HDAC.

- **Human and Mouse – Histone methyltransferase**

  Human HOX loci, which encode for homeobox transcription factors, associate with many ncRNAs that are spatially expressed along the developmental axes. A long ncRNA transcribed from the HOXC locus, termed HOTAIR, represses transcription in *trans* of the HOXD locus located ~40kb away from the HOXC locus. HOTAIR interacts with PRC2 (Polycomb Repressive Complex 2) and induces H3K27 methylation of the HOXD locus, resulting in transcription repression of HOXD (Rinn et al., 2007).

  X-chromosome inactivation (XCI) in female mouse is mediated by Xist, a ~17kb ncRNA transcribed form the X chromosome prior to XCI that localizes to the inactive X chromosome. Xist recruits PRC2 that results in spreading of H3K27me and establishing XCI (Zhao et al., 2008).

The examples summarized above demonstrated the wide range of ncRNA functions. The upstream ncRNAs of *fbp1* seem to function without the requirement of protein partners. Or, more specifically, this regulation seems to depend on the action of transcription but not the ncRNAs. Other ncRNAs, on the other hand, seem to serve as a recruiting platform for histone modification enzymes to the same loci or as a targeting molecule for histone modification enzymes to other loci. This indicates that RNA-interacting proteins have an important role in the ncRNA-mediated regulation.

Future Directions:

In the *S. pombe* genome, 595 genes (more than 1/10 of the entire genome) were experimentally tested or predicted to have RNA binding ability and among these 70 genes have the typical RRM (RNA-recognition motifs), a motif that binds to single strand RNA (genome statistics acquired from GeneDB). Some of these genes are known to be involved in splicing, RNA 3' processing, RNA export, RNA stability and so on, while functions of many other genes remain unexplored. Meiosis in *S. pombe* has a great demand on RNA binding proteins at many stages. The most striking RNA binding protein is Mei2, the master meiotic inducer, that functions during early/middle meiotic events. Other meiosis-specific RNA binding proteins (including *crp79, mug28, spo5, mde7 and etc.*) seem to be important for middle and late meiosis, but their target RNAs and their molecular functions are largely unknown. To explore the biological functions of ncRNAs, an alternative method is to ask what proteins interact with them.

meiRNA and Mei2

The master meiosis regulator Mei2 is an RNA binding protein that contains three RRMs. To date, the ncRNA meiRNA is the only RNA identified that binds to Mei2 at meiotic prophase (Watanabe et al., 1994).

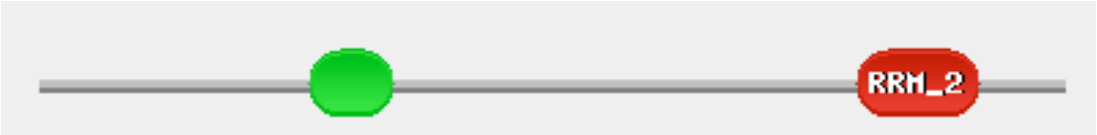

Pfam-A	Description	Entry type	Sequence		HMM	
			Start	End	From	To
RRM_1	RNA recognition motif. (a.k.a. RRM, RBD, or RNP domain)	Domain	197	265	1	74
RRM_1	RNA recognition motif. (a.k.a. RRM, RBD, or RNP domain)	Domain	334	361	47	74
RRM_2	RNA recognition motif 2	Family	596	692	1	97

Figure 4.4. Mei2 contains three RNA recognition motifs (RRM). The second RRM1 is not shown on the top panel due to the lower confidence. (Figure generated with Pfam web tool.)

Mei2 is cytoplasmic during meiotic interphase and Mei2 shuttles into the nucleus prior to Meiosis I (MI) to form a dot at the DNA locus of *sme2,* the gene that encodes meiRNA. In this case, *sme2/*meiRNA serves as a recruiting platform (Yamashita et al., 1998). Mei2 interacts with meiRNA through RRM2. A point mutation in the RRM2 (*mei2-F644A*) abolishes MI, a phenotype that was also observed in a *sme2Δ* strain (Watanabe et al., 1997). This suggests that Mei2-meiRNA interaction is important for MI. The first RRM1 is also important since *mei2-33* (F240L point mutation in the first RRM1) arrests before DNA synthesis at higher temperature or arrests before MI at lower temperature (Watanabe et al., 1994). These observations suggest that Mei2 may interact with other RNAs, besides meiRNA, through both RRM1 and RRM2 for proper DNA synthesis and MI. The identification of Mei2 interacting RNAs will provide insights to the Mei2 functions. I predict that novel ncRNAs are involved. I had requested TAP-tagged *mei2* strain and this strain is suitable for RNA-IP (or CLIP) followed by tiling array (or sequencing) to indentify Mei2-interacting RNAs. We can also test which RRM is involved in the interaction since I also requested the *mei2-F644A* and *mei2-33* strains.

Similar methods can be used to identify RNAs that interact with other RNA binding proteins.

3. Forkhead transcription factor

The first forkhead factor was identified in a genetic screen for embryonic defects in *Drosophila*, where the head exoskeletons of *fkh*$^{-}$ mutants fly were "forked" (Figure 4.5) (Weigel et al., 1989). These reports had established the importance of forkhead factors in developmental process, and subsequently forkhead factors (or FOX) were found to play central roles in cell cycle, metabolism, avian vocal development, human diseases and many other processes. The human genome contains at least 43 forkhead factors, whereas both fission yeast and budding yeast genomes contain four forkhead factors. Forkhead factors share a conserved winged-helix domain, termed the forkhead box or FKH, which is reminiscent of the chromatin-binding domain of linker histone (Clark et al., 1993). However, unlike linker histone, binding by forkhead factors, at least FOXA, relaxes the compact chromatin structure at target promoter sites, resulting in target gene expression (Cirillo et al., 2002). The FKH domain is a DNA-binding domain (Clark et al., 1993), the core DNA binding motif (GTAAAYA) for forkhead transcription factors is well conserved in fission yeast (Horie et al., 1998; Oliva et al., 2005) and likely across species (Pierrou et al., 1994; Kaufmann et al., 1995). Although there are many breakthroughs on the functions of forkhead factors in recent years, very little is known about the mechanism by which forkhead factors choose amongst similar DNA binding sites in the genome.

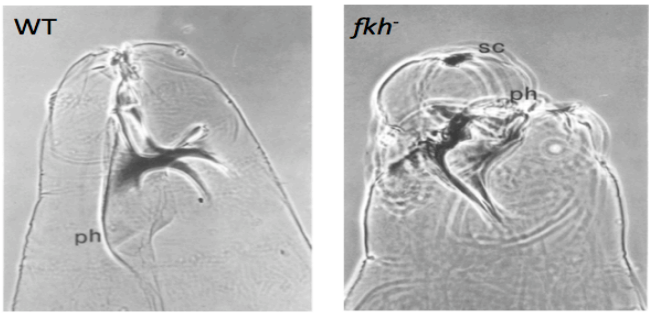

Figure 4.5 Forkhead phenotype. The head phenotypes of WT (left) and *fkh2*$^{-}$ (right) *Drosophila* embryos. head selerite (sc), pharynx floor (ph). Figure adapted from (Jürgens et al., 1988.)

Future Directions:

Understand Forkhead binding specificity

Fkh2 seems to repress transcription of a subset of meiotic genes, but how does this suppression function in vegetative cells and how this repression is relieved in meiosis are questions that I want to answer. To investigate the mechanism of Fkh2-mediated repression and to understand the DNA binding specificity of different forkhead factors, we plan to perform genome wide ChIP-on-chip experiments on all four *S. pombe* forkhead factors. Fellow graduate student Angad Garg has tagged *fkh2, sep1, fhl1* and *mei4* with the TAP-tag and conducted the initial ChIP experiment. We aim to have data sets on all four factors in unsynchronized cell populations, *fkh2* and *sep1* in different stages of the cell cycle and *fkh2* and *mei4* across a meiotic time course. These data will be analyzed to identify motifs that associated with individual forkhead factors. If such motifs are found, we will validate the motifs experimentally.

Summary

My research has uncovered several mechanisms that *S. pombe* utilizes to keep meiotic genes off in vegetative cells and to fine-tune the expression timing of genes during meiosis. These mechanisms are surprising at first, at least to me, because cells seem to spend a lot of energy on repression. Whether to make RNAs just for degradation in the Mmi1-mediated decay pathway or to make a lot of antisense RNAs in the antisense-mediated gene repression. However, searching the literature one can easily identify similar strategies that are used in many organisms and in many cellular processes. I would like to conclude my work with one thought: Life (science) is full of surprises!

References

The ENCODE (ENCyclopedia Of DNA Elements) Project. (2004). Science *306*, 636-640.

Abe, H., and Shimoda, C. (2000). Autoregulated expression of Schizosaccharomyces pombe meiosis-specific transcription factor Mei4 and a genome-wide search for its target genes. Genetics *154*, 1497-1508.

Adhya, S., and Gottesman, M. (1982). Promoter occlusion: transcription through a promoter may inhibit its activity. Cell *29*, 939-944.

Allmang, C., Petfalski, E., Podtelejnikov, A., Mann, M., Tollervey, D., and Mitchell, P. (1999). The yeast exosome and human PM-Scl are related complexes of 3' --> 5' exonucleases. Genes Dev *13*, 2148-2158.

Almeida, R., and Allshire, R.C. (2005). RNA silencing and genome regulation. Trends Cell Biol *15*, 251-258.

Alvarez, B., and Moreno, S. (2006). Fission yeast Tor2 promotes cell growth and represses cell differentiation. J Cell Sci *119*, 4475-4485.

Amorim, M.J., Cotobal, C., Duncan, C., and Mata, J. (2010). Global coordination of transcriptional control and mRNA decay during cellular differentiation. Mol Syst Biol *6*, 380.

Aranda, A., and Proudfoot, N.J. (1999). Definition of transcriptional pause elements in fission yeast. Mol Cell Biol *19*, 1251-1261.

Asakawa, H., Haraguchi, T., and Hiraoka, Y. (2007). Reconstruction of the kinetochore: a prelude to meiosis. Cell Div *2*, 17.

Averbeck, N., Sunder, S., Sample, N., Wise, J.A., and Leatherwood, J. (2005). Negative control contributes to an extensive program of meiotic splicing in fission yeast. Mol Cell *18*, 491-498.

Ayte, J., Leis, J.F., Herrera, A., Tang, E., Yang, H., and DeCaprio, J.A. (1995). The Schizosaccharomyces pombe MBF complex requires heterodimerization for entry into S phase. Mol Cell Biol *15*, 2589-2599.

Bentley, D.L. (2005). Rules of engagement: co-transcriptional recruitment of pre-mRNA processing factors. Curr Opin Cell Biol *17*, 251-256.

Birikh, K.R., Heaton, P.A., and Eckstein, F. (1997). The structure, function and application of the hammerhead ribozyme. Eur J Biochem *245*, 1-16.

Birney, E., Kumar, S., and Krainer, A.R. (1993). Analysis of the RNA-recognition motif and RS and RGG domains: conservation in metazoan pre-mRNA splicing factors. Nucleic Acids Res *21*, 5803-5816.

Brawerman, G. (1981). The Role of the poly(A) sequence in mammalian messenger RNA. CRC Crit Rev Biochem *10*, 1-38.

Brown, C.E., and Sachs, A.B. (1998). Poly(A) tail length control in Saccharomyces cerevisiae occurs by message-specific deadenylation. Mol Cell Biol *18*, 6548-6559.

Buck, V., Ng, S.S., Ruiz-Garcia, A.B., Papadopoulou, K., Bhatti, S., Samuel, J.M., Anderson, M., Millar, J.B., and McInerny, C.J. (2004). Fkh2p and Sep1p regulate mitotic gene transcription in fission yeast. J Cell Sci *117*, 5623-5632.

Buhler, M., Spies, N., Bartel, D.P., and Moazed, D. (2008). TRAMP-mediated RNA surveillance prevents spurious entry of RNAs into the Schizosaccharomyces pombe siRNA pathway. Nat Struct Mol Biol *15*, 1015-1023.

Bulmer, R., Pic-Taylor, A., Whitehall, S.K., Martin, K.A., Millar, J.B., Quinn, J., and Morgan, B.A. (2004). The forkhead transcription factor Fkh2 regulates the cell division cycle of Schizosaccharomyces pombe. Eukaryot Cell *3*, 944-954.

Burkard, K.T., and Butler, J.S. (2000). A nuclear 3'-5' exonuclease involved in mRNA degradation interacts with Poly(A) polymerase and the hnRNA protein Npl3p. Mol Cell Biol *20*, 604-616.

Callahan, K.P., and Butler, J.S. (2010). TRAMP complex enhances RNA degradation by the nuclear exosome component Rrp6. J Biol Chem *285*, 3540-3547.

Cam, H.P., Sugiyama, T., Chen, E.S., Chen, X., FitzGerald, P.C., and Grewal, S.I. (2005). Comprehensive analysis of heterochromatin- and RNAi-mediated epigenetic control of the fission yeast genome. Nat Genet *37*, 809-819.

Camblong, J., Iglesias, N., Fickentscher, C., Dieppois, G., and Stutz, F. (2007). Antisense RNA stabilization induces transcriptional gene silencing via histone deacetylation in S. cerevisiae. Cell *131*, 706-717.

Carmichael, J.B., Provost, P., Ekwall, K., and Hobman, T.C. (2004). ago1 and dcr1, two core components of the RNA interference pathway, functionally diverge from rdp1 in

regulating cell cycle events in Schizosaccharomyces pombe. Mol Biol Cell *15*, 1425-1435.

Cervantes, M.D., Farah, J.A., and Smith, G.R. (2000). Meiotic DNA breaks associated with recombination in S. pombe. Mol Cell *5*, 883-888.

Cirillo, L.A., and Barton, M.C. (2008). Many forkheads in the road to regulation. Symposium on forkhead transcription factor networks in development, signalling and disease. EMBO Rep *9*, 721-724.

Cirillo, L.A., Lin, F.R., Cuesta, I., Friedman, D., Jarnik, M., and Zaret, K.S. (2002). Opening of compacted chromatin by early developmental transcription factors HNF3 (FoxA) and GATA-4. Mol Cell *9*, 279-289.

Clark, K.L., Halay, E.D., Lai, E., and Burley, S.K. (1993). Co-crystal structure of the HNF-3/fork head DNA-recognition motif resembles histone H5. Nature *364*, 412-420.

Cooke, C., Hans, H., and Alwine, J.C. (1999). Utilization of splicing elements and polyadenylation signal elements in the coupling of polyadenylation and last-intron removal. Mol Cell Biol *19*, 4971-4979.

Cramer, P., Pesce, C.G., Baralle, F.E., and Kornblihtt, A.R. (1997). Functional association between promoter structure and transcript alternative splicing. Proc Natl Acad Sci U S A *1997*, 21.

Darieva, Z., Bulmer, R., Pic-Taylor, A., Doris, K.S., Geymonat, M., Sedgwick, S.G., Morgan, B.A., and Sharrocks, A.D. (2006). Polo kinase controls cell-cycle-dependent transcription by targeting a coactivator protein. Nature *444*, 494-498.

Dass, B., Tardif, S., Park, J.Y., Tian, B., Weitlauf, H.M., Hess, R.A., Carnes, K., Griswold, M.D., Small, C.L., and Macdonald, C.C. (2007). Loss of polyadenylation protein tauCstF-64 causes spermatogenic defects and male infertility. Proc Natl Acad Sci U S A *104*, 20374-20379.

Davey, J. (1992). Mating pheromones of the fission yeast Schizosaccharomyces pombe: purification and structural characterization of M-factor and isolation and analysis of two genes encoding the pheromone. EMBO J *11*, 951-960.

Davis, C.A., and Ares, M., Jr. (2006). Accumulation of unstable promoter-associated transcripts upon loss of the nuclear exosome subunit Rrp6p in Saccharomyces cerevisiae. Proc Natl Acad Sci U S A *103*, 3262-3267.

Delaney, K.J., Xu, R., Zhang, J., Li, Q.Q., Yun, K.Y., Falcone, D.L., and Hunt, A.G. (2006). Calmodulin interacts with and regulates the RNA-binding activity of an Arabidopsis polyadenylation factor subunit. Plant Physiol *140*, 1507-1521.

Ding, R., and Smith, G.R. (1998). Global control of meiotic recombination genes by Schizosaccharomyces pombe rec16 (rep1). Mol Gen Genet *258*, 663-670.

Dreyfus, M., and Regnier, P. (2002). The poly(A) tail of mRNAs: bodyguard in eukaryotes, scavenger in bacteria. Cell *111*, 611-613.

Dutrow, N., Nix, D.A., Holt, D., Milash, B., Dalley, B., Westbroek, E., Parnell, T.J., and Cairns, B.R. (2008). Dynamic transcriptome of Schizosaccharomyces pombe shown by RNA-DNA hybrid mapping. Nat Genet *40*, 977-986.

Dziembowski, A., Lorentzen, E., Conti, E., and Seraphin, B. (2007). A single subunit, Dis3, is essentially responsible for yeast exosome core activity. Nat Struct Mol Biol *14*, 15-22.

Garcia, I., Tajadura, V., Martin, V., Toda, T., and Sanchez, Y. (2006). Synthesis of alpha-glucans in fission yeast spores is carried out by three alpha-glucan synthase paralogues, Mok12p, Mok13p and Mok14p. Mol Microbiol *59*, 836-853.

Ge, X., Rubinstein, W.S., Jung, Y.C., and Wu, Q. (2008). Genome-wide analysis of antisense transcription with Affymetrix exon array. BMC Genomics *9*, 27.

Geer, L.Y., Marchler-Bauer, A., Geer, R.C., Han, L., He, J., He, S., Liu, C., Shi, W., and Bryant, S.H. (2010). The NCBI BioSystems database. Nucleic Acids Res *38*, D492-496.

Grewal, S.I., and Elgin, S.C. (2007). Transcription and RNA interference in the formation of heterochromatin. Nature *447*, 399-406.

Harigaya, Y., Tanaka, H., Yamanaka, S., Tanaka, K., Watanabe, Y., Tsutsumi, C., Chikashige, Y., Hiraoka, Y., Yamashita, A., and Yamamoto, M. (2006). Selective elimination of messenger RNA prevents an incidence of untimely meiosis. Nature *442*, 45-50.

Hartmann, A.M., Nayler, O., Schwaiger, F.W., Obermeier, A., and Stamm, S. (1999). The interaction and colocalization of Sam68 with the splicing-associated factor YT521-B in nuclear dots is regulated by the Src family kinase p59(fyn). Mol Biol Cell *10*, 3909-3926.

Hilleren, P., McCarthy, T., Rosbash, M., Parker, R., and Jensen, T.H. (2001). Quality control of mRNA 3'-end processing is linked to the nuclear exosome. Nature *413*, 538-542.

Hilleren, P., and Parker, R. (2001). Defects in the mRNA export factors Rat7p, Gle1p, Mex67p, and Rat8p cause hyperadenylation during 3'-end formation of nascent transcripts. RNA *7*, 753-764.

Hirota, K., Miyoshi, T., Kugou, K., Hoffman, C.S., Shibata, T., and Ohta, K. (2008). Stepwise chromatin remodelling by a cascade of transcription initiation of non-coding RNAs. Nature *456*, 130-134.

Hofmann, J.F., and Beach, D. (1994). cdt1 is an essential target of the Cdc10/Sct1 transcription factor: requirement for DNA replication and inhibition of mitosis. EMBO J *13*, 425-434.

Hongay, C.F., Grisafi, P.L., Galitski, T., and Fink, G.R. (2006). Antisense transcription controls cell fate in Saccharomyces cerevisiae. Cell *127*, 735-745.

Horie, S., Watanabe, Y., Tanaka, K., Nishiwaki, S., Fujioka, H., Abe, H., Yamamoto, M., and Shimoda, C. (1998). The Schizosaccharomyces pombe mei4+ gene encodes a meiosis-specific transcription factor containing a forkhead DNA-binding domain. Mol Cell Biol *18*, 2118-2129.

Hornyik, C., Duc, C., Rataj, K., Terzi, L.C., and Simpson, G.G. (2010). Alternative polyadenylation of antisense RNAs and flowering time control. Biochem Soc Trans *38*, 1077-1081.

Huang, Y., Bayfield, M.A., Intine, R.V., and Maraia, R.J. (2006). Separate RNA-binding surfaces on the multifunctional La protein mediate distinguishable activities in tRNA maturation. Nat Struct Mol Biol *13*, 611-618.

Huber, W., Toedling, J., and Steinmetz, L.M. (2006). Transcript mapping with high-density oligonucleotide tiling arrays. Bioinformatics *22*, 1963-1970.

Ibrahim, H., Wilusz, J., and Wilusz, C.J. (2008). RNA recognition by 3'-to-5' exonucleases: the substrate perspective. Biochim Biophys Acta *1779*, 256-265.

Imai, Y., and Yamamoto, M. (1994). The fission yeast mating pheromone P-factor: its molecular structure, gene structure, and ability to induce gene expression and G1 arrest in the mating partner. Genes Dev *8*, 328-338.

Ito, S., Sakai, A., Nomura, T., Miki, Y., Ouchida, M., Sasaki, J., and Shimizu, K. (2001). A novel WD40 repeat protein, WDC146, highly expressed during spermatogenesis in a stage-specific manner. Biochem Biophys Res Commun *280*, 656-663.

Ji, Z., Lee, J.Y., Pan, Z., Jiang, B., and Tian, B. (2009). Progressive lengthening of 3' untranslated regions of mRNAs by alternative polyadenylation during mouse embryonic development. Proc Natl Acad Sci U S A *106*, 7028-7033.

Jia, H., Osak, M., Bogu, G.K., Stanton, L.W., Johnson, R., and Lipovich, L. (2010). Genome-wide computational identification and manual annotation of human long noncoding RNA genes. RNA *16*, 1478-1487.

Jin, Y.H., Yoo, E.J., Jang, Y.K., Kim, S.H., Kim, M.J., Shim, Y.S., Lee, J.S., Choi, I.S., Seong, R.H., Hong, S.H.*, et al.* (1998). Isolation and characterization of hrp1+, a new member of the SNF2/SWI2 gene family from the fission yeast Schizosaccharomyces pombe. Mol Gen Genet *257*, 319-329.

Kadaba, S., Wang, X., and Anderson, J.T. (2006). Nuclear RNA surveillance in Saccharomyces cerevisiae: Trf4p-dependent polyadenylation of nascent hypomethylated tRNA and an aberrant form of 5S rRNA. RNA *12*, 508-521.

Kaufer, N.F., and Potashkin, J. (2000). Analysis of the splicing machinery in fission yeast: a comparison with budding yeast and mammals. Nucleic Acids Res *28*, 3003-3010.

Kaufmann, E., Hoch, M., and Jackle, H. (1994). The interaction of DNA with the DNA-binding domain encoded by the Drosophila gene fork head. Eur J Biochem *223*, 329-337.

Kaur, J., Sebastian, J., and Siddiqi, I. (2006). The Arabidopsis-mei2-like genes play a role in meiosis and vegetative growth in Arabidopsis. Plant Cell *18*, 545-559.

Keller, W., and Minvielle-Sebastia, L. (1997). A comparison of mammalian and yeast pre-mRNA 3'-end processing. Curr Opin Cell Biol *9*, 329-336.

Kerwitz, Y., Kuhn, U., Lilie, H., Knoth, A., Scheuermann, T., Friedrich, H., Schwarz, E., and Wahle, E. (2003). Stimulation of poly(A) polymerase through a direct interaction with the nuclear poly(A) binding protein allosterically regulated by RNA. EMBO J *22*, 3705-3714.

Kishida, M., Nagai, T., Nakaseko, Y., and Shimoda, C. (1994). Meiosis-dependent mRNA splicing of the fission yeast Schizosaccharomyces pombe mes1+ gene. Curr Genet *25*, 497-503.

Kiss, D.L., and Andrulis, E.D. (2010). Genome-wide analysis reveals distinct substrate specificities of Rrp6, Dis3, and core exosome subunits. RNA.

Kitamura, K., Katayama, S., Dhut, S., Sato, M., Watanabe, Y., Yamamoto, M., and Toda, T. (2001). Phosphorylation of Mei2 and Ste11 by Pat1 kinase inhibits sexual differentiation via ubiquitin proteolysis and 14-3-3 protein in fission yeast. Dev Cell *1*, 389-399.

Klapholz, S., and Esposito, R.E. (1980). Isolation of SPO12-1 and SPO13-1 from a natural variant of yeast that undergoes a single meiotic division. Genetics *96*, 567-588.

Koranda, M., Schleiffer, A., Endler, L., and Ammerer, G. (2000). Forkhead-like transcription factors recruit Ndd1 to the chromatin of G2/M-specific promoters. Nature *406*, 94-98.

Krogan, N.T., and Long, J.A. (2009). Why so repressed? Turning off transcription during plant growth and development. Curr Opin Plant Biol *12*, 628-636.

Kuhn, U., Gundel, M., Knoth, A., Kerwitz, Y., Rudel, S., and Wahle, E. (2009). Poly(A) tail length is controlled by the nuclear poly(A)-binding protein regulating the interaction between poly(A) polymerase and the cleavage and polyadenylation specificity factor. J Biol Chem *284*, 22803-22814.

Kumar, R., Reynolds, D.M., Shevchenko, A., Goldstone, S.D., and Dalton, S. (2000). Forkhead transcription factors, Fkh1p and Fkh2p, collaborate with Mcm1p to control transcription required for M-phase. Curr Biol *10*, 896-906.

LaCava, J., Houseley, J., Saveanu, C., Petfalski, E., Thompson, E., Jacquier, A., and Tollervey, D. (2005). RNA degradation by the exosome is promoted by a nuclear polyadenylation complex. Cell *121*, 713-724.

Lange, H., Sement, F.M., Canaday, J., and Gagliardi, D. (2009). Polyadenylation-assisted RNA degradation processes in plants. Trends Plant Sci *14*, 497-504.

Lebreton, A., and Seraphin, B. (2008). Exosome-mediated quality control: substrate recruitment and molecular activity. Biochim Biophys Acta *1779*, 558-565.

Lee, Y.J., and Glaunsinger, B.A. (2009). Aberrant herpesvirus-induced polyadenylation correlates with cellular messenger RNA destruction. PLoS Biol *7*, e1000107.

Lemay, J.F., D'Amours, A., Lemieux, C., Lackner, D.H., St-Sauveur, V.G., Bahler, J., and Bachand, F. (2010). The nuclear poly(A)-binding protein interacts with the exosome to promote synthesis of noncoding small nucleolar RNAs. Mol Cell *37*, 34-45.

Li, P., and McLeod, M. (1996). Molecular mimicry in development: identification of ste11+ as a substrate and mei3+ as a pseudosubstrate inhibitor of ran1+ kinase. Cell *87*, 869-880.

Liu, D., Brockman, J.M., Dass, B., Hutchins, L.N., Singh, P., McCarrey, J.R., MacDonald, C.C., and Graber, J.H. (2007). Systematic variation in mRNA 3'-processing signals during mouse spermatogenesis. Nucleic Acids Res *35*, 234-246.

Liu, F., Marquardt, S., Lister, C., Swiezewski, S., and Dean, C. (2010). Targeted 3' processing of antisense transcripts triggers Arabidopsis FLC chromatin silencing. Science *327*, 94-97.

Liu, J., Tang, X., Wang, H., and Balasubramanian, M. (2000). Bgs2p, a 1,3-beta-glucan synthase subunit, is essential for maturation of ascospore wall in Schizosaccharomyces pombe. FEBS Lett *478*, 105-108.

Liu, X., McLeod, I., Anderson, S., Yates, J.R., 3rd, and He, X. (2005). Molecular analysis of kinetochore architecture in fission yeast. EMBO J *24*, 2919-2930.

Mahajan, A., Yuan, C., Lee, H., Chen, E.S., Wu, P.Y., and Tsai, M.D. (2008). Structure and function of the phosphothreonine-specific FHA domain. Sci Signal *1*, re12.

Malapeira J, Moldón A, Hidalgo E, Smith GR, Nurse P, and J., A. (2005). A Meiosis-Specific Cyclin Regulated by Splicing Is Required for Proper Progression through Meiosis. Mol Cell Biol *25*, 6330-6337.

Maniatis, T., and Reed, R. (2002). An extensive network of coupling among gene expression machines. Nature *416*, 499-506.

Martin, V., Ribas, J.C., Carnero, E., Duran, A., and Sanchez, Y. (2000). bgs2+, a sporulation-specific glucan synthase homologue is required for proper ascospore wall maturation in fission yeast. Mol Microbiol *38*, 308-321.

Mata, J., Lyne, R., Burns, G., and Bahler, J. (2002). The transcriptional program of meiosis and sporulation in fission yeast. Nat Genet *32*, 143-147.

Mata, J., Wilbrey, A., and Bahler, J. (2007). Transcriptional regulatory network for sexual differentiation in fission yeast. Genome Biol *8*, R217.

McLeod, M., and Beach, D. (1988). A specific inhibitor of the ran1+ protein kinase regulates entry into meiosis in Schizosaccharomyces pombe. Nature *332*, 509-514.

McLeod, M., Stein, M., and Beach, D. (1987). The product of the mei3+ gene, expressed under control of the mating-type locus, induces meiosis and sporulation in fission yeast. EMBO J *6*, 729-736.

McPheeters, D.S., Cremona, N., Sunder, S., Chen, H.M., Averbeck, N., Leatherwood, J., and Wise, J.A. (2009). A complex gene regulatory mechanism that operates at the nexus of multiple RNA processing decisions. Nat Struct Mol Biol *16*, 255-264.

Meijer, H.A., Bushell, M., Hill, K., Gant, T.W., Willis, A.E., Jones, P., and de Moor, C.H. (2007). A novel method for poly(A) fractionation reveals a large population of mRNAs with a short poly(A) tail in mammalian cells. Nucleic Acids Res *35*, e132.

Millevoi, S., Geraghty, F., Idowu, B., Tam, J.L., Antoniou, M., and Vagner, S. (2002). A novel function for the U2AF 65 splicing factor in promoting pre-mRNA 3'-end processing. EMBO Rep *3*, 869-874.

Millevoi, S., and Vagner, S. (2010). Molecular mechanisms of eukaryotic pre-mRNA 3' end processing regulation. Nucleic Acids Res *38*, 2757-2774.

Milligan, L., Torchet, C., Allmang, C., Shipman, T., and Tollervey, D. (2005). A nuclear surveillance pathway for mRNAs with defective polyadenylation. Mol Cell Biol *25*, 9996-10004.

Minvielle-Sebastia, L., and Keller, W. (1999). mRNA polyadenylation and its coupling to other RNA processing reactions and to transcription. Curr Opin Cell Biol *11*, 352-357.

Mitchell, P., Petfalski, E., Shevchenko, A., Mann, M., and Tollervey, D. (1997). The exosome: a conserved eukaryotic RNA processing complex containing multiple 3'-->5' exoribonucleases. Cell *91*, 457-466.

Moldon, A., Malapeira, J., Gabrielli, N., Gogol, M., Gomez-Escoda, B., Ivanova, T., Seidel, C., and Ayte, J. (2008). Promoter-driven splicing regulation in fission yeast. Nature *455*, 997-1000.

Moreno, M.B., Duran, A., and Ribas, J.C. (2000). A family of multifunctional thiamine-repressible expression vectors for fission yeast. Yeast *16*, 861-872.

Moreno, S., Klar, A., and Nurse, P. (1991). Molecular genetic analysis of fission yeast Schizosaccharomyces pombe. Methods Enzymol *194*, 795-823.

Moser, B.A., and Russell, P. (2000). Cell cycle regulation in Schizosaccharomyces pombe. Curr Opin Microbiol *3*, 631-636.

Muller, W.E., Zahn, R.K., and Seidel, H.J. (1971). Inhibitors acting on nucleic acid synthesis in an oncogenic RNA virus. Nat New Biol *232*, 143-145.

Nakamura, T., Kishida, M., and Shimoda, C. (2000). The Schizosaccharomyces pombe spo6+ gene encoding a nuclear protein with sequence similarity to budding yeast Dbf4 is required for meiotic second division and sporulation. Genes Cells *5*, 463-479.

Nakamura, T., Nakamura-Kubo, M., and Shimoda, C. (2002). Novel fission yeast Cdc7-Dbf4-like kinase complex required for the initiation and progression of meiotic second division. Mol Cell Biol *22*, 309-320.

Nakashima, N., Tanaka, K., Sturm, S., and Okayama, H. (1995). Fission yeast Rep2 is a putative transcriptional activator subunit for the cell cycle 'start' function of Res2-Cdc10. EMBO J *14*, 4794-4802.

Neiman, A.M., Stevenson, B.J., Xu, H.P., Sprague, G.F., Jr., Herskowitz, I., Wigler, M., and Marcus, S. (1993). Functional homology of protein kinases required for sexual differentiation in Schizosaccharomyces pombe and Saccharomyces cerevisiae suggests a conserved signal transduction module in eukaryotic organisms. Mol Biol Cell *4*, 107-120.

Numata, K., Okada, Y., Saito, R., Kiyosawa, H., Kanai, A., and Tomita, M. (2007). Comparative analysis of cis-encoded antisense RNAs in eukaryotes. Gene *392*, 134-141.

Nurse, P. (1997). Regulation of the eukaryotic cell cycle. Eur J Cancer *33*, 1002-1004.

O'Brien, K.P., Remm, M., and Sonnhammer, E.L. (2005). Inparanoid: a comprehensive database of eukaryotic orthologs. Nucleic Acids Res *33*, D476-480.

Ohkura, H., Kinoshita, N., Miyatani, S., Toda, T., and Yanagida, M. (1989). The fission yeast dis2+ gene required for chromosome disjoining encodes one of two putative type 1 protein phosphatases. Cell *57*, 997-1007.

Ohnacker, M., Barabino, S.M., Preker, P.J., and Keller, W. (2000). The WD-repeat protein pfs2p bridges two essential factors within the yeast pre-mRNA 3'-end-processing complex. EMBO J *19*, 37-47.

Oliva, A., Rosebrock, A., Ferrezuelo, F., Pyne, S., Chen, H., Skiena, S., Futcher, B., and Leatherwood, J. (2005). The cell cycle-regulated genes of Schizosaccharomyces pombe. PLoS Biol *3*, e225.

Parisi, S., McKay, M.J., Molnar, M., Thompson, M.A., van der Spek, P.J., van Drunen-Schoenmaker, E., Kanaar, R., Lehmann, E., Hoeijmakers, J.H., and Kohli, J. (1999). Rec8p, a meiotic recombination and sister chromatid cohesion phosphoprotein of the Rad21p family conserved from fission yeast to humans. Mol Cell Biol *19*, 3515-3528.

Perez-Hidalgo, L., Moreno, S., and San-Segundo, P.A. (2003). Regulation of meiotic progression by the meiosis-specific checkpoint kinase Mek1 in fission yeast. J Cell Sci *116*, 259-271.

Perissi, V., Jepsen, K., Glass, C.K., and Rosenfeld, M.G. (2010). Deconstructing repression: evolving models of co-repressor action. Nat Rev Genet *11*, 109-123.

Perocchi, F., Xu, Z., Clauder-Munster, S., and Steinmetz, L.M. (2007). Antisense artifacts in transcriptome microarray experiments are resolved by actinomycin D. Nucleic Acids Res *35*, e128.

Perreault, A., Bellemer, C., and Bachand, F. (2008). Nuclear export competence of pre-40S subunits in fission yeast requires the ribosomal protein Rps2. Nucleic Acids Res *36*, 6132-6142.

Perreault, A., Lemieux, C., and Bachand, F. (2007). Regulation of the nuclear poly(A)-binding protein by arginine methylation in fission yeast. J Biol Chem *282*, 7552-7562.

Pierrou, S., Hellqvist, M., Samuelsson, L., Enerback, S., and Carlsson, P. (1994). Cloning and characterization of seven human forkhead proteins: binding site specificity and DNA bending. EMBO J *13*, 5002-5012.

Prescott, E.M., and Proudfoot, N.J. (2002). Transcriptional collision between convergent genes in budding yeast. Proc Natl Acad Sci U S A *99*, 8796-8801.

Qu, X., Lykke-Andersen, S., Nasser, T., Saguez, C., Bertrand, E., Jensen, T.H., and Moore, C. (2009). Assembly of an export-competent mRNP is needed for efficient release of the 3'-end processing complex after polyadenylation. Mol Cell Biol *29*, 5327-5338.

Reynolds, D., Shi, B.J., McLean, C., Katsis, F., Kemp, B., and Dalton, S. (2003). Recruitment of Thr 319-phosphorylated Ndd1p to the FHA domain of Fkh2p requires Clb kinase activity: a mechanism for CLB cluster gene activation. Genes Dev *17*, 1789-1802.

Rinn, J.L., Kertesz, M., Wang, J.K., Squazzo, S.L., Xu, X., Brugmann, S.A., Goodnough, L.H., Helms, J.A., Farnham, P.J., Segal, E.*, et al.* (2007). Functional demarcation of

active and silent chromatin domains in human HOX loci by noncoding RNAs. Cell *129*, 1311-1323.

Rudra, D., Zhao, Y., and Warner, J.R. (2005). Central role of Ifh1p-Fhl1p interaction in the synthesis of yeast ribosomal proteins. EMBO J *24*, 533-542.

Ruprecht, R.M., Goodman, N.C., and Spiegelman, S. (1973). Conditions for the selective synthesis of DNA complementary to template RNA. Biochim Biophys Acta *294*, 192-203.

Rustici, G., Mata, J., Kivinen, K., Lio, P., Penkett, C.J., Burns, G., Hayles, J., Brazma, A., Nurse, P., and Bahler, J. (2004). Periodic gene expression program of the fission yeast cell cycle. Nat Genet *36*, 809-817.

Salles, F.J., and Strickland, S. (1999). Analysis of poly(A) tail lengths by PCR: the PAT assay. Methods Mol Biol *118*, 441-448.

Samarsky, D.A., Ferbeyre, G., Bertrand, E., Singer, R.H., Cedergren, R., and Fournier, M.J. (1999). A small nucleolar RNA:ribozyme hybrid cleaves a nucleolar RNA target in vivo with near-perfect efficiency. Proc Natl Acad Sci U S A *96*, 6609-6614.

Sato, M., Watanabe, Y., Akiyoshi, Y., and Yamamoto, M. (2002). 14-3-3 protein interferes with the binding of RNA to the phosphorylated form of fission yeast meiotic regulator Mei2p. Curr Biol *12*, 141-145.

Schmid, M., and Jensen, T.H. (2008). The exosome: a multipurpose RNA-decay machine. Trends Biochem Sci *33*, 501-510.

Shigehisa, A., Okuzaki, D., Kasama, T., Tohda, H., Hirata, A., and Nojima, H. (2010). Mug28, a meiosis-specific protein of Schizosaccharomyces pombe, regulates spore wall formation. Mol Biol Cell *21*, 1955-1967.

Shinozaki-Yabana, S., Watanabe, Y., and Yamamoto, M. (2000). Novel WD-repeat protein Mip1p facilitates function of the meiotic regulator Mei2p in fission yeast. Mol Cell Biol *20*, 1234-1242.

Shobuike, T., Tatebayashi, K., Tani, T., Sugano, S., and Ikeda, H. (2001). The dhp1(+) gene, encoding a putative nuclear 5'-->3' exoribonuclease, is required for proper chromosome segregation in fission yeast. Nucleic Acids Res *29*, 1326-1333.

Shonn, M.A., McCarroll, R., and Murray, A.W. (2002). Spo13 protects meiotic cohesin at centromeres in meiosis I. Genes Dev *16*, 1659-1671.

Spiegelman, S., Burny, A., Das, M.R., Keydar, J., Schlom, J., Travnicek, M., and Watson, K. (1970). DNA-directed DNA polymerase activity in oncogenic RNA viruses. Nature *227*, 1029-1031.

St-Andre, O., Lemieux, C., Perreault, A., Lackner, D.H., Bahler, J., and Bachand, F. (2010). Negative regulation of meiotic gene expression by the nuclear poly(A)-binding protein in fission yeast. J Biol Chem.

Steege, D.A. (2000). Emerging features of mRNA decay in bacteria. RNA *6*, 1079-1090.

Sugimoto, A., Iino, Y., Maeda, T., Watanabe, Y., and Yamamoto, M. (1991). Schizosaccharomyces pombe ste11+ encodes a transcription factor with an HMG motif that is a critical regulator of sexual development. Genes Dev *5*, 1990-1999.

Swiezewski, S., Liu, F., Magusin, A., and Dean, C. (2009). Cold-induced silencing by long antisense transcripts of an Arabidopsis Polycomb target. Nature *462*, 799-802.

Szilagyi, Z., Batta, G., Enczi, K., and Sipiczki, M. (2005). Characterisation of two novel fork-head gene homologues of Schizosaccharomyces pombe: their involvement in cell cycle and sexual differentiation. Gene *348*, 101-109.

Takahashi, K., Yamada, H., and Yanagida, M. (1994). Fission yeast minichromosome loss mutants mis cause lethal aneuploidy and replication abnormality. Mol Biol Cell *5*, 1145-1158.

Takeuchi, M., and Yanagida, M. (1993). A mitotic role for a novel fission yeast protein kinase dsk1 with cell cycle stage dependent phosphorylation and localization. Mol Biol Cell *4*, 247-260.

Vanacova, S., Wolf, J., Martin, G., Blank, D., Dettwiler, S., Friedlein, A., Langen, H., Keith, G., and Keller, W. (2005). A new yeast poly(A) polymerase complex involved in RNA quality control. PLoS Biol *3*, e189.

Wade, J.T., Hall, D.B., and Struhl, K. (2004). The transcription factor Ifh1 is a key regulator of yeast ribosomal protein genes. Nature *432*, 1054-1058.

Wahle, E. (1991). A novel poly(A)-binding protein acts as a specificity factor in the second phase of messenger RNA polyadenylation. Cell *66*, 759-768.

Wahle, E. (1995). Poly(A) tail length control is caused by termination of processive synthesis. J Biol Chem *270*, 2800-2808.

Wang, S.W., Asakawa, K., Win, T.Z., Toda, T., and Norbury, C.J. (2005). Inactivation of the pre-mRNA cleavage and polyadenylation factor Pfs2 in fission yeast causes lethal cell cycle defects. Mol Cell Biol *25*, 2288-2296.

Wang, S.W., Toda, T., MacCallum, R., Harris, A.L., and Norbury, C. (2000). Cid1, a fission yeast protein required for S-M checkpoint control when DNA polymerase delta or epsilon is inactivated. Mol Cell Biol *20*, 3234-3244.

Watanabe, Y., Shinozaki-Yabana, S., Chikashige, Y., Hiraoka, Y., and Yamamoto, M. (1997). Phosphorylation of RNA-binding protein controls cell cycle switch from mitotic to meiotic in fission yeast. Nature *386*, 187-190.

Watanabe, Y., and Yamamoto, M. (1994). S. pombe mei2+ encodes an RNA-binding protein essential for premeiotic DNA synthesis and meiosis I, which cooperates with a novel RNA species meiRNA. Cell *78*, 487-498.

Weigel, D., Jurgens, G., Kuttner, F., Seifert, E., and Jackle, H. (1989). The homeotic gene fork head encodes a nuclear protein and is expressed in the terminal regions of the Drosophila embryo. Cell *57*, 645-658.

Weisman, R., and Choder, M. (2001). The fission yeast TOR homolog, tor1+, is required for the response to starvation and other stresses via a conserved serine. J Biol Chem *276*, 7027-7032.

Werner, A., and Sayer, J.A. (2009). Naturally occurring antisense RNA: function and mechanisms of action. Curr Opin Nephrol Hypertens *18*, 343-349.

Wilhelm, B.T., Marguerat, S., Watt, S., Schubert, F., Wood, V., Goodhead, I., Penkett, C.J., Rogers, J., and Bahler, J. (2008). Dynamic repertoire of a eukaryotic transcriptome surveyed at single-nucleotide resolution. Nature *453*, 1239-1243.

Wilusz, J.E., Sunwoo, H., and Spector, D.L. (2009). Long noncoding RNAs: functional surprises from the RNA world. Genes Dev *23*, 1494-1504.

Win, T.Z., Draper, S., Read, R.L., Pearce, J., Norbury, C.J., and Wang, S.W. (2006). Requirement of fission yeast Cid14 in polyadenylation of rRNAs. Mol Cell Biol *26*, 1710-1721.

Wood, V., Gwilliam, R., Rajandream, M.A., Lyne, M., Lyne, R., Stewart, A., Sgouros, J., Peat, N., Hayles, J., Baker, S.*, et al.* (2002). The genome sequence of Schizosaccharomyces pombe. Nature *415*, 871-880.

Wyers, F., Rougemaille, M., Badis, G., Rousselle, J.C., Dufour, M.E., Boulay, J., Regnault, B., Devaux, F., Namane, A., Seraphin, B.*, et al.* (2005). Cryptic pol II transcripts are degraded by a nuclear quality control pathway involving a new poly(A) polymerase. Cell *121*, 725-737.

Yamamoto, M. (1996). Regulation of meiosis in fission yeast. Cell Struct Funct *21*, 431-436.

Yamanaka, S., Yamashita, A., Harigaya, Y., Iwata, R., and Yamamoto, M. (2010). Importance of polyadenylation in the selective elimination of meiotic mRNAs in growing S. pombe cells. EMBO J.

Yamashita, A., Watanabe, Y., Nukina, N., and Yamamoto, M. (1998). RNA-assisted nuclear transport of the meiotic regulator Mei2p in fission yeast. Cell *95*, 115-123.

Yanow, S.K., Lygerou, Z., and Nurse, P. (2001). Expression of Cdc18/Cdc6 and Cdt1 during G2 phase induces initiation of DNA replication. EMBO J *20*, 4648-4656.

Yassour, M., Pfiffner, J., Levin, J.Z., Adiconis, X., Gnirke, A., Nusbaum, C., Thompson, D.A., Friedman, N., and Regev, A. (2010). Strand-specific RNA sequencing reveals extensive regulated long antisense transcripts that are conserved across yeast species. Genome Biol *11*, R87.

Young, D., Riggs, M., Field, J., Vojtek, A., Broek, D., and Wigler, M. (1989). The adenylyl cyclase gene from Schizosaccharomyces pombe. Proc Natl Acad Sci U S A *86*, 7989-7993.

Zhao, J., Sun, B.K., Erwin, J.A., Song, J.J., and Lee, J.T. (2008). Polycomb proteins targeted by a short repeat RNA to the mouse X chromosome. Science *322*, 750-756.

Zhou, D., Frendewey, D., and Lobo Ruppert, S.M. (1999). Pac1p, an RNase III homolog, is required for formation of the 3' end of U2 snRNA in Schizosaccharomyces pombe. RNA *5*, 1083-1098.